Journal *of*
Energy & Environmental Research

NETL

Carbon Sequestration I

Journal Papers, Conversion and Utilization

Message From the Director

I am pleased to introduce the first issue of the *Journal of Energy and Environmental Research*. The Journal will highlight work being conducted by U.S. Department of Energy, National Energy Technology Laboratory (NETL) researchers, in collaboration with investigators from industry, academia, and other national laboratories. The Journal will also feature articles written by invited experts in various fields of energy and environmental studies.
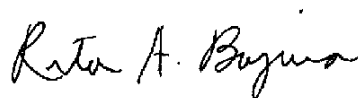
NETL's programs assist in providing the United States with acceptable, affordable, and available energy. They also provide the quality science that contributes to the development of sound energy policies.

Through our contracted, cost-shared research projects, NETL helps maintain U.S. leadership in the energy industry, and appropriately transfers technology to developing countries to improve geopolitical stability. Our research programs are conducted through partnerships with private industry, universities, and national laboratories to develop advanced energy and environmental technologies. NETL also helps provide a trained energy workforce through university research programs.

The challenge we face in addressing our nation's energy issues is formidable. Our academic, scientific, and technological communities must continue to share information to develop solutions to this challenge.

Technology is producing beneficial outcomes in many areas of our lives. Thoughtfully applied to energy, it will allow us to enjoy a thriving economy, a healthy environment, and the quality of life we all desire. NETL's *Journal of Energy and Environmental* is an important step in communicating with you to make this happen.

Your comments, questions, and suggestions for future issues are welcome. We look forward to hearing from you about our first issue.

Rita A. Bajura
Director, NETL

Editorial Board

Production Staff

**Carbon Sequestration Research in the Office of Science and Technology
at the National Energy Technology Laboratory**

Curt M. White (cwhite@netl.doe.gov; 412 386-5808)
Robert P. Warzinski (warzin@netl.doe.gov; 412 386-5863)
James S. Hoffman (jhoffman@netl.doe.gov; 412 386-5740)
Karl T. Schroeder (kschroeder@netl.doe.gov; 412 386-5910)
Daniel Fauth (fauth@netl.doe.gov; 412 386-4618)
U.S. Department of Energy
National Energy Technology Laboratory
P.O. Box 10940, Pittsburgh, PA 15236-0940

Introduction
The National Energy Technology Laboratory (NETL) is the nation's newest National Laboratory. It has campuses in Pittsburgh, PA, and Morgantown, WV. It is the premier DOE laboratory for fossil fuel research and has a history of more than 75-years of providing science-based, technological solutions to issues associated with the environmental, supply, and reliability constraints of producing and using fossil resources. Since 1993, researchers in the NETL's Office of Science and Technology (OST) have been performing carbon sequestration research. The OST research program has expanded in recent years as concerns about the impact of rising atmospheric CO_2 levels on climate and global ecosystems intensify. A Carbon Sequestration Science Focus Area has been established within OST to foster the development of the growing research program.

Carbon Sequestration Science is a relatively new field. It is remarkably broad-based, encompassing major parts of chemistry, physics, biological and geological sciences, as well as engineering, computational science, and other disciplines. The OST Carbon Sequestration Science Focus Area divides its effort into six major tasks, consisting of 16 individual projects that include 1) Capture and Separation (5 projects), 2) Geological Sequestration (7 projects), 3) Oceanic Sequestration (1 project), 4) Chemical Sequestration (1 project) , 5) Geological Sequestration Modeling (1 project), and 6) Process Modeling and Economic Assessment (1 project). Other major areas of Carbon Sequestration Science, such as sequestration in terrestrial ecosystems and biological sequestration, are not addressed in the OST work plans. A conscious, deliberate decision was made early in the planning stage to omit sequestration in terrestrial ecosystems from our efforts. OST intends to initiate work in biological sequestration in the future. The report, _Carbon Sequestration Research and Development_ (1), a road mapping document, was used as a guide to frame the overall approach to the work, and as a source to focus individual research projects on specific goals.

Task 1. Capture and Separation
The Capture and Separation task contains five projects that can be divided among those that use dry scrubbing (3 projects), and electrochemical pumping (1), as well as a project whose goal is to develop NETL's facilities to capture and separate CO_2 (1 project).   In addition to conducting research to capture and separate CO_2 from conventional flue gas, NETL is also investigating the

separation and capture of CO_2 from gasifiers. Projects within the Capture and Separation Task include the following:

CO₂ Scrubbing With Regenerable Sorbents
Novel Amine Enriched Absorbents for Capture
Sorbent Development PSA/TSA
Electrochemical Devices
Scoping Exercise: Capture Facility.

The objective of the project entitled *CO₂ Scrubbing With Regenerable Sorbents* is to identify potential regenerable sorbents that could be used for the capture of CO_2 from a gas stream and to validate a potential dry, regenerable sorbent process that is capable of removing CO_2 from a gaseous stream. The experimental approach taken in this research effort is to utilize a thermogravimetric analyzer (TGA) to track sorbent weight change as the material is exposed to gases under conditions representative of absorption or regeneration. Change in sorbent weight can be linked to the extent of chemical reaction, from which kinetic information can be extracted. Additionally, scaled-up experiments will be performed in a packed-bed reactor to complement the TGA study.

An experimental study was performed to evaluate the potential of alkali- and alkaline-earth metals for use as dry, regenerable sorbents for the capture of CO_2 from a gas stream. Thermodynamic analysis identified ranges of temperature for absorption and regeneration that would be thermodynamically feasible. Potassium carbonate is applicable for CO_2 capture at low absorption temperature (less than 145 °C), while calcium oxide is applicable for much higher absorption temperature (less than 860 °C).

Experiments were conducted in both a TGA reactor and a packed-bed reactor using sorbent fabricated from potassium carbonate supported on a high surface area activated alumina. Sorbent batches with potassium loadings (as potassium carbonate) of 12.2 and 17.1 weight percent were prepared for experimental evaluation. Chemical analyses indicated approximately one-third of the surface area was lost upon impregnation of the metal, but the potassium loading is uniform across the cross-section of the sorbent sample.

A typical weight/time curve for a TGA experiment is shown in Figure 1. This particular experiment used Batch #1 sorbent that was evaluated at an absorption temperature of 80°C. The sample is dried at 150°C in nitrogen for 3-4 hours, followed by humidification, and then CO_2 absorption. Some CO_2 is desorbed (physical sorption) upon removal of CO_2 as an input, and then humidification of the sample is ceased, resulting in additional weight loss as moisture desorbs from the sample as shown in Figure 1. The chemical equation for the capture reaction is shown in equation 1. Considerable time is required for the sample to achieve steady state during each particular phase of the experiment. The experiment depicted in Figure 1 lasted almost four days.

$$K_2CO_3 + CO_2 + H_2O \iff 2\,KHCO_3 \qquad\qquad \text{equation } [1]$$

The weight/time data from the TGA can be interpreted in several manners. Preliminary attempts were made to obtain the temporal rate of weight changes during absorption and desorption, but are not reported here. If such information could become available, then the information could be linked to kinetic rate law expressions. An overall capacity of the sorbent proved to be more reproducibly quantifiable. The sorbent capacity is based on the difference in weight, under humidified conditions, of the sorbent after all CO_2, which was physically sorbed, has been desorbed. In the example of Figure 1, the weight gain (from forming potassium bicarbonate) equaled 26 percent of the theoretical weight gain if all of the potassium carbonate was converted to potassium bicarbonate. Hence the sorbent capacity (i.e., utilization) is reported as 26%.

TGA experiments were typically conducted using a gas composition of 10 mole % CO_2, 10 mole % H_2O, with balance N_2. TGA results indicate CO_2 capture is favored at low absorption temperature (50-60 °C), with sorbent utilization strongly decreasing with higher absorption temperature (80-100 °C). Higher potassium loading on the sorbent did not provide additional benefit for CO_2 capture, as evidenced by lower sorbent utilization for the higher loaded sorbent. The sorbent was thermally regenerated at 150 °C, which is consistent with the predicted temperature based on thermodynamic analysis.

Task 2. Geological Sequestration
The Geological Sequestration task contains seven projects that encompass investigations of CO_2 sequestration in brine fields, in active and depleted oil and gas fields (including natural gas hydrates), and in coal seams. One project, entitled *Sequestration in Brine Fields, Oil and Gas Fields, and Natural Gas Hydrates* attempts to develop an understanding on a macro level of what occurs when large volumes of CO_2 are pumped into a geological formation; while another, entitled *An Investigation of CO_2/Water/Rock Interactions and Chemistry,* seeks to develop insight into what occurs on a chemical/mineralogical level. This project addresses the aqueous chemistry of CO_2 with brines and rock. With the United States Geological Survey's (USGS) Hydrothermal Laboratory as our partner, NETL is beginning to investigate the uncertainties associated with heterogeneous reactions that may occur with minerals and strata, as well as the uncertainties associated with the complex ionic equilibria and kinetics of CO_2/water/rock interactions. A second component of this project is concerned with developing a better understanding of low temperature, low pressure formation of carbonate minerals from brine reactions with CO_2 both in the presence, and absence, of rock. Projects within the Geological Sequestration Task include the following:

> *Sequestration in Brine Fields, Oil and Gas Fields, and Natural Gas Hydrates*
> *An Investigation of Gas/Water/Rock Interactions and Chemistry*
> *Chemistry of Carbon Dioxide Sequestration in Coal Seams*
> *Sequestration of CO_2 in Coal Seams and Production of Methane Therefrom*
> *Comprehensive Monitoring Techniques*
> *Scoping Exercise for a Geological Sequestration Simulation Facility (GSSF)*
> *Collection of Brines and Surrounding Strata.*

The injection of CO_2 into coal-seams to promote the production of coal-bed methane has recently become of considerable interest to the private sector and the U.S. DOE (1-3). By preferentially absorbing CO_2 onto the coal surface and displacing sorbed methane, this technology may

substantially increase methane production above the level achievable without injection of CO_2 (4). If such increases can be demonstrated, then favorable economics may make coal-seam injection one of the most attractive options for CO_2 sequestration.

The objective of the project entitled *Chemistry of Carbon Dioxide Sequestration in Coal Seams* is to obtain information useful for assessing the technical feasibility of CO_2 sequestration in coal-seams by defining those parameters that affect both the capacity of a coal-seam to adsorb CO_2 and the stability of the formation once formed. The work involves studying the interaction of a number of the Argonne Coal Samples (5,6) with CO_2 under different environmental conditions. The variables of interest are listed in Table 1. The goal is to provide data relating storage capacity and stability to coal and environmental properties, which can then be used as part of the evaluation of whether a candidate seam is appropriate for geologic sequestration. The Argonne coals have been especially prepared to be representative and reproducible from sample to sample. They were mined, ground, thoroughly mixed, and stored under nitrogen.

Gas-phase CO_2 adsorption isotherms were determined using a common manometric technique. The temperature and pressure were maintained at values below the critical temperature and pressure of CO_2 thereby maintaining gas-phase conditions. A reference-cell, contained within a thermostated bath ($\pm 0.1\ ^{o}C$), was pressurized to the desired level as indicated on a pressure transducer. The maximum pressure for any given isotherm was limited by the operating temperature and the condensation pressure of CO_2 at that temperature. A sample-cell of known void volume, which was also contained within the same thermostated bath, was pressurized from the reference-cell. Using the change in pressure in the reference-cell and accounting for the gas compressibility, the number of moles of gas transferred from the reference-cell was calculated. Similarly, the gas-phase moles of gas in the sample-cell after the gas transfer were calculated from the post-transfer sample-cell pressure. The missing moles of gas were attributed to adsorption onto (into) the coal.

n = (moles transferred from reference) - (moles in gas-phase in sample-cell)   equation [2]

The reference-cell was then pressurized to a higher pressure and the process repeated. The individual incremental gas adsorption values are summed to generate the adsorption isotherm in a step-wise fashion as shown in Figure 2. The adsorption isotherm for a given temperature is plotted with the total number of millimoles of carbon dioxide adsorbed per gram of coal (y-axis) as a function of the equilibrium sample-cell pressure (x-axis). After completing the experiment at one temperature, the temperature of the thermostated bath was raised, and the process repeated. From the temperature dependence of the adsorption isotherms, the isosteric heat of adsorption was calculated from the modified Clausius-Clapeyron equation:

$$\ln (P_2/P_1) = Q_{isosteric} (T_2-T_1) / RT_1T_2 \qquad \text{equation} [3]$$

In the pressure-temperature region studied, the CO_2 adsorption isotherms appear to be non-Langmuir, Figure 2, in that they fail to approach a limiting value at high pressures, as would be predicted by the Langmuir equation. The incremental amount of CO_2 that can be adsorbed by the coal drops off dramatically at higher pressures. For example, the amount of CO_2 adsorbed

during the application of the first 100 psi of CO_2 pressure (0-100 psia) amounts to 0.6 to 0.9 mmole per gram of coal, depending on the temperature. However, the additional amount of CO_2 adsorbed during the addition of the last 100 psi of CO_2 pressure (600-700 psi) amounts to less than an additional 0.1 mmole per gram. From a practical stand-point, this means that disproportionately higher pumping costs per pound of CO_2 will be incurred at higher sequestration pressures. The effect of increasing temperature is to decrease the equilibrium adsorption capacity of the coal. This is expected because higher temperatures increasingly favor the gas-phase due to the $T\Delta S$ entropy term in the free energy expression. This means that otherwise equivalent, but deeper, warmer seams will adsorb less CO_2 than more shallow, cooler ones. The isosteric heat of adsorption was calculated to be 4.85 ± 0.26 kcal per mole of CO_2 adsorbed. This is higher than the heat of vaporization of CO_2 in this temperature range which is only about 1.3 kcal/mol, even at the lowest temperature. It is, however, less than the 12 kcal/mole which has been measured in low-coverage experiments. Thus, it appears that in this case, the binding falls between simple pore-condensation and the higher energy adsorption of the more active sites. On the average, the strength of interaction is about the same as for a typical hydrogen bond (ca. 5 kcal/mol).

Task 3. Oceanic Sequestration
An important issue in determining the fate of CO_2 in the deep ocean is understanding the possible occurrence and impact of the CO_2 clathrate hydrate compound ($CO_2 \cdot nH_2O$; 6<n<8), hereafter referred to as hydrate, which can form in the ocean as discrete particles or as shells on CO_2 drops at depths below about 500 m (1). Theoretically, pure CO_2 hydrate particles should sink in the ocean (7). This would facilitate sequestration by transporting the CO_2 to even greater depths than used for injection. However, it has been previously demonstrated that hydrate particles will initially float if formed from a two-phase, liquid CO_2/seawater system, such as would be present in current direct injection scenarios (8). On the other hand, if the CO_2 is first dissolved in the seawater, this single-phase system produces a sinking hydrate upon reaching hydrate-forming conditions (9). If a hydrate shell formed on a CO_2 drop, it would retard the dissolution of the CO_2 into seawater and would therefore frustrate sequestration if the hydrate-encased CO_2 drops rise to shallower depths before dissolving (8). Finally, hydrate formation has recently been shown to rapidly occur in actual experiments in the ocean under the scenario where CO_2 is introduced at depths greater than 3000 m where the CO_2 is more dense than seawater and therefore sinks to the bottom (9). Rather than just forming a protective layer on a CO_2 lake, dynamic hydrate formation resulted in rapid expansion of the CO_2 mass. These examples show that understanding hydrate formation occurrences and processes is therefore critical to successful deployment of strategies to introduce CO_2 into the deep ocean in a manner that leads to long-term sequestration.

NETL is constructing a High-Pressure Water Tunnel Facility (HWTF) that will permit an accurate simulation of the ocean water column encountered by injected CO_2. In the HWTF a fluid particle, such as a CO_2 drop, is held in an observation section solely by a countercurrent flow of water or seawater. Screens or other restraining devices are not required. Such devices can impact hydrate nucleation and also have unnatural heat transfer characteristics relative to the open ocean. In the HWTF, specialized internal geometries and flow conditioning elements are used to modify the velocity profile in the observation section to provide both axial and radial stability of the fluid particle for extended periods. A generalized schematic of such a water

tunnel device is shown in Figure 3. This device is placed in a flow loop that provides recirculation of water through the system. For a positively buoyant object, the flow of water or seawater enters the top of the water tunnel and passes through a stilling section (not shown in Figure 3). At the end of the stilling section, a flow conditioning element is placed to provide the velocity profile required for radial stabilization of the buoyant object in the observation section immediately below it. The top flow conditioning element shown in Figure 3 represents a bundle of small tubes of different length. Various other configurations are possible. Increasing the length of the tubes in the center results in more head loss in this region and results in flow redistribution with the desired local velocity minimum in the center of the observation section of the water tunnel. The diameter of the observation section increases from top to bottom $(x2 > x1)$ which provides the downstream axial velocity drop required for axial stabilization. At the exit of the test section, another flow conditioning element may be used. In Figure 3, this lower element depicts another possible tube bundle shape that could be used. A final stilling section is located after the test section (again not shown in Figure 3). To stabilize a sinking fluid particle the system is essentially inverted. Design variables affecting the velocity profile in the observation section include the geometries of the conditioning elements and the divergent cone.

Task 4. Chemical Sequestration
OST's chemical sequestration portfolio is narrow and focuses upon one topic--mineral carbonation. This project attempts to form calcium and magnesium carbonates from minerals high in these metals, such as olivine and serpentine. Metal carbonates are desirable because they are benign, very stable and long-lived in the environment. Once these carbonate minerals are formed, they are appropriate for long-term unmonitored storage. Mineral carbonation can be defined as the reaction of CO_2 with non-carbonate materials to form geologically stable mineral carbonates, such as calcite ($CaCO_3$) or magnesite ($MgCO_3$).   Drawing on mineral carbonation to reduce CO_2 emissions has a myriad of potential advantages. First, mineral carbonation mimics the natural weathering of rock. Mineral carbonates, the principal product of the process, are known to be stable over geological time (millions of years).   For this reason, mineral carbonation ensures permanent fixation rather than temporary storage of CO_2. Second, Mg-rich silicates, especially serpentines, already exist in readily minable deposits/outcrops in quantities far in excess of that needed to carbonate all anthropogenic CO_2 that could be emitted from the world's fossil fuel reserves. Finally, the silicate mineral carbonation reaction is strongly exothermic, providing clear energy and process cost advantages. NETL has been conducting a series of mineral carbonation tests at its Pittsburgh, PA facility over the past 2 years as part of a Mineral Carbonation Study Program within DOE. Other participants in this program include Los Alamos National Laboratory, Arizona State University, and Albany Research Center.

We have studied the effect of NaCl (i.e., 0.5 M Na_2CO_3/0.5 M $NaHCO_3$, and different concentrations of NaCl) on the extent of reaction utilizing an olivine sample, a non-hydrous magnesium silicate, from the Twin Sisters Range, Washington, USA. Each carbonation reaction was conducted using a continuously stirred tank reactor (CSTR) under identical conditions: T= 185° C; P_{CO_2} = 115 atm; time = 3 hours.   The initial test was performed in a sodium carbonate/sodium bicarbonate only solution (0.5 M Na_2CO_3/0.5 M $NaHCO_3$) whereas the two remaining tests were performed employing the identical sodium carbonate/sodium bicarbonate solution along with 1.0 M NaCl and 2.0 M NaCl additions, respectively.

The relationship between NaCl concentration and extent of the carbonation reaction is depicted graphically in Figure 4. As shown, the solutions containing 2.0 M NaCl and 1.0 M NaCl had increased yields of carbonated product. The yields of magnesite ($MgCO_3$) were 80% for 2.0 M NaCl and 67% for 1.0 M NaCl. In comparison, the sodium carbonate/sodium bicarbonate solution only experiment produced a lower yield (i.e., 61%).

Mineral carbonation experiments utilizing a coal-derived Ca and Mg rich fly ash and a waste product obtained from the Dravo-Lime, Corporation, Pittsburgh, PA were also performed using a CSTR. Each carbonation test was conducted under identical conditions: T= 185° C; P_{CO2} = 115 atm; time = 3 hours, solution = 0.5 M Na_2CO_3/0.5 M $NaHCO_3$; 1.0 M NaCl. Duplicate carbonation experiments performed on the fly ash gave a 79% yield of carbonates, with calcite and dolomite being the principal products. Experiments conducted with the Dravo-Lime waste yielded a 50% conversion to calcite.

Task 5. Geological Sequestration Modeling
Advances in high-speed computing and improved understanding of chemical behavior and fluid flow in porous media permit the use of simulations and modeling as tools for designing, optimizing, analyzing, and better understanding of chemical and physical processes. The Geological Sequestration Modeling task will integrate computational science capabilities within the Carbon Sequestration Science Focus Area, and build upon the solid foundation of experimental research at NETL. It will complement and support the laboratory and field work, and will promote a more thorough understanding of the fundamental science we are seeking to provide. The major emphasis of the OST laboratory effort in the Carbon Sequestration Science Focus Area is on geological sequestration and capture technologies. Accordingly, a complementary suite of computational science capabilities will be developed in these areas as well. In FY01 and in future years, a holistic approach (consisting of laboratory and modeling and simulation studies conducted in concert) to acquiring the fundamental body of knowledge required to successfully take carbon sequestration to fruition will be undertaken.

Task 6. Process Modeling and Economic Assessment
Another essential element of this effort is an attempt to develop a thorough and accurate understanding of the costs and benefits of any new carbon dioxide separation and capture process technologies. In the Process Modeling and Economic Assessment task, evolutionary improvements to existing capture process designs will be sought, and the overall economics of various capture technologies will be evaluated. This work will be conducted outside of OST within the NETL's Process Engineering Division. NETL is developing models of existing carbon dioxide capture technologies such as those used in plants that employ monoethanolamine and the Selexol Process. Once modeled, the scientific and technological aspects of each process will be closely studied to determine if the most recent advances in science and technology could further improve their efficacy and economic viability if they were incorporated into the plant design.

Common Themes
Investigation of the chemical interactions between CO_2/water/rock is a constant theme throughout the Carbon Sequestration Science Focus Area. It permeates the Geological Sequestration, Oceanic Sequestration and Chemical Sequestration tasks, and pervades the

Geological Modeling task. Developing a comprehensive understanding of the formation of $Ca/MgCO_3$ by the reaction of CO_2 with minerals, or CO_2 with water to form carbonate anion, bicarbonate anion, and carbonic acid, and their subsequent reactions with minerals or brine, either above or below ground, is vital to much of the work. The kinetics of these reactions must be better defined. The interactions of CO_2 and seawater (brine) to form hydrates is the major emphasis of the work in the Oceanic Sequestration task.

Another common theme is the development of facilities and capabilities to permit NETL to perform state-of-the-art Carbon Sequestration Science R&D. Three projects are concerned with improving NETL's facilities and capabilities. Specifically, we are undertaking two scoping exercises. The first is directed at finalizing the design of a versatile facility to investigate novel and modified techniques for CO_2 capture from fossil fuel processing. The second scoping exercise is to plan and design a state-of-the-art facility where geotechnical properties of candidate sequestration strata and chemical reactions between CO_2, brine, oil, natural gas, coal, and associated strata can be investigated. The concept is to plan and design a research facility where geotechnical properties and chemical reactions can be investigated for a variety of geological formations into which CO_2 can be injected. The strategy is to produce a flexible Geological Sequestration Simulation Facility (GSSF). Similarly, NETL hopes to improve its ability to perform meaningful studies of sequestration in deep brine aquifers by acquiring brines and associated strata from five to ten potential deep aquifer sequestration sites scattered throughout the country. This will be performed in conjunction with the USGS.

REFERENCES
(1) *Carbon Sequestration Research and Development*, A U. S. Department of Energy Report, December, 1999. (http://www.ornl.gov/carbon_sequestration/).
(2) Byrer, C. W.; Guthrie, H. D. **1997**, "Assessment of World Coal Resources for Carbon Dioxide (CO_2) Storage Potential While Enhancing Potential Coalbed Methane," pp. 573-76 in *Greenhouse Gas Mitigation, Proceedings of Technologies for Activities Implemented Jointly*, held in Vancouver, Canada, May 26-29, eds. Reimer, P.W.F.; Smith, A.Y.; Thambimuthu, K.V. (Elsevier, Amsterdam, The Netherlands).
(3) Reznik, A. A.; Singh, P. K.; Foley, W. L. **1982**, *Enhanced Recovery of In-Situ Methane By Carbon Dioxide Injection: An Experimental Feasibility Study*, Chemical and Petroleum Engineering Department, University of Pittsburgh, Pittsburgh, PA (work performed for the DOE under Contract DE-FG21-80 MC14262).
(4) Dean, W. E.; Anderson, R. Y. **1978,** Salinity Cycles: Evidence for subaqueous deposition of Castile formation and lower part of Salado Formation, Delaware Basin, Texas and New Mexico, in Austin, G. S. Compiler, Geology and mineral depostis of Ochoan rocks in Delaware Basin and adjacent areas: New Mexico Bureau of Mines and Mineral Resources Circular 159, p. 15-20.
(5) Vorres, K. S. *Energy & Fuels* **1990**, *4*, 420-426.
(6) Haggin, J. *Chemical & Engineering News* **1988**, October 3, 29-32.
(7) Holder, G. D.; Cugini, A. V.; Warzinski, R. P. *Environ. Sci. Tech.* **1995**, 29, 276-278.
(8) Warzinski, R. P.; Holder, G. D. *Proc. Int. Conf. Coal Sci.* **1997**, 3, 1879-1882.
(9) Brewer, P. G.; Friederich, G.; Peltzer, E. T.; Orr, F. M., Jr. *Science* **1999**, 2843, 943-945.

Table 1. Variables of Interest		
Parameters	**Values**	**Rationale**
pH	2	some thermal springs, water containing pyrite oxidation products
	6	bicarbonate buffered water
	9	sea water, high extreme
Salinity	0	Low extreme
	30 g/L NaCl	Seawater
Gas	CO_2	Pure sample
	Combustion gas	"dirty" sample
Temperature(C)	15,25,35,45	Range of geologic sequestration, determination of binding energies
Pressure (atm)	1,50,100,150	Range for geologic sequestration

Figure 1. Typical TGA experiment (Batch #1 sorbent @ 80C absorption).
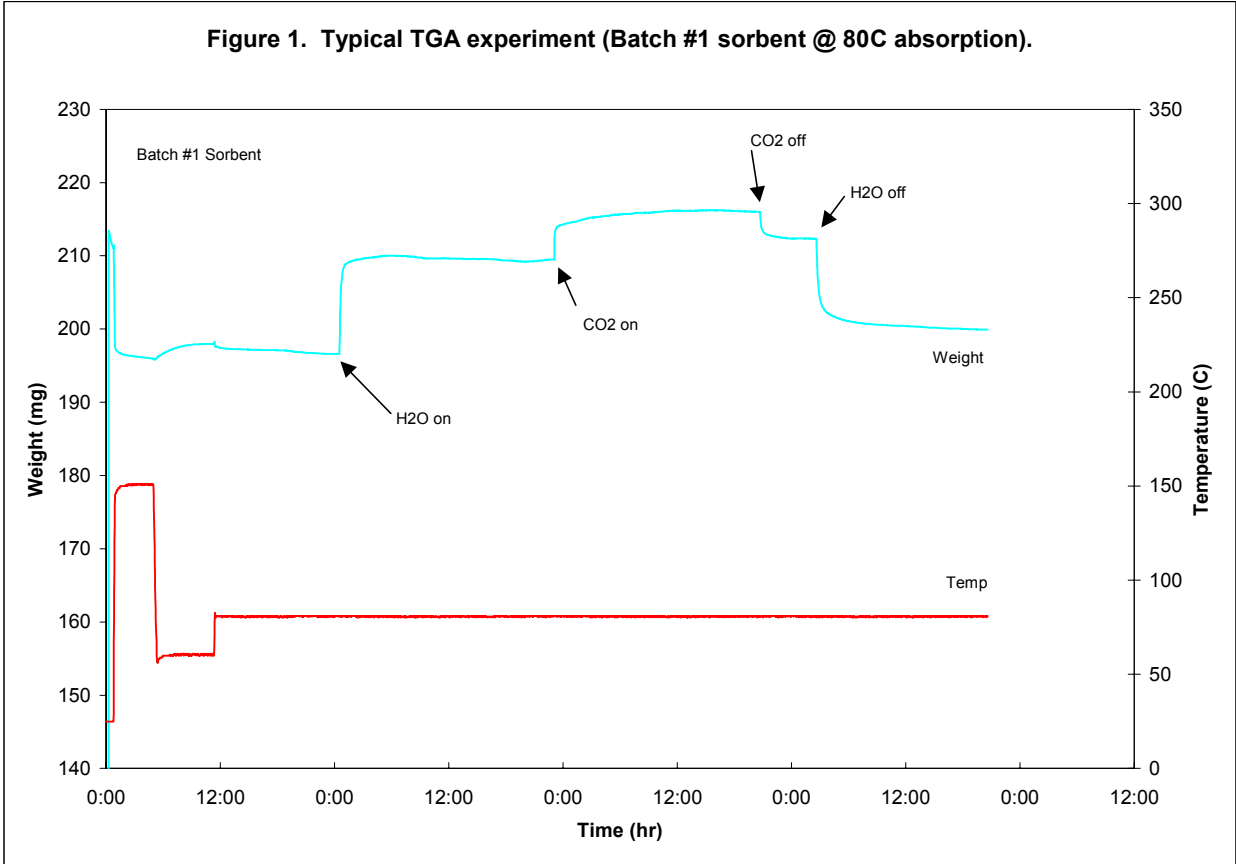
**Figure 2. Temperature Effect on
CO2 Adorption of Upper Freeport Coal**
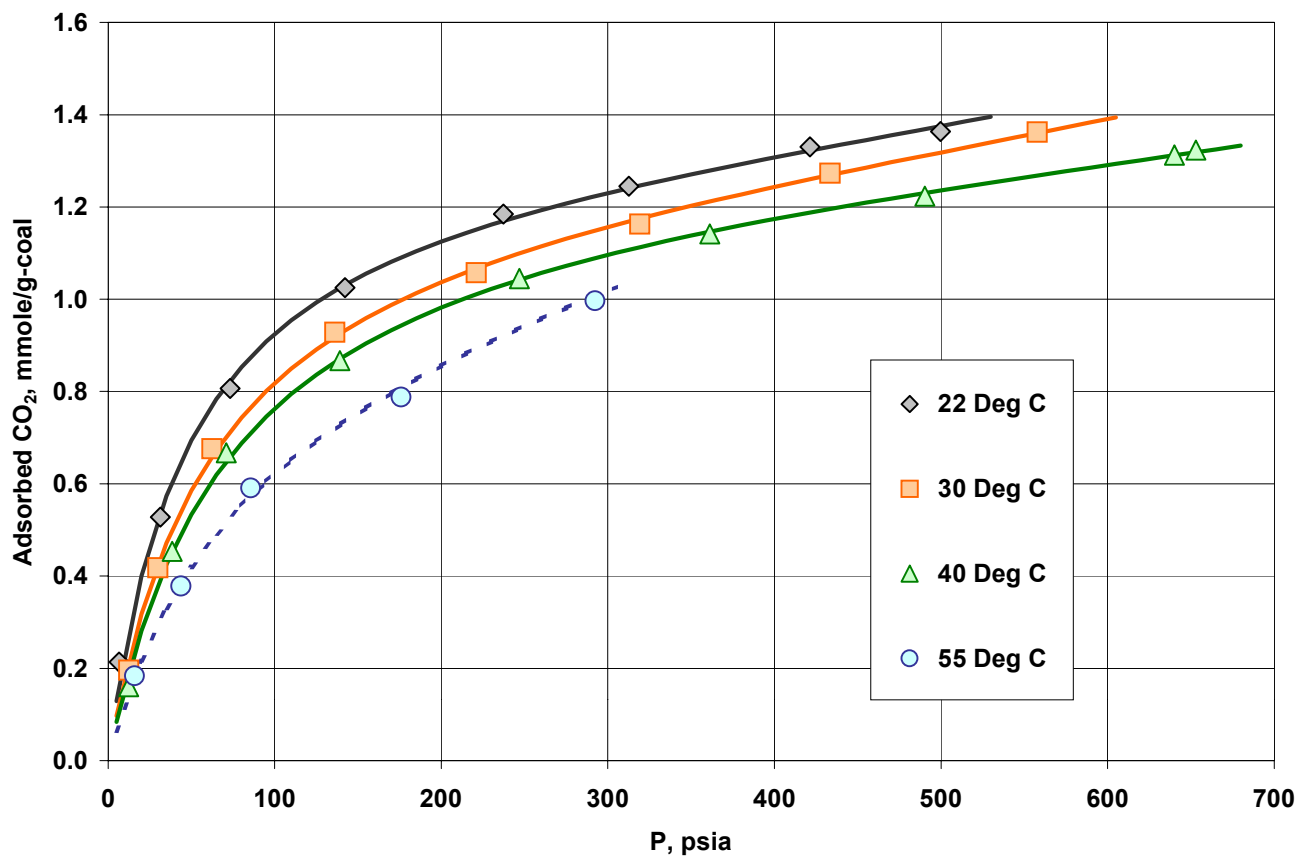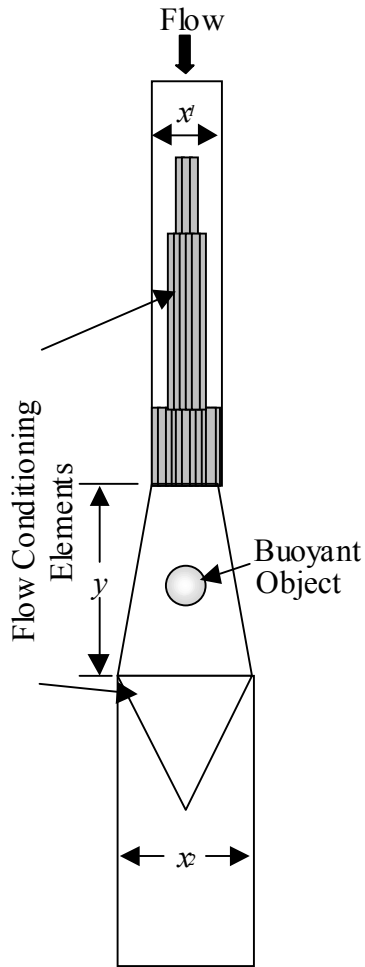
Figure 3. Schematic diagram of a water tunnel device

Figure 4. Effect of NaCl on Conversion
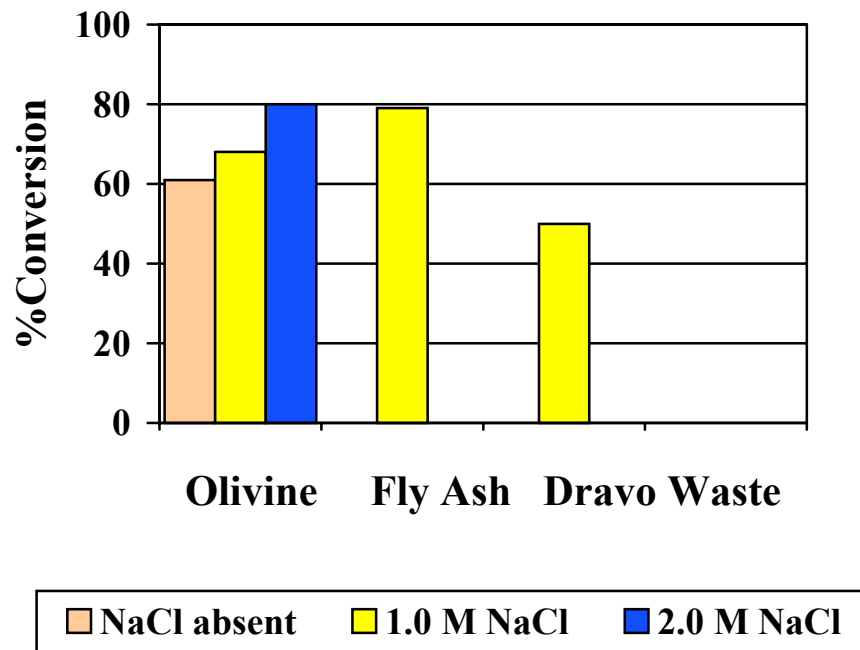
ADSORPTION AND DESORPTION OF CO$_2$ ON SOLID SORBENTS

Ranjani Siriwardane (rsiiw@netl.doe.gov; 304-285-4513)
Ming Shen (mshen@netl.doe.gov; 304-285-4112)
Edward Fisher (efishe@netl.doe.gov; 304-285-4011)
James Poston (jposto@netl.doe.gov; 304-285-4635)
Abolghasem Shamsi (ashams@netl.doe.gov; 304-285-4360)

U.S. Department of Energy, National Energy Technology Laboratory, 3610 Collins Ferry Road, P.O.Box 880, Morgantown, WV 26507-0880

INTRODUCTION

Fossil fuels supply more than 98% of the world's energy needs. However, the combustion of fossil fuels is one of the major sources of the green house gas CO$_2$. It is necessary to develop technologies that will allow us to utilize the fossil fuels while reducing the emissions of green house gases. Commercial CO$_2$ capture technology that exists today is very expensive and energy intensive. Improved technologies for CO$_2$ capture are necessary to achieve low energy penalties. Pressure swing adsorption (PSA) is one of the potential techniques that could be applicable for removal of CO$_2$ from high pressure gas streams such as those encountered in Integrated Gasification Combined Cycle (IGCC) systems.

PSA processes[1-4] are based on preferential adsorption of the desired gas (eg. CO$_2$) on porous materials at a high pressure. When the pressure is decreased, the gas is desorbed from the porous sorbent and the sorbent can be reused for subsequent adsorption. PSA technology has gained interest due to low energy requirements and low capital investment costs. Development of regenerable sorbents that have high selectivity for CO$_2$ and high adsorption capacity for CO$_2$ is critical for the success of the PSA process.

OBJECTIVE

The objective of this work is to understand the adsorption properties of CO$_2$ on molecular sieves and activated carbon[5] that can be utilized in PSA processes. In this work adsorption and desorption of CO$_2$ was studied on three sorbents namely molecular sieve 13X, natural zeolite ZS500A and activated carbon. Volumetric adsorption and desorption studies of CO$_2$, N$_2$, O$_2$ or H$_2$ with the three sorbents were conducted at 25 ^{0}C up to a pressure of 300 psi (~2x 10^6 Pa). Competitive gas adsorption studies were also conducted with CO$_2$ containing gas mixtures in the presence of water vapor.

APPROACH

Zeochem-Z10-02/13X molecular sieve and activated carbon sorbents were obtained from Sud Chemie. Natural zeolite GSA ZS 500A was obtained from GSA Resources. Adsorption and

desorption isotherms at 25 ^{0}C of pure CO_2, N_2, O_2 and H_2 on molecular sieve 13X and activated carbon were measured up to an equilibrium pressure of about 300 psi (~2x 10^6 Pa) utilizing a volumetric adsorption apparatus. Approximately 10 ml of the sorbent materials were placed in the sample chamber, which was evacuated to ~ 5x10^{-5} Torr. The amount of CO_2 adsorbed was calculated utilizing the pressure measurements before and after the exposure of the sample chamber to CO_2. Desorption studies were conducted by gradually decreasing the pressure from 300 psi after the adsorption cycle. After each cycle the sorbent was evacuated overnight. Competitive gas adsorption studies were conducted in lab scale fixed bed reactors at 14.7 psi and 250 psi using a gas mixture with a composition of 15%CO_2, 82%N_2, 3% O_2.in the presence of water vapor at ambient temperature. The samples were heated at 100 ^{0}C for one hour and cooled down to ambient temperature before the introduction of the gas mixture.

RESULTS AND DISCUSSION

Volumetric adsorption isotherms of CO_2, N_2, O_2 and H_2 on molecular sieve 13X at 25 ^{0}C are shown in Figure 1. The CO_2 adsorption increased rapidly when the pressure was increased up to 50 psi but the CO_2 adsorption after 50 psi appeared to be gradual. At all pressures, adsorption isotherms of nitrogen were lower than those of CO_2, and adsorption isotherms of hydrogen were significantly lower than those of CO_2. Preferential adsorption of CO_2 indicates that this material can be used for separation of CO_2 from some gas mixtures. The adsorption and desorption isotherms of CO_2 on molecular sieve 13X are also shown in Figure 1. The adsorption and desorption isotherms were very similar. This indicates that the adsorption of CO_2 on molecular sieve 13X is reversible. So the adsorbed CO_2 can be recovered by lowering the pressure.

The results of the competitive gas adsorption studies conducted utilizing a gas mixture of 15%CO_2, 82%N_2, 3% O_2 and water vapor on molecular sieve 13X in the atmospheric micro reactor are shown in Figure 2. The gas mixture was introduced to 1g of molecular sieve 13 X at a flow rate of 15 cc/min and at 25 ^{0}C. After the introduction of the gas mix to the molecular sieve 13X, the CO_2 concentration decreased to almost zero until the breakthrough. This indicates that an excellent separation of CO_2 can be obtained from a gas mixture of N_2, O_2, H_2O and CO_2 with molecular sieve 13X. The total amount of CO_2 adsorbed at the breakthrough or saturation as calculated from the data was about 3 moles/kg of the sorbent. This value is very similar to the amount of CO_2 adsorbed at 1 atm from volumetric equilibrium adsorption studies, as shown in Figure 1. This indicates that the full capacity of the molecular sieve 13X was utilized for CO_2 adsorption during competitive gas adsorption from a CO_2, N_2, O_2 and water vapor mixture. This indicated that the water vapor does not affect the adsorption of CO_2 on molecular sieve 13X.

The results of the competitive gas adsorption studies conducted utilizing 15%CO_2, 82%N_2, 3% O_2 and water vapor on molecular sieve 13X in the high pressure reactor are shown in Figure 3. The gas mixture was introduced to 1.3 g of molecular sieve 13 X at a flow rate of 19 cc/min, at 25 ^{0}C and at 250 psi. After the introduction of the gas mix to the molecular sieve 13X, the CO_2 concentration decreased to almost zero until the breakthrough. This indicates that an excellent separation of CO_2 from a gas mixture of N_2 and CO_2 can be obtained with molecular sieve 13X even at high pressure. The amount of CO_2 adsorbed per kg of the sorbent calculated from the data at breakthrough is about 6-7 moles/kg as shown in Figure 4. This is very similar to the amount of

CO_2 adsorbed at 250 psi from volumetric equilibrium adsorption studies, as shown in Figure 1. This indicates that the full capacity of the molecular sieve 13X was utilized for CO_2 adsorption during competitive gas adsorption at high pressure. There is some decrease in the CO_2 adsorption in the second cycle but the amount of adsorption was still very high. This sorbent may be suitable for separation of gases from high pressure gas mixtures.

The adsorption isotherms for activated carbon are shown in Figure 5. The CO_2 uptake for activated carbon was lower than that of the molecular sieve 13X at lower pressures, but at higher pressures (>100 psi) the CO_2 uptake for activated carbon was higher than that of the molecular sieves. The adsorption isotherm for activated carbon is also shown in Figure 5. The desorption isotherm was higher than that of the adsorption isotherm which indicated that the CO_2 is not fully desorbed during the desorption experiments. The hysteresis observed with activated carbon indicates that it is not possible to recover the adsorbed CO_2 by lowering the pressure. However, the activated carbon can be fully regenerated by evacuating the sample to $5x10^{-5}$ Torr.

When the competitive gas adsorption studies were conducted utilizing 15%CO_2, 82%N_2,3% O_2 and water vapor on activated carbon (0.5g) in the atmospheric reactor, it was necessary to use a lower flow rate (5 cc/min) for the adsorption of CO_2. After the introduction of the gas mix to the activated carbon, the CO_2 concentration decreased to almost zero and remained until the breakthrough. However, CO_2 uptake (1.1-1.2 moles/kg) at breakthrough was considerably lower in the presence of water vapor and oxygen in the gas mixture. The results of the gas adsorption studies with activated carbon (0.73g at flow rate 19 cc/min) conducted at 250 psi utilizing the same gas mixture are shown in Figure 6. The CO_2 concentration only decreased to 2% after the introduction of the gases and uptake (4 moles/kg) was lower than that for the molecular sieve 13X as shown in Figures 6 and 7. The activated carbon showed lower CO_2 uptake during competitive gas adsorption studies than that was observed during the equilibrium adsorption studies.

Adsorption isotherms of CO_2, H_2, O_2 and H_2 on natural zeolite GSA ZS 500 A are shown in Figure 8. It is clear that there is preferential adsorption of CO_2 on this natural zeolite indicating that it is suitable for separations of CO_2 from gas mixtures. The desorption isotherm also shown in Figure 8, was similar to that of the adsorption isotherm. This indicates that there is no substantial hysteresis during desorption and CO_2 can be fully recovered during desorption. The results of the competitive gas adsorption studies conducted utilizing 15%CO_2, 82%N_2, 3% O_2 and water vapor on natural zeolite GSA ZS 500A in the atmospheric reactor are shown in Figure 9. The gas mixture was introduced to 0.846g of the natural zeolite in the atmospheric reactor at a flow rate of 5 cc/min, at 25 ^{0}C. The separation of CO_2 from the gas mixture was very good as shown in Figure 9. There is a substantial amount of CO_2 adsorbed (1.2 moles/kg) at breakthrough even though the amount is slightly lower than that was adsorbed during equilibrium adsorption.

CONCLUSIONS

All three sorbents, molecular sieves 13X, activated carbon, and natural zeolite showed preferential adsorption of CO_2 over nitrogen, oxygen and water vapor at all pressures up to 250 psi. The molecular sieve 13X showed better CO_2 uptake than the natural zeolite. Water vapor and oxygen did not affect the adsorption of CO_2 on molecular sieve 13X during competitive gas adsorption studies at both low and high pressures but activated carbon showed lower CO_2 uptake in the presence of water vapor and oxygen. A very high CO_2 uptake was observed with molecular sieve 13X during high pressure competitive gas adsorption studies.

REFERENCES

1. Skarstrom, C.W., U.S.Patent 2,944,627 (**1960**)
2. Guerrin de Montgareuil, P., and D. Domine, U.S. Patent 3,155,468 (**1964**).
3. Cheu, K., Jong-Nam, K., Yun-Jong, Y., and Soon-Haeng C., Fundamentals of Adsorption, Proc. Int.Conf., D. LeVan(ed), Kluwer Academi Publishers, Boston, Massachusetts, **1996**, 203-210.
4. Dong, F., Lou, H., Goto, M., Hirose, T., Separation &Purification Technology, **1990,** *15,* 31-40.
5. Siriwardane, R.V., Shen, M., Fisher, E.,and Poston, J. , Energy and Fuels (Accepted for publication in the March 2001 issue)

Figure 1
Sorption-Desorption Isotherms of Molecular Sieve 13X
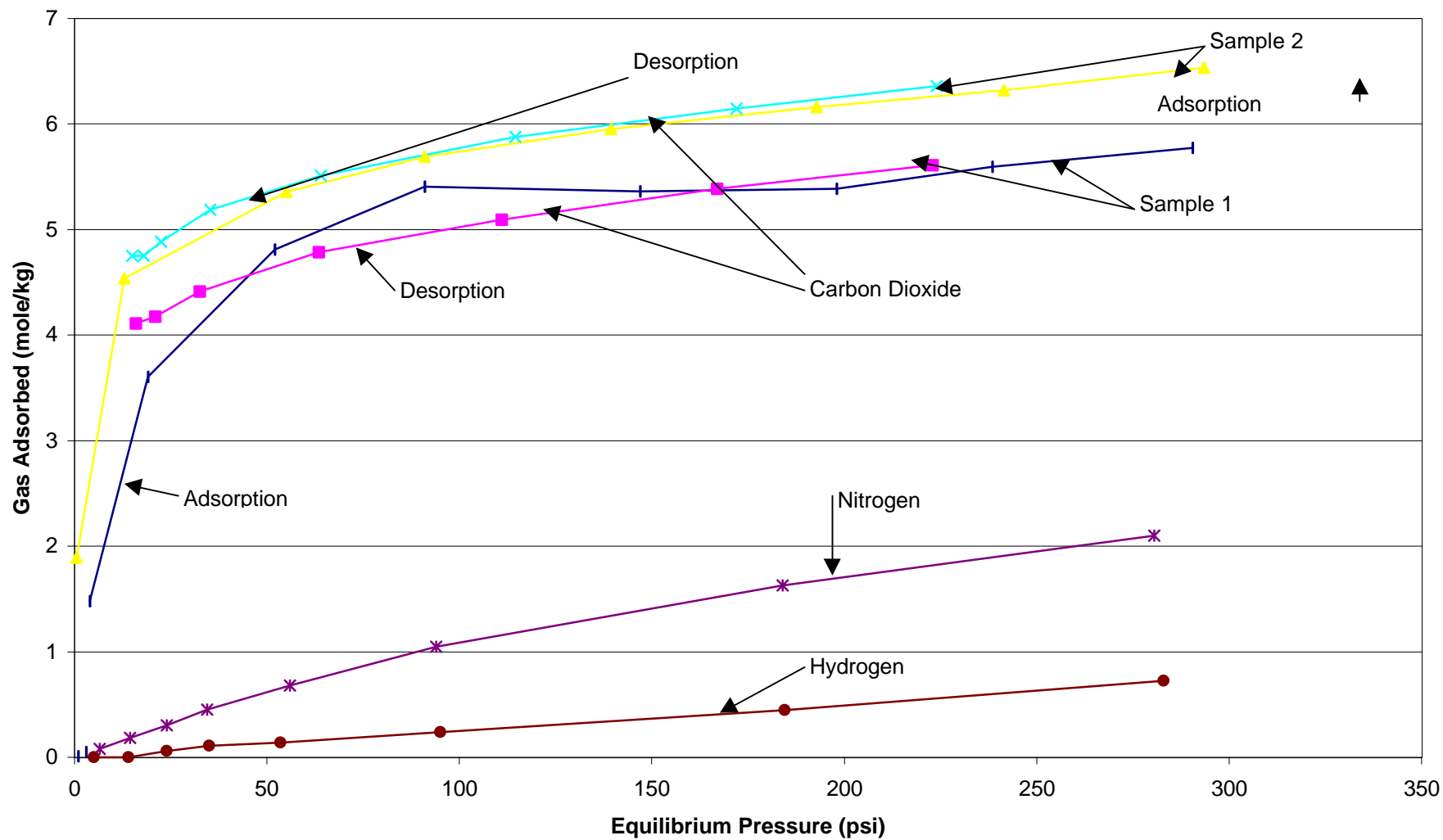
Figure 2
Adsorption of CO2, N2, and O2 on Molecular Sieve 13X in Atmospheric Reactor
(15% CO2, 3%O2, 82% N2, and saturated with water vapor at 25 C, 15 cc/min)
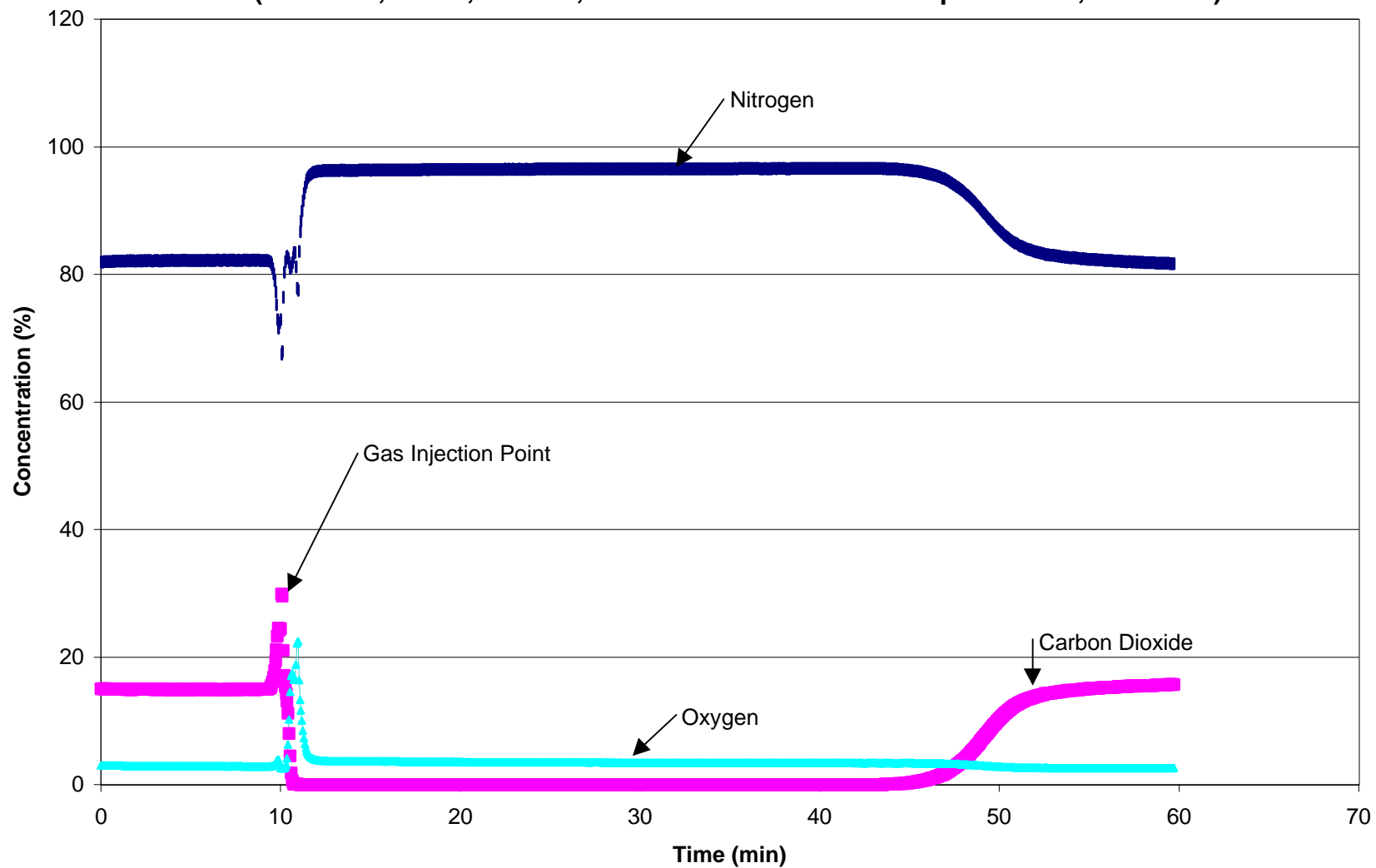
Figure 3

Adsorption of CO_2 on 13X at 22 ^{o}C, 250 psi

(15%CO_2, 82% N_2 and 3% O_2, and H_2O, 19.0 cc/min)
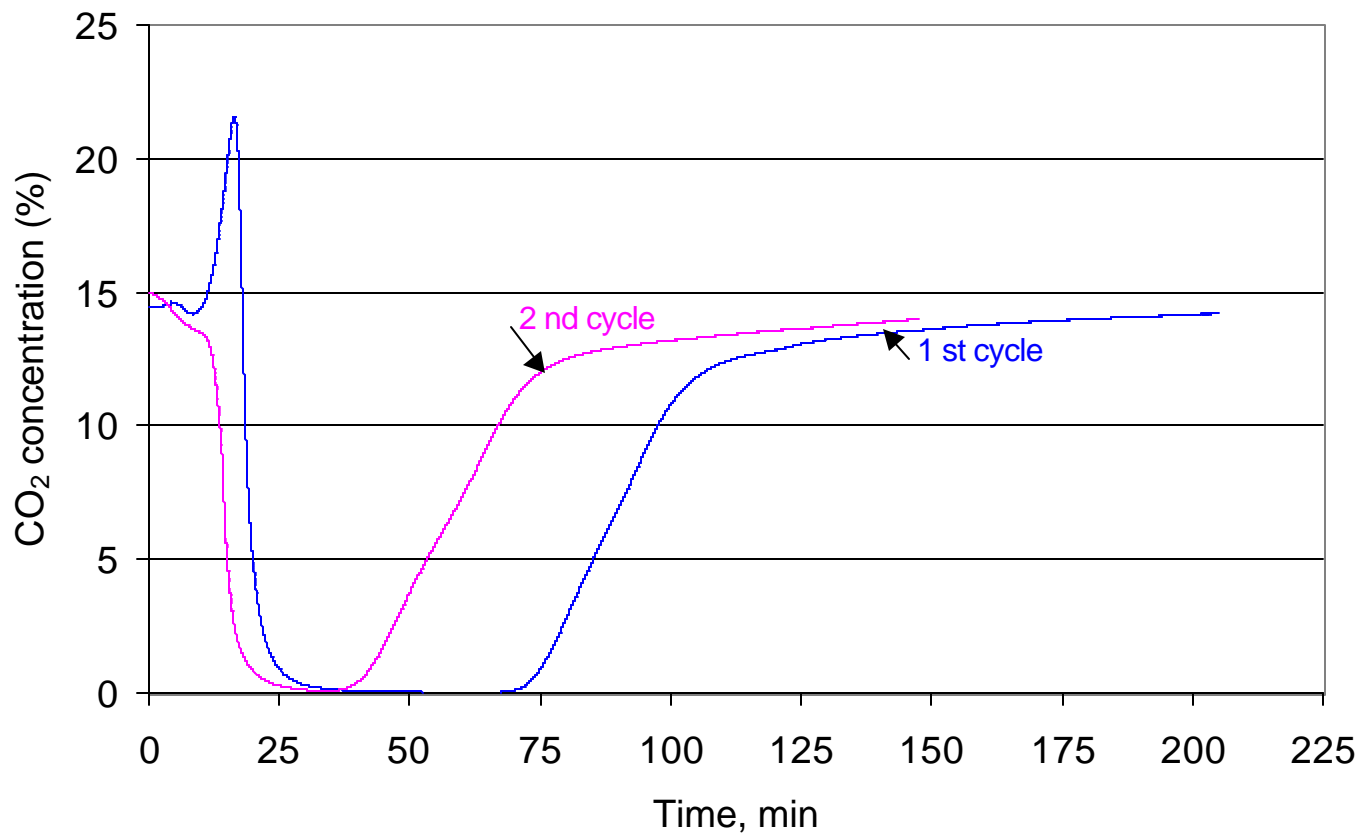
Figure 4

Adsorption of CO_2 on 13X at 22 ^{o}C, 250 psi
(15%CO2, 82% N_2 and 3% O_2, and H_2O, 19.0 cc/min)

Figure 5
Adsorption - Desorption Isotherms of Activated Carbon
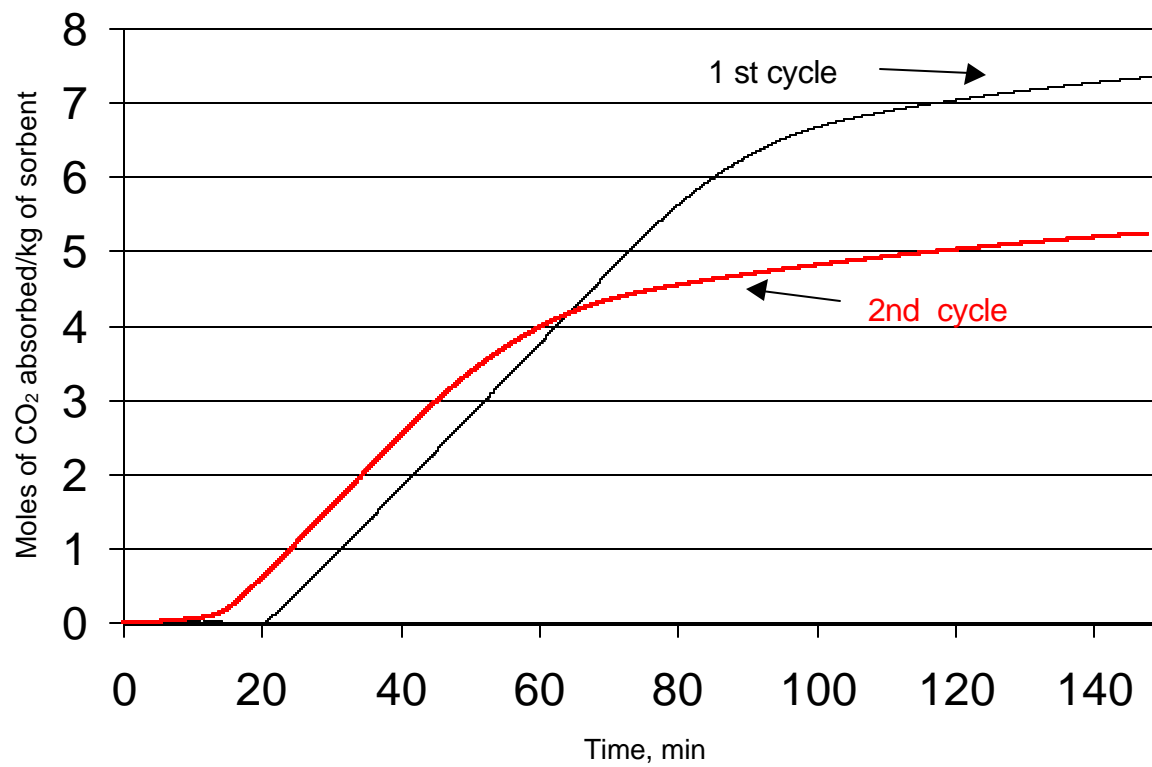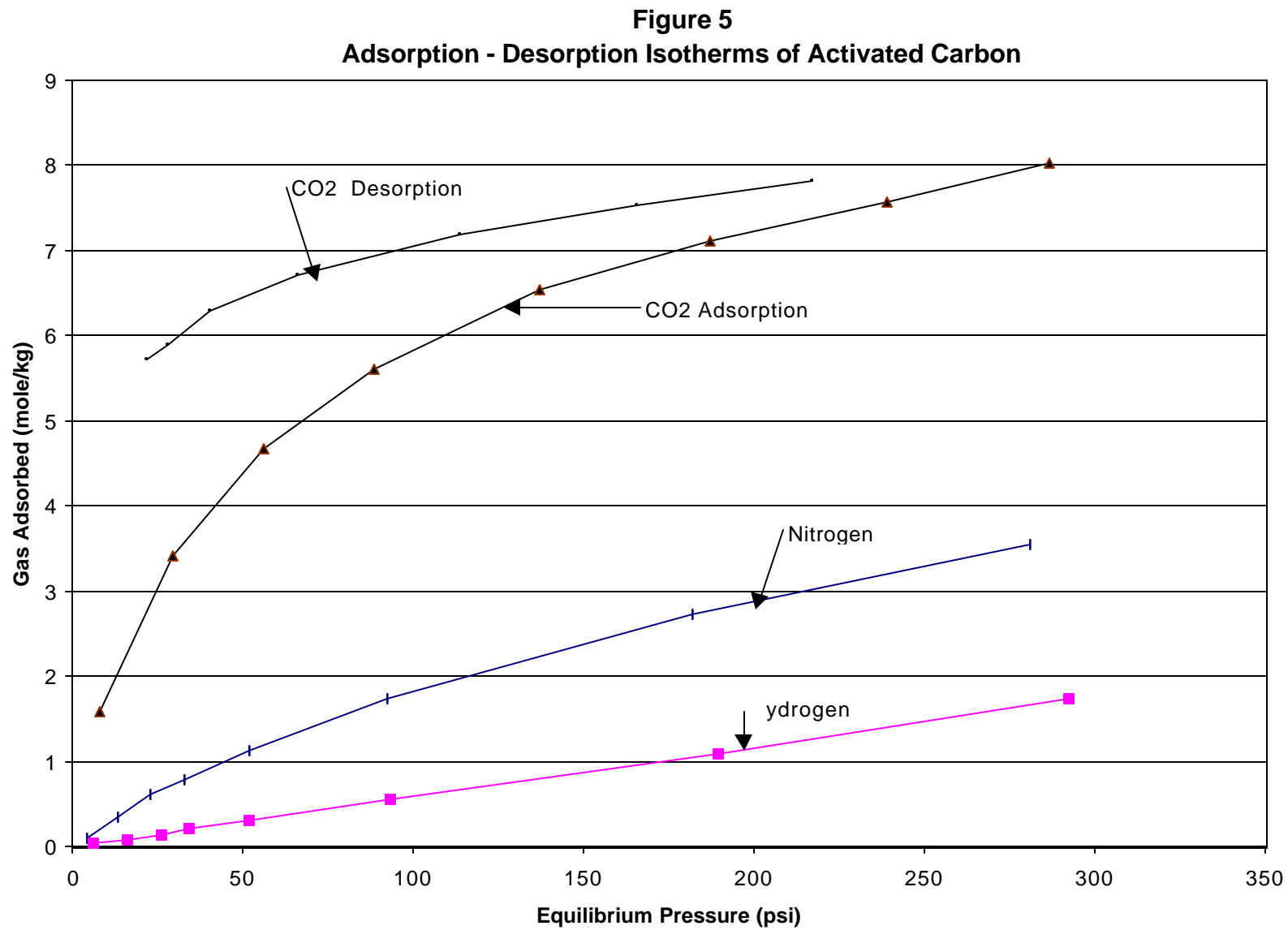
Figure 6.
Adsorption of CO_2 on activated carbon at 22 ^oC, 250 psi,
(15%CO_2, 82% N_2 and 3% O_2, and H_2O, 19 cc/min)
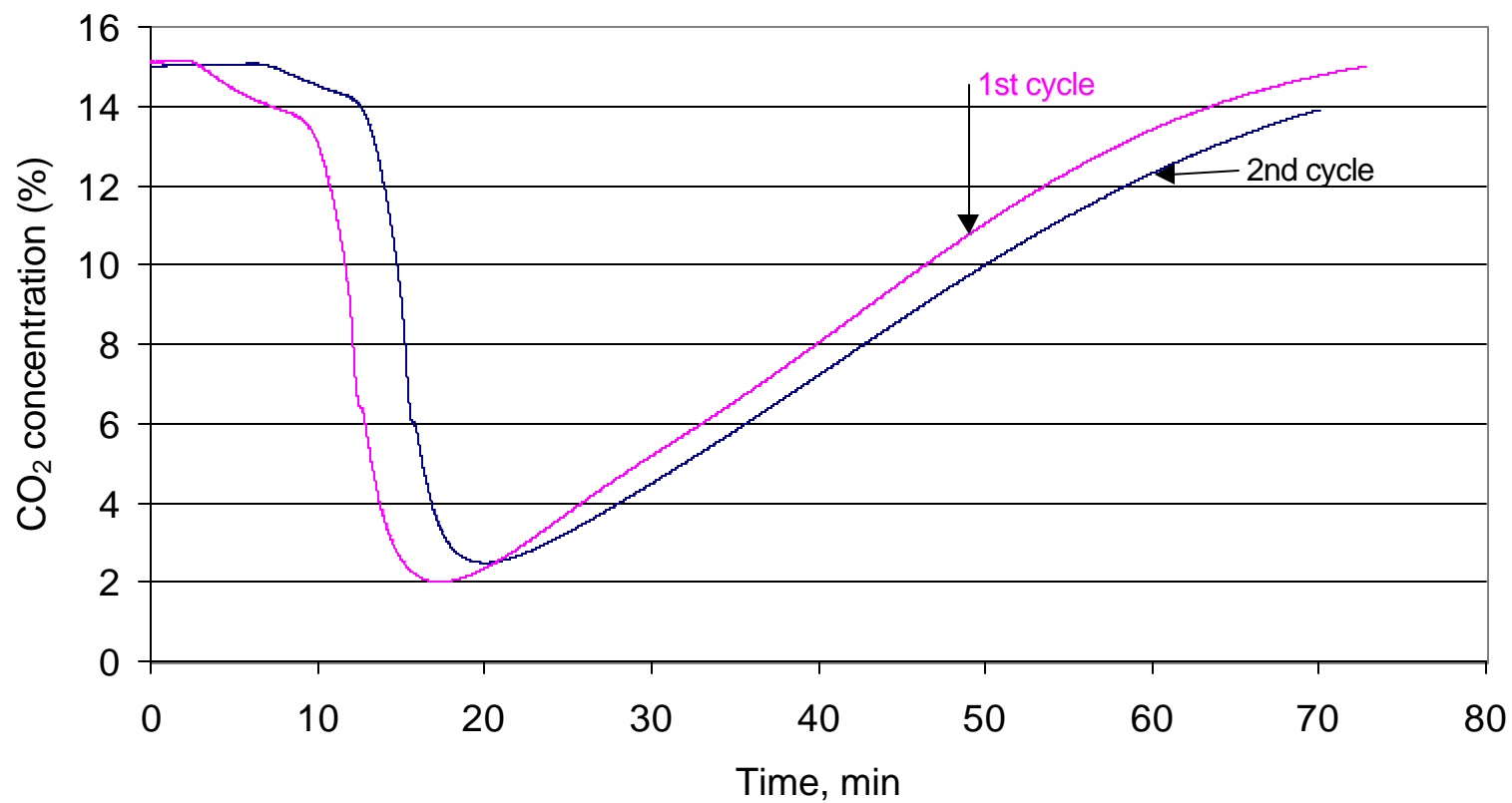
Figure 7.

Adsorption of CO_2 on activated carbon, 250 psi, 22 ^{o}C
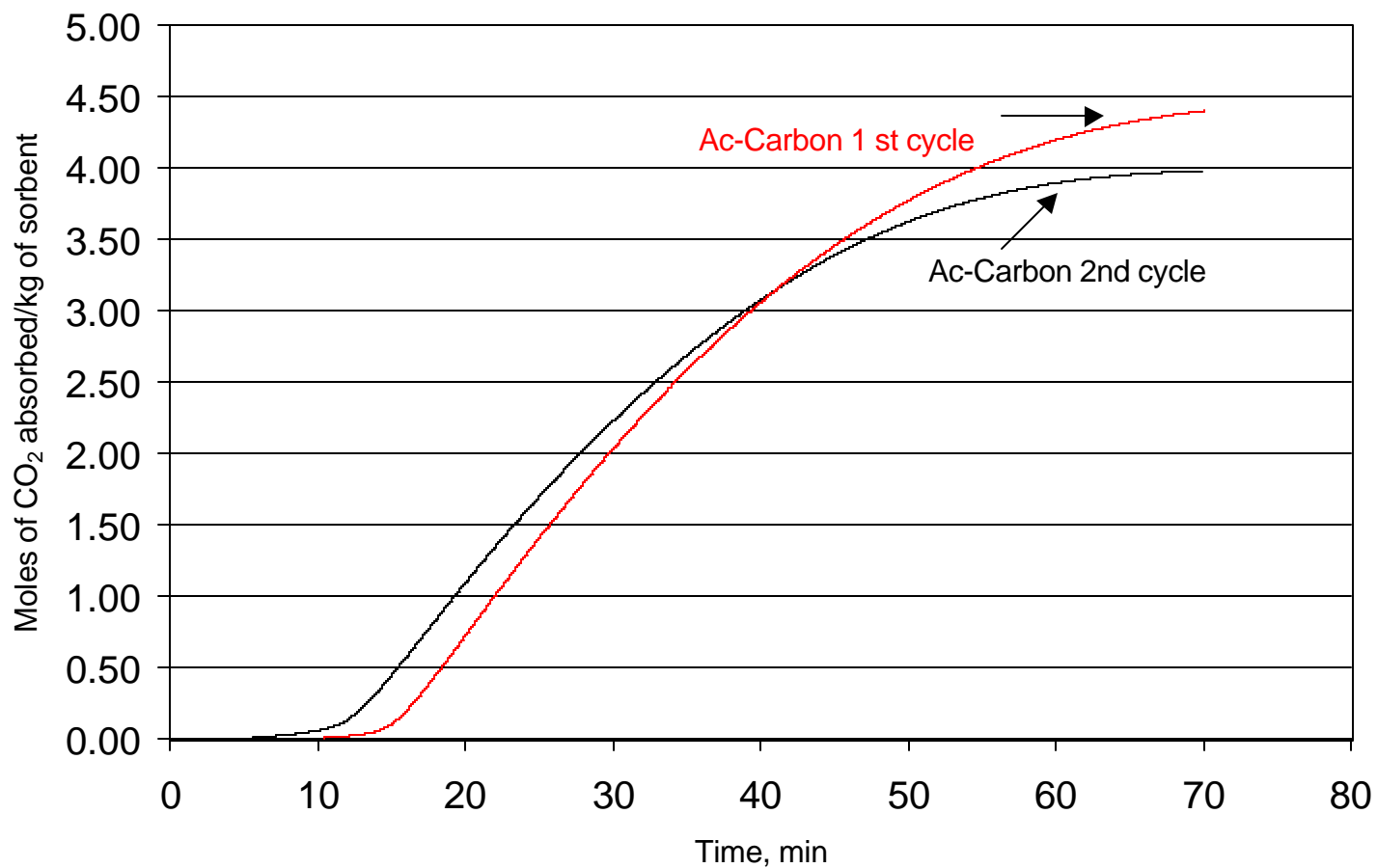
Figure 8
Adsorption-Desorption Isotherms of Natural Zeolite GSA ZS 500 A
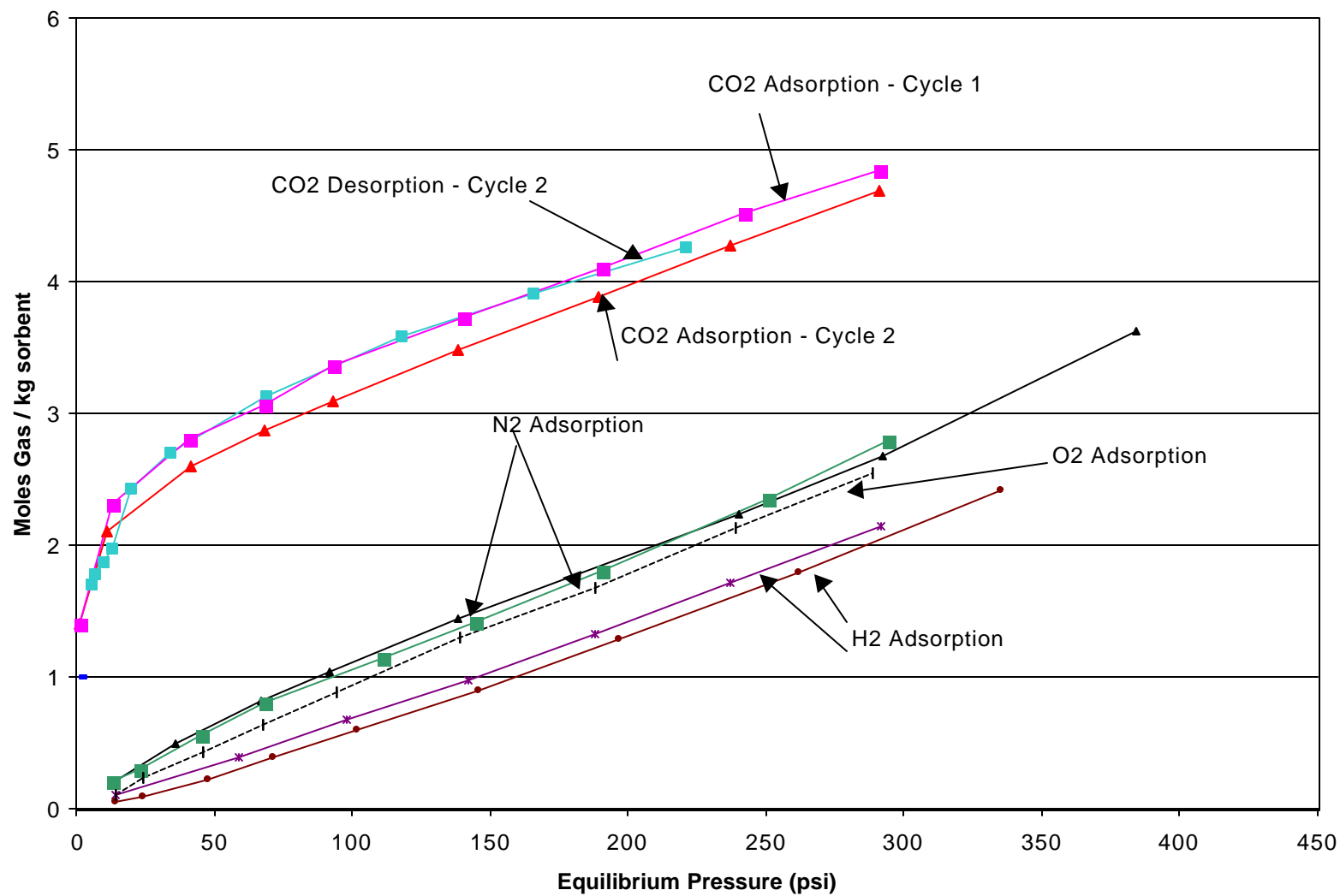
Figure 9
Adsorption of CO2, N2, and O2 on Natural Zeolite
GSA ZS500A (15% CO2, 3% O2, 82% N2 and H2O at 25 C)
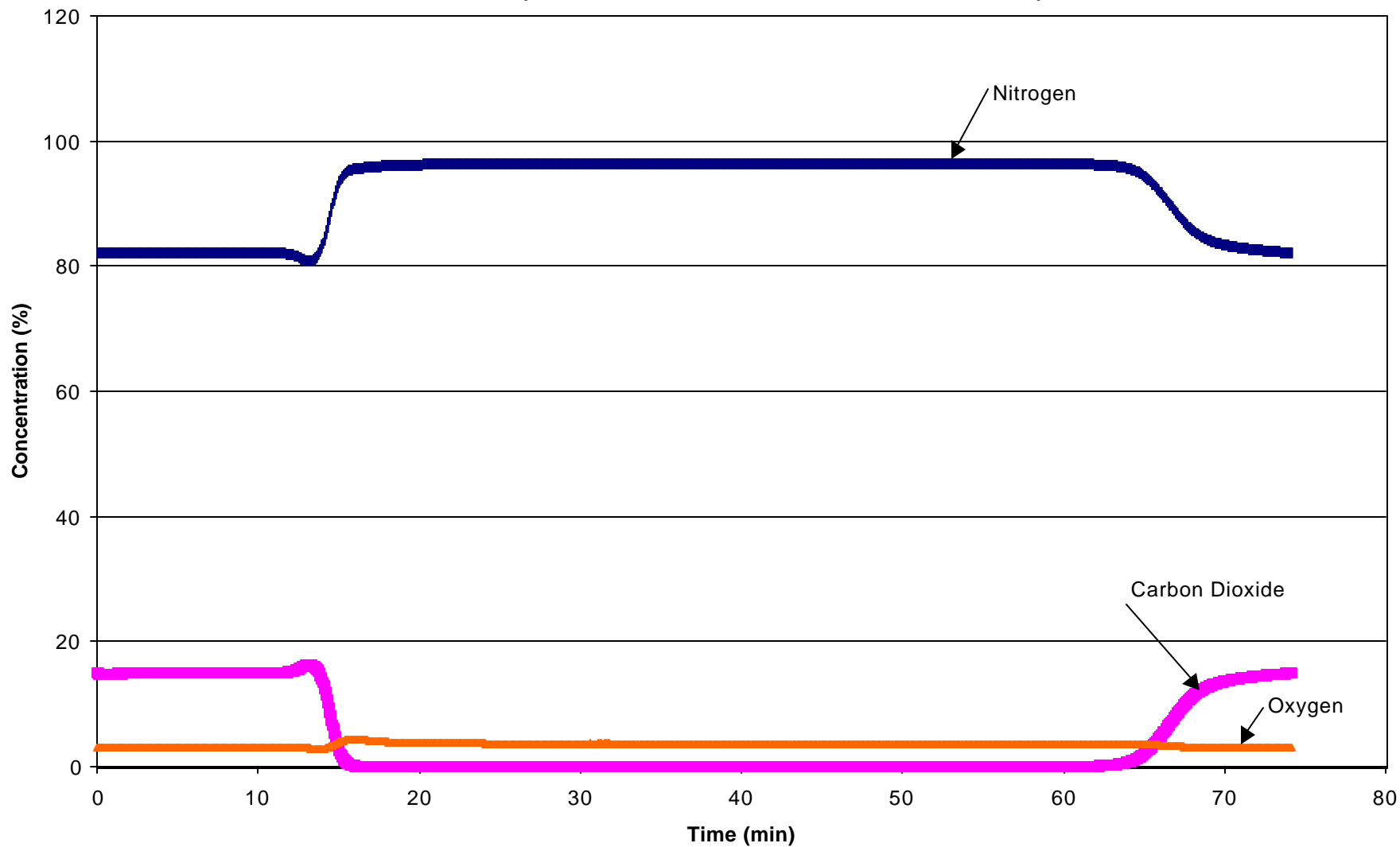
Degradation of Monoethanolamine Used in Carbon Dioxide Capture from Flue Gas of a Coal-fired Electric Power Generating Station

Brian R. Strazisar (strazisa@netl.doe.gov; 412-386-5988)
Richard R. Anderson (anderson@netl.doe.gov; 412-386-6143)
Curt M. White (cwhite@netl.doe.gov; 412-386-5808)

National Energy Technology Laboratory
Clean Air Technology Division
P.O. Box 10940
Pittsburgh, PA 15236

Introduction

The development of techniques for the separation and capture of CO_2 is considered to be one of the highest priorities in the field of carbon sequestration science. This is mainly because the capture cost is expected to make up about 75% of the total costs for geological or oceanic sequestration[1], with the other 25% going into transportation and injection costs. The technology for separation of CO_2 from flue gas or from other gaseous streams using chemical absorption has existed and been in use for decades.[2,3] To date, chemical absorption is the only technique that has been used commercially to capture CO_2 from flue gas. The general method involves exposing a gas stream to an aqueous amine solution which reacts with the CO_2 in the gas by an acid-base neutralization reaction to form a soluble carbonate salt:

$$2RNH_2 + CO_2 + H_2O \rightarrow (RHN_3)_2CO_3 \qquad [1]$$
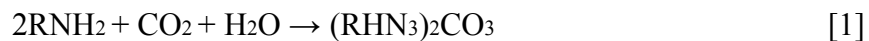
This reaction is reversible, allowing the CO_2 gas to be liberated by heating in a separate stripping column. Therefore, the major advantage to this technique is that, in the ideal situation, the amine is not consumed and may be continuously recycled through the process.

The amine used in this process is most commonly one of several alkanolamines including monoethanolamine (MEA), diethanolamine (DEA), methyldiethanolamine (MDEA), or diisopropanolamine (DIPA). The technology was originally developed not for the purpose of carbon sequestration, but in order to "sweeten" natural gas streams by removing CO_2.[4] More recently, it was successfully adapted for recovery of CO_2 from flue gas of coal-fired electric power generating plants.[5] In this case, rather than CO_2 sequestration, the CO_2 has been used for commercial purposes such as enhanced oil recovery and the carbonation of brine as well as food industry uses. Currently there are three electric power generating stations in the U. S. that capture CO_2 from flue and six

other major flue gas CO_2 capture facilities worldwide. All nine use MEA as the chemical sorbant.[6]

There is only one operation in the world that performs CO_2 separation for the purpose of sequestration. Statoil's Sleipner plant separates about 2,800 tons of CO_2 from a natural gas stream daily using chemical absorption and injects it into a saline aquifer below the North Sea.[7] This project was made economically attractive by a Norwegian tax based on CO_2 emissions. In order for current sequestration goals to be met, it may be necessary for many fossil fuel fired power plants to adopt similar capture and sequestration capabilities. Unfortunately, such a large scale CO_2 separation program would be cost prohibitive under the current state of technology. One possible solution is to improve upon the existing technology in a way that will decrease the cost.

A significant problem with the MEA absorption technique in its current form is the degradation of the amine over time. The byproducts of MEA degradation are known to decrease the efficiency of CO_2 capture. and have also been implicated in the corrosion of machinery[8] In order to compensate for this degradation, current facilities include distillation of the amine to remove byproducts while continuously adding fresh amine to the system. Unfortunately, this leads to increased material and waste disposal costs. In addition, degradation processes have forced the use of lower concentrations of MEA (<20%) leading to larger overall equipment size, higher solvent circulation rate, and therefore increased energy requirements for CO_2 regeneration from the rich amine.[9] This increased energy requirement is especially significant since it increases the parasitic load on the power plant leading to increased fuel consumption, higher maintenance costs, and (ironically) increased CO_2 production relative to the power output of the plant.

Using current technology, it has been estimated that CO_2 capture from fossil fuel-fired power plants for geological or ocean sequestration would increase electricity costs by 50%.[9] This does not include transportation and injection costs, which would increase the economic burden even further. It is clear that CO_2 separation technology based on chemical absorption could be improved by limiting or eliminating solvent degradation. It is crucial that we learn more about the processes that lead to solvent degradation. A clear understanding of the chemical processes involved under current conditions will be necessary in order to guide the development of improved solvents or technology.

Reactions of MEA with carbon dioxide[10,11] and with oxygen[12] have been well studied over the past 50 years. It is thought that CO_2 initiated degradation begins with the formation of 2-oxazolidone:

$$HO\diagdown\diagup NH_2 + CO_2 \rightleftarrows \quad \text{(2-oxazolidone)} + H_2O \qquad [2]$$
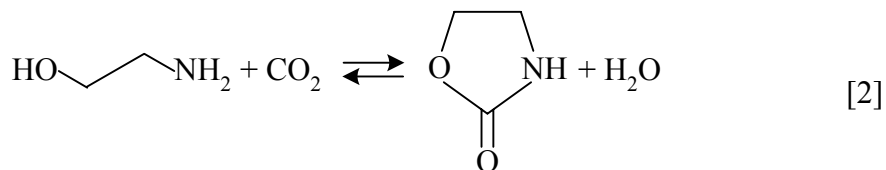
which can, in turn, react with another MEA molecule to form N-(2-hydroxyethyl)-ethylenediamine via intermediates of N,N′-di(hydroxyethyl)urea and 1-(2-hydroxyethyl)-2-imidazolidone:

[3]
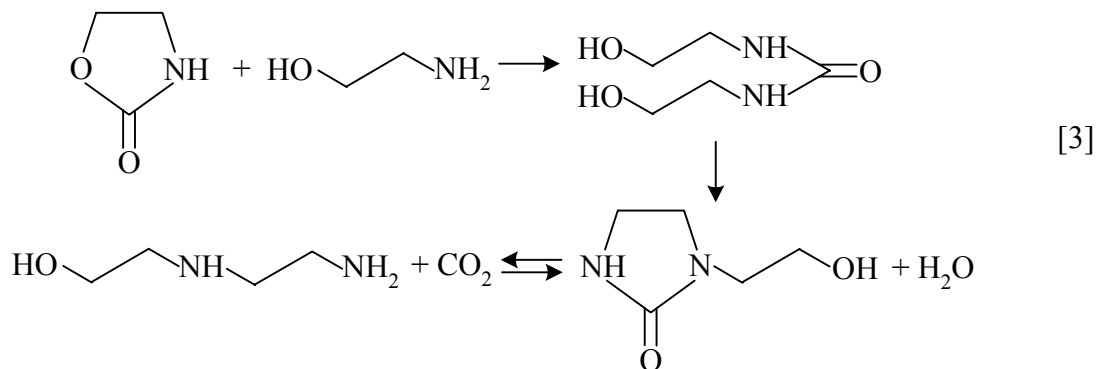
The majority of work that has been done in this area was aimed at understanding natural gas sweetening processes. However, in flue gas from a fossil fuel fired boiler, the process becomes much more complicated due to the presence of a mixture of CO_2, O_2, CO, SO_x, NO_x, and fly ash. The degradation process in this case remains poorly understood, particularly under conditions that are common to power plants.[13]

In order to begin to develop an understanding of how the degradation products are formed, the first step is to determine what the major products are under actual plant conditions. Once the formation mechanisms are elucidated, it may be possible to take steps to minimize them or prevent them from occurring.

Approach

The IMC Chemicals Facility in Trona, California is a plant that has been performing CO_2 capture from flue gas since 1978, longer than any other such plant in the world. CO_2 is separated from flue gas of a coal-fired boiler, which is used to produce electricity. In this case, the captured CO_2 is used for the carbonation of brine from Searles Lake, California for the commercial production of sodium carbonate.[5] For the current study, MEA samples were obtained from this plant in order to identify the degradation products from the CO_2 separation process. There were two samples obtained as well as a sample of the virgin concentrated MEA. The first sample was "lean" MEA. This is the material that is introduced to the absorption column where it is contacted by flue gas. The second was the reclaimer bottoms, which is the still bottoms waste that remains after the amine is distilled to remove the degradation products.

A variety of analytical techniques were used to characterize these samples. In order to identify the volatile organic compounds, the mixture was separated and analyzed using combined gas chromatography-mass spectrometry (GC-MS) and combined gas chromatography-Fourier transform infrared absorption spectrophotometry (GC-FTIR).

Two separate gas chromatographic columns were used for separation. The first was a 60 m × 0.32 mm i. d. fused silica column coated with a 0.25-μm film of 14%-(cyanopropyl-phenyl)-methylpolysiloxane (DB-1701 from J&W Scientific). This column was temperature programmed from 35 to 280°C at 1 C°/min. The second column, a 60 m × 0.25 mm i. d. column coated with 0.25-μm modified polyethylene glycol (Nukol™ from Supelco), was temperature programmed from 50 to 200°C at 5 C°/min. Helium carrier gas was used with initial linear velocities of 40 and 36 cm/s, respectively. In both cases, samples were introduced via a split injector held at 250°C. GC-MS experiments were done using an HP 5973 mass selective detector (MSD) and GC-FTIR experiments employed an HP 5965A infrared detector (IRD).

In addition, precise molecular masses of the organic compounds were obtained using low voltage high-resolution mass spectrometry (LVHRMS).[14] Mass spectra were acquired on a Kratos MS-50 high-resolution mass spectrometer. The ionizing voltage was set to about 11.5 electron volts in order to minimize fragmentation and therefore enhance detection of molecular ions. In this experiment, the samples were introduced to the ion source directly without prior separation.

Results

Since the focus of this study was on the MEA degradation products, the reclaimer bottoms sample, where these products were concentrated as a result of distillation provided the most important information. Portions of the total ion chromatograms obtained from GC-MS analysis of this sample on both the DB-1701 and the Nukol™ columns are shown in Figures 1 and 2, respectively. The numbered peaks are identified in table 1 along with the methods of identification. An "x" in the GC-MS or GC-FTIR column indicates a positive match from an electronic search of either MS or FTIR libraries. MS library searches were done using the NIST Mass Spectral Search Program for the NIST/NIH/EPA Mass Spectral Library.[15] FTIR searches were done using the FTIRsearch.com service.[16] The LVHRMS column indicates whether a match within 0.003 amu of the mass of the indicated molecule was present in the mass spectrum of the entire sample. Also included in Table 1 is an indication of which column or columns were used to detect each compound. The % of total area refers to the integrated peak area from the total ion chromatogram as a percentage of the total signal intensity for each column. Other than the MEA, none of the peaks shown in Figures 1 and 2 were present in identical experiments performed on the virgin MEA

The use of two separate GC columns (one intermediate and one polar stationary phase) was necessary due to the large variation in polarity of the degradation products, a result of the large number of heteroatoms present in the compounds. This is illustrated by the fact that each chromatogram (Figures 1 and 2) has some major peaks that are not present in the other.
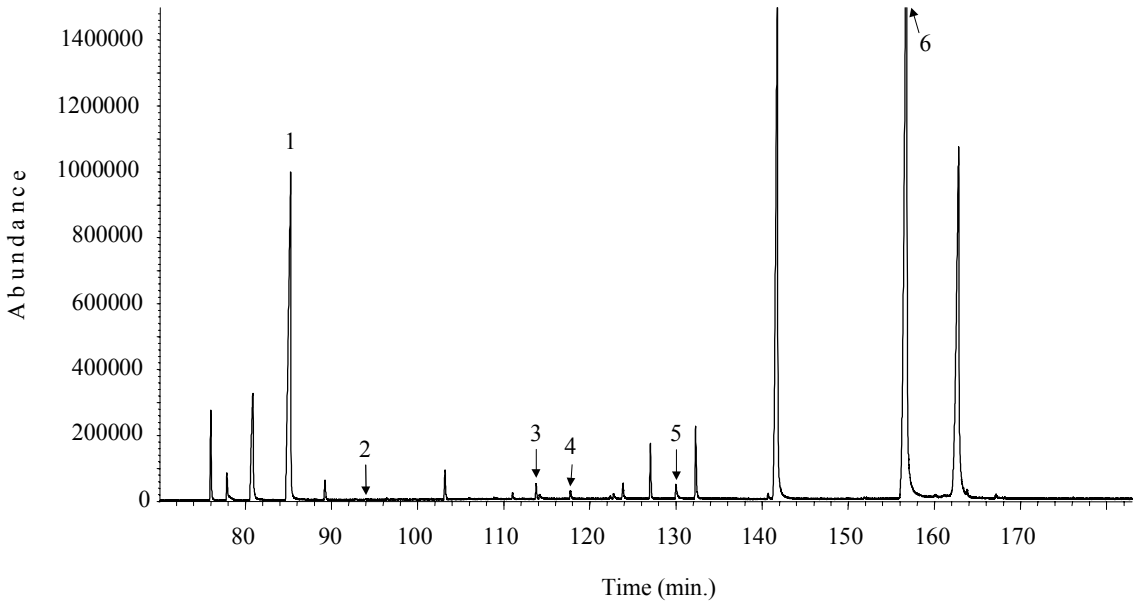
Figure 1. Portion of total ion chromatogram of the reclaimer bottoms sample obtained using the DB-1701 column. Numbered peaks are identified in Table 1. (MEA peak at 9.3 minutes not shown.)
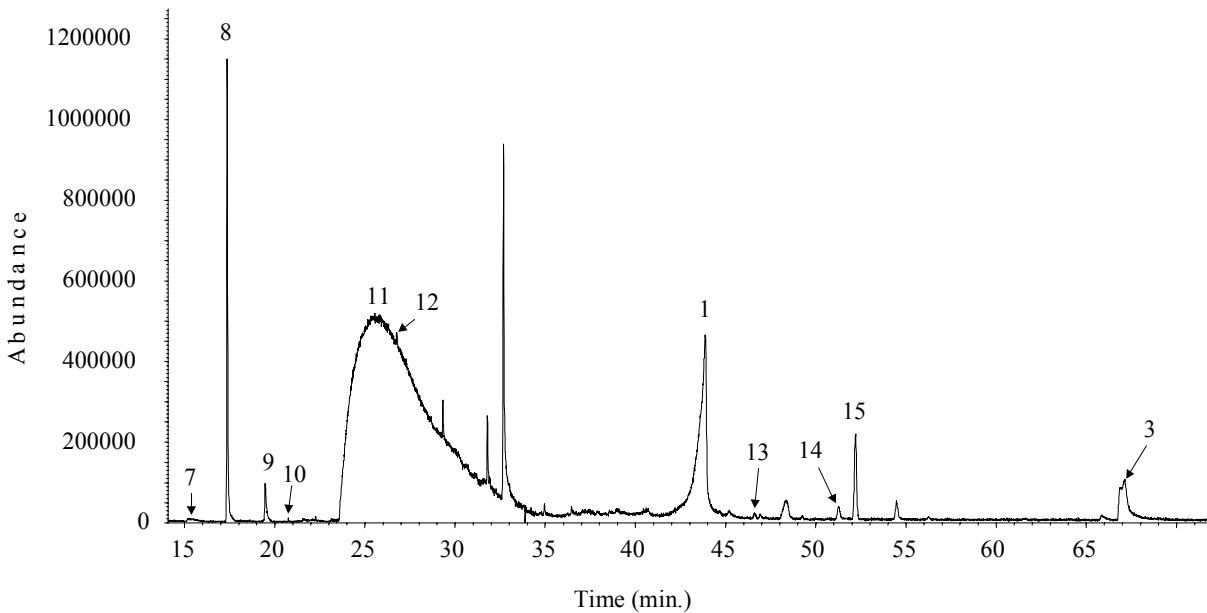
Figure 2. Portion of total ion chromatogram of the reclaimer bottoms sample obtained using the Nukol™ column. Numbered peaks are identified in Table 1.

Table 1. Identified compounds from monoethanolamine reclaimer from a CO_2 capture facility.

peak	compound	method of identification			GC column		%of total area	
		GC-MS	GC-FTIR	LVHRMS	DB-1701	Nukol	DB-1701	Nukol
1	N-acetylethanolamine ($C_4H_9NO_2$)	x		x	x	x	8.86	6.28
2	N-glycylglycine ($C_4H_8N_2O_3$)	x		x	x		<0.01	
3	N-(hydroxyethyl)-succinimide ($C_6H_9NO_3$)	x		x	x	x	0.16	*
4	N-(2-hydroxyethyl)-lactamide ($C_5H_{11}NO_3$)	x	x	x	x		0.07	
5	1-(2-hydroxyethyl)-2-imidazolidinone ($C_5H_{10}N_2O_2$)	x	x		x		0.24	
6	N,N-diacetylethanolamine ($C_6H_{11}NO_3$)		x	x	x		21.83	
7	ammonia (NH_3)	x				x		0.10
8	acetic acid ($C_2H_4O_2$)	x		x		x		2.02
9	propionic acid ($C_3H_6O_2$)	x				x		0.30
10	*n*-butyric acid ($C_4H_8O_2$)	x		x		x		0.01
11	monoethanolamine (C_2H_7NO)	x	x	x	x	x	*	35.18
12	2,6-dimethyl-4-pyridinamine ($C_7H_{10}N_2$)	x		x		x		0.05
13	2-imidazolecarboxaldehyde ($C_4H_4N_2O$)	x		x		x		0.05
14	1-methyl-2-imidazolecarboxaldehyde ($C_5H_6N_2O$)	x		x		x		0.17
15	2-oxazolidone ($C_3H_5NO_2$)	x		x		x		0.80

* Area percentage not calculated due to overlap with other peaks

Peaks 5 and 15 are known products of the degradation of MEA induced by CO_2 as shown in equations [2] and [3]. However, these are relatively minor components. The other two compounds from equation [3], N,N′-di(hydroxyethyl)urea and N-(2-hydroxyethyl)-ethylenediamine are not present at a detectable level. The largest identified peaks from MEA degradation products are due to N-acetylethanolamine and N,N-diacetylethanolamine (peaks 1 and 6), indicating that degradation may be dominated by a process other than simple reaction between MEA and CO_2. The acetic, propionic and butyric acid (peaks 8,9, and 10) are suspected to be present in the flue gas in small amounts as combustion products which may be captured by the MEA and may react with it. The acetylated MEA compounds show that reaction between acetic acid and MEA may be a major source of degeradation.

Future Activities

At the time of submission, positive identification of all of the major degradation products was not yet fully accomplished. In order to identify the remaining compounds as well as to provide further confirmation of the identity of the compounds listed on table 1, preparative GC will be used to isolate the compounds. Both proton and carbon-13 nuclear magnetic resonance (NMR) spectra may then be obtained for each as well as the single species LVHRMS. In addition, authentic standards of each identified compound will be obtained in order to verify gas chromatographic retention times under identical experimental conditions. The standards will also be used to determine response factors in order to calculate relative concentrations for each compound. This will provide a more complete picture of the organic MEA degradation products so that degradation pathways and mechanisms may be postulated.

The work described thus far has been aimed primarily at identifying organic molecular compounds in the MEA degradation samples. It is known that ionic species are also generated in alkanolamine degradation.[12] Identification of ionic species is currently in progress using ion chromatography (IC) as well as inductively coupled plasma emission spectrophotometry (ICP). The reclaimer sample also contained a solid residue that will be isolated and analyzed as well.

Acknowledgments

References

1. DOE report, DOE/SC/FE-1, "Carbon Sequestration Research and Development", (December, 1999).
2. R. R. Bottoms, U. S. Patent No. 1,783,901, Dec. 2, 1930.
3. A. S. Allen, U. S. Patent No. 1,934,472, Nov. 7, 1933.
4. R. N. Maddox, *Gas And Liquid Sweetening*, 2nd Ed. (Campbell Petroleum Series, Norman, OK,1974).
5. D. S. Arnold, D. A. Barrett, R. H. Isom, *Oil & Gas Journal* **80**(47), 130-136 (1982).
6. H. Herzog, "An Introduction to CO_2 Separation and Capture Technologies," Energy Laboratory Working Paper, Massachusetts Institute of Technology (August, 1999).
7. T. Hammerstad, "Carbon Dioxide Storage Prized," from www.statoil.com (2000).
8. M. S DuPart, T. R. Bacon, D. J. Edwards, *Hydrocarbon Processing*, 75-80 (April 1993).
9. C. L. Leci, *Energy Convers. Mgmt*. **38**, S45-S50 (1997).
10. L. D. Polderman, C. P. Dillon, A. B. Steele, *Oil & Gas Journal* **54**(2), 180-183 (1955).
11. N. V. Yazvikova, L. G. Zelenskaya, L. V. Balyasnikova, *J. Appl. Chem. USSR* **48**, 699-702 (1975).
12. P. C. Rooney, M. S. DuPart, T. R. Bacon, *Hydrocarbon Processing*, 109-113 (July 1998).
13. A. Meisen, X. Shuai, *Energy Conserv. Mgmt*. **38**, S37-S42 (1997).
14. C. E. Schmidt, R. F. Specher, B. D. Batts, *Anal. Chem*. **59**, 2027-2033 (1987).
15. S. Stein, A. Levitsky, O. Fateev, G. Mallard*, The NIST Mass Spectral Search Program for the NIST/EPA/NIH Mass Spectral Library* Version 1.6, (National Institute of Standards and Technology, 1998).
16. *FTIRsearch.com* (Galactic Industries Corp. and Thermo Nicolet Corp.,2001).

Argonne National Laboratory
9700 S. Cass Avenue
Argonne, Illinois 60439

Life-Cycle Analysis of a Shell Gasification-Based Multi-Product System with CO_2 Recovery

Richard D. Doctor, John C. Molburg, Norman F. Brockmeier
Argonne National Laboratory

Lynn Manfredo, Victor Gorokhov, Massood Ramezan
Science Applications International Corporation

Gary J. Stiegel
DOE-National Energy Technology Laboratory

March 30, 2001

Life-Cycle Analysis of a Shell Gasification-Based Multi-Product System with CO$_2$ Recovery

Richard D. Doctor (rdoctor@anl.gov; 630-252-5913)
John C. Molburg (molburg@anl.gov; 630-252-3264)
Norman F. Brockmeier (nbrockmeier@anl.gov; 630-252-9984)
Argonne National Laboratory
9700 S. Cass Avenue
Argonne, Illinois 60439

Lynn Manfredo (manfredo@netl.doe.gov; 412-386-6839)
Victor Gorokhov (victor.a.gorokhov@saic.com; 703-676-7192)
Massood Ramezan (Ramezan@netl.doe.gov; 412-386-6451)
Science Applications International Corporation
P.O. Box 18689
Pittsburgh, Pennsylvania 15236

Gary J. Stiegel (stiegel@netl.doe.gov; 412-386-4499)
National Energy Technology Laboratory
P.O. Box 10940
Pittsburgh, Pennsylvania 15236

INTRODUCTION

The U.S. Department of Energy (DOE) is investigating CO$_2$ recovery from fossil-fuel cycles as a greenhouse gas mitigation strategy. Recognizing this, we used life-cycle analysis tools to compare two integrated gasification combined-cycle (IGCC) plant designs based on the Shell entrained-flow gasifier. One option, called the "co-product case," uses high-sulfur Illinois #6 coal to produce electricity and hydrogen (H$_2$) as energy carriers. At the same time, 90% of the carbon dioxide (CO$_2$) is recovered for disposal in geological storage or for use, such as enhanced-oil recovery (EOR). The second option, called the "base case," is a conventional IGCC power plant releasing CO$_2$ by combustion of the synthesis gas in a gas turbine. The life-cycle analysis task has been aided by use of LCAdvantage^{TM}. Process design has been aided by the use of the ASPEN© simulation for critical design areas. Special attention is paid to the transport issues for the CO$_2$ product, because transportation technology is a determinant of product specifications, which affect plant design. Separating and purifying the H$_2$ for fuel cell use should yield an impressive gain in overall process efficiency, offsetting the losses in efficiency from recovery and compression of CO$_2$ to supercritical conditions.

OBJECTIVE - LOW GREENHOUSE IMPACT GASIFICATION CYCLES

Plant Design Basis

The Shell (entrained-flow) coal gasification system has been selected as the basis for the co-product plant. The energy and environmental performances of the co-product plant are

compared with those of a base-case plant that also uses the Shell gasification technology but produces only electricity as a salable product. The base-case IGCC plant and the co-product plant are substantially different in design. The most significant common elements are the use of the Shell gasifier and the consumption of the same amount and type of coal. Principal features and differences are summarized in Table 1.

Shell Gasification-Based Combined Cycle with Hydrogen, Electricity and CO_2
Figure 1 presents an overview of some of the critical process areas of the co-product plant, clarifying the differences noted in Table 1. The plant is conceptually divided into five main plant areas. Each area consists of a set of related processes. The processes in turn are composed of equipment or unit operations and process streams connect these. A two-digit taxonomy has been adapted for consistency in referring to these plant elements. The first digit designates the plant area, while the second designates the process. Table 2 presents a summary and comparison of the plant performance for a Base Case integrated gasification combined-cycle plant (IGCC), the proposed plant and an IEA study.

Coal Mining, Coal Washing, Transportation and Preparation
Coal characteristics and the impacts of the coal-preparation circuit appear in Table 3. The mining, coal-sizing and washing circuits are considered integral to the design of the gasification system. An underground mine near Seeser Illinois supplies Illinois #6 coal using long-wall continuous mining feeds 4,967 tons/day of raw coal to a washing circuit employing a jig, two crushers, three screens, a centrifuge and a thickener. This provides a more uniform product in the 5 x 1.5 in. size range with considerable reduction of the ash and modest reductions of pyritic sulfur. Employing this washing circuit shows a considerable advantage in reducing the tonnage of coal shipped by rail to the plant because the mining operation brings in roof and floor material. Calculations show that 81% of the energy from the raw coal reaches the product. At the same time, only 65% of the original tonnage of coal needs to be transported and handled. We have assumed that cleaning plant refuse is returned to the mine. The water use is 11.3 gallons/ton of raw coal, and the electricity use is 7 kWh/ton of raw coal. As a consequence of shaking and abrasion, coal losses of 0.05%/100 miles of rail transport are included.

10-Raw Materials Preparation

A material balance for the major process streams appear in Tables 4.1-4.3. The front end of the plant is nearly unchanged through Area 20. Hence, the gasification; heat recovery; particulate removal; and COS hydrolysis follow the base-case performance as originally modeled by Wally Shelton, EG&G.

11-Coal Preparation: After delivery by unit train a pulverizing circuit prepares the coal for transport into the gasifier using hot inert nitrogen from the 12-Air Separation Unit. In pulverizing and transporting the coal, further drying takes place so that a net 2,977 tons/day of coal is feed to the gasifier. The coal is combined with steam in transport, but does not mix with oxygen until the gasifier.

12-Air Separation Unit (ASU): A cryogenic unit provides 2,558 tons/day of oxygen feed to the gasifier at 95% purity. Nitrogen at 2.1% and Argon at 2.9% are inert diluents that carry through the rest of the cycle.

13-Water treatment: Conditioning of raw water for feed to the boiler and gasifier are essential so that steam service maintains a high efficiency. The process consumes 87 tons/day of steam as a chemical reagent in the gasification while a further 160 tons/day is consumed in the 31- Shift block. Sour water and blow-down streams also are treated in the plant.

20-Gasification

21-Gasification: The Shell gasifier receives the dry coal feed into an oxygen-blown, entrained-flow slagging unit that operates at 367 psi. The gasifier exit conditions are controlled by a feedback system on the oxygen so that the exit temperature before quench is 2,500 F. One critical design decision is to employ a gas recycle stream from 24-COS Hydrolysis block rather than quenching the hot raw gas with a water spray. This significantly reduces the water treatment from this system as contrasted with other commercial oxygen-blown, entrained-flow gasifiers.

22-Heat Recovery and 23-Particulate Removal: The raw gas product has considerable enthalpy that is converted to steam and employed for power generation. Because of the dust loading coming off the gasifier, the design of these sections present some particularly challenging materials of construction, fabrication, and heat-transfer issues. A dust-free raw product gas at 450 F with a minor pressure drop is delivered for 24-COS Hydrolysis treatment.

24-COS Hydrolysis: This section converts the COS produced in gasification to H_2S. It is included in the 20-Gasification process block because nearly 30% of the product stream is recycled to the raw gas exiting the gasifier to serve as a quench. Any HCl and nearly all the ammonia entering with the raw gas stream is captured in this section and reports to the sour water.

30-Gas Conversion

31-Shift Reaction: The shift reaction uses 160 tons/day of steam to convert CO in the gasifier product stream to CO_2 and Hydrogen. The reaction takes place in two beds of sulfur-tolerant shift catalyst. The first bed of lower activity catalyst yields a 76% conversion. The temperature of the shift product form the first stage must be returned to 452 F so that 98% conversion in the second bed is feasible. Because these reactions are exothermic, cooling of the shift product from the two stages provides an additional 4.9 MW of power in the 32-Heat Recovery process block.

40-Gas Separation and Purification

41-H_2S Recovery: Glycol-based absorber-stripper processes for H_2S and CO_2 are commonly employed for gas clean up. Commercial systems generally employ an optimized mixture of five or more glycols, however, the vendors of these systems have provided warnings that the physical properties data for their mixtures are not well-simulated using data in the open literature. The current ASPEN 10.2 simulation solely employs tetra-Ethylene Glycol di-Methyl Ether ($C_{10}H_{22}O5$) as a surrogate for the commercial mixture. Using this physical solvent and a 25 molar % water mix, more than 98% of the H_2S is captured in this section. This H_2S is

recovered for treatment in the 44-Claus process block that will yield a sulfur product. The next stage of glycol-based scrubbing recovers a very high fraction of residual H_2S so that a product specification of 10 ppm H_2S in the turbine fuel is met. While the glycols are more selective for H_2S than for CO_2, nearly 60% of the CO_2 is captured here.

42-CO_2 Recovery: A second glycol-based absorber-stripper system is employed for polishing so that a total of 90% of the CO_2 is captured for recovery and pipeline transport. After drying, 6,612 tons/day of CO_2 is compressed to 2,100 psi and transported from the plant using a super-critical pipeline. Commercial experience shows that other species such as H_2S are permissible in co-mixtures with CO_2 for injection into underground reservoirs. An effort to determine whether this co-mixture could be adequately simulated is reported in a later paper.

43-Pressure Swing Adsorption: This approach is commonly used in the purification of hydrogen. It is a semi-continuous process, which yields 357 tons/day of a very high purity hydrogen product, with some minor Argon dilution. The blow down product from this system has a significant heating value and is employed as a turbine fuel for power generation.

50-Power Generation

51-Combustion Turbine; 52-Heat Recovery Steam Generator; 53-Steam Cycle: These process areas are configured so that after the gas turbine (61.95 MW) the Heat recovery Steam Generator employs three steam pressures.

Additional output from steam cycle with incorporation of raw gas cooling: 86.63 MW
Low pressure turbine output from shift system heat: 4.9 MW
Total power generation: 153.48 MW.
Internal power requirements: -77.4 MW

Looking at the power balance over the entire plant, it is clear that most of the power is being exported over the fence as hydrogen.

APPROACH TO LIFE-CYCLE ASSESSMENT

Life-Cycle Assessment (LCA) is a tool for analyzing the environmental burden of products at all stages of their life cycle, "from cradle to grave" – extraction of resources; production of materials, product parts, and the product itself; use of the product; and management after discarding, either by reuse, recycling, or final disposal. Over the last decade, the U.S. and European branches of the Society of Environmental Toxicology and Chemistry[1] (SETAC) have led the intensive development of LCA methodologies, producing a "Code of Practice" – the first internationally accepted technical framework for LCA. This SETAC work is the basis for the LCA protocol in the ISO 14000 environmental management standards of the International

---

[1]SETAC, a worldwide professional society, was founded in 1979 to provide a forum for individuals and institutions engaged in the study of environmental problems, the management and regulation of natural resources, education, research, and development, and manufacturing and distribution.

Organization for Standardization (ISO). SETAC defines the inherent features of LCA as follows [1-3]:

- A system-wide or "cradle-to-grave" perspective, implying coverage of the multiple operations and activities throughout a life cycle;
- A multimedia perspective, implying coverage of resource use and emissions to different environmental media (e.g., air, water, and soil); and
- A functional unit accounting system that normalizes energy carriers, material resources, emissions, and wastes across the system (i.e., full fuel cycle) and across media after unit process allocation procedures. Only those percentages of emissions or resource use specific to the function are included in the balance sheet (LCA inventory table).

The methodological framework accepted worldwide for LCA currently recognizes four distinct components of a life-cycle assessment. The first step is a *goal definition and scoping* activity that serves to define the specific objectives and the expected products of a given study, as well as to identify time and spatial boundaries, boundary conditions and assumptions, and impact and improvement objectives. The second step, *inventory analysis*, quantifies and catalogs the materials and energy used and the environmental releases arising from all stages of the life of a product or process, from raw material acquisition to ultimate disposal. The third step, *impact assessment*, examines potential and actual environmental, human health, and resource depletion effects related to the use of resources (energy and materials) and environmental releases. The fourth step (optional) is an *improvement assessment* of the changes needed to bring about environmental, human health, and/or resource management improvements in the product or process. The scope of the current project is limited to the first three steps.

LCA GOAL DEFINITION AND SCOPING

Two major goals are pursued by the current LCA analysis:

- To create an "environmental footprint" of an IGCC-based multi-product system with CO_2 recovery and
- To compare that footprint with that of a conventional IGCC-based system with only electricity generation.

For consistency of analysis, both plants are assumed to be located in Stevens Point, Wisconsin, and fueled by coal from a seam near Sesser, Illinois. To reflect the full life-cycle concept, both analyzed systems include three distinct activity areas, as shown in Figure 2:

1. Production plant (including gasification, gas conversion and purification, and power production by combined cycle);
2. Auxiliary operations and activities (including extraction and processing of coal and other significant major natural resources, transportation of major consumables and construction materials to the power plant, by-products and waste transportation/disposal/reuse, and production of power plant consumables and construction materials); and
3. Power plant construction and demolition, as well as construction of hydrogen and CO_2 transportation pipelines.

DESCRIPTION OF INVENTORY
COLLECTION AND ANALYSIS

To perform the LCA, an inventory of raw materials, products, and emissions associated with activities within this scope was collected for the base and the co-product cases. This inventory has been allocated to the products as described below.

Inventory Collection

Inventory collection and analysis were performed by using the LCAdvantage[TM] computer program developed by Battelle [4]. LCAdvantage[TM] combines life-cycle modeling features with a graphical user interface, database structure, and calculation engine. The LCAdvantage[TM] database comprises materials inventories based on U.S. experience for the production of basic commodities, including power generation, fuels production and distribution, and cradle-to-grave operations for such selected products as metals, cement, and basic chemicals. The quantities of materials, consumables, and effluents associated with IGCC process operations, as well as the pollutant emissions from relevant activities, were obtained from various sources, including the Aspen[TM] simulations, supplemental mass and energy balances, the LCAdvantage database, other reports on LCA analyses, literature, EPA resources, and personal communications with individuals and experts in different industries. The LCAdvantage creates an inventory for all processes involved in construction, operation, and demolition of the plant. The inventory categories are resources, products, and airborne, liquid, and solid residues.

Shell Gasification Combined-Cycle Plant

The major process streams from the Shell gasification combined-cycle plant that need to be considered in the life-cycle assessment are:

- Major resource inputs: coal, water, MDEA and Selexol (used for removal of H_2S and CO_2 from flue gas), catalyst for the reduction of H_2S to elemental sulfur (Claus process), catalyst for chemical reduction of SO_2 to H_2S (SCOT process) to improve total sulfur removal by the Claus plant, and auxiliary electricity.
- Major products: electricity, hydrogen, CO_2, and by-product sulfur.
- Solid waste: coal slag, spent Claus and SCOT catalyst, and dewatered sludge from raw water coagulation process.
- Liquid waste: gasifier blowdown, scrubbing processes blowdown, HRSG blowdown, cooling tower blowdown, and water treatment unit blowdown.
- Airborne residues: SO_2 and CO_2 from SCOT plant stack (base case only), stack gas from combustion turbine, de-aerator vent, N_2 from the air separation unit, and solid particulate drift from the cooling tower.

Auxiliary Operations and Activities

Both cycles include the following processes: coal mining, coal cleaning, coal transportation to the power plant, solid waste collection and transportation, power generation and transmission, and wastewater treatment. In addition, for the multi-product system we include separation of H_2 and CO_2 and delivery of these products to clients via pipelines.

Run-of-mine Illinois #6 coal, mined underground at Sesser County in Illinois, is used in the ASPEN modeling to fuel both plants. Coarse cleaning at the mine mouth is assumed, with refuse returned to the mine. Coal is transported to the plant by rail only. Emissions associated with coal transportation to the power plant include those from diesel fuel use and open rail cars loaded with crushed coal. We do not include emissions associated with manufacturing of diesel fuel and with manufacturing and maintaining rail cars.

It is assumed that power plant solid waste (slag, solids from water treatment, and spent catalysts) is collected in a dewatering pond located on the plant site. After dewatering, this waste is transported to a landfill 40 to 80 km from the power plant. The landfill is designed to prevent leachate, so emissions from solid waste collection and landfill are only from the fuel used for solid waste transportation by rail. Usually, sulfur produced in the Claus cycle is stored at the power plant and sold to clients. No emissions are expected from the sulfur storage process. Finally, depending on the selected water treatment process, most wastewater does not require treatment before being discharged.

Construction and Demolition of the Power Plant
Hydrogen and CO_2 Pipelines
The power plant construction and demolition analysis applies to both power plant cases. The amount of materials required for the construction of a power plant is broadly proportional to the size and complexity of the plant. The bulk construction materials required are steel, cement, and aggregates in the ratio 1:1:6. Other materials include aluminum, copper, glass, and iron, but in insignificant amounts compared to the first three materials. We have assumed that construction of the co-product and base-case plants would require equal amounts of construction materials. The gasifier sections for these plants are identical. Also, the reduction in material use for the power island of the co-product case is offset by the increase in material use for enhanced gas treatment. Fuel use and emissions from the production of these construction materials have been estimated based on the energy required to produce the materials. In addition, we have included fugitive emissions of particulates during construction. Decommissioning will involve some expenditure of energy, depending on the future use of the site. One study advised [5] that the net energy consumption for decommissioning is approximately 10% of the energy consumed in construction. There are two primary solid waste outputs from decommissioning. One of them is scrap metal, which will be partially reused for steel manufacturing. The second is spent shift, SCOT, and Claus catalyst, plus resins from the water treatment unit. This flow of material will be directed to the solid waste module.

Amounts of materials and energy required for power plant construction and demolition activities, as well as emissions associated with these activities, were calculated on the basis of information presented in Gorokhov et al. [6]. All emissions associated with plant construction and demolition were distributed over the assumed 30-yr plant life (alternatively, they could be assigned to the construction period before power plant commissioning and to a demolition period after plant decommissioning).

Construction of H_2 and CO_2 pipelines is included in the scope of analysis. Both pipelines are assumed to be 100 km long. Initial pressurization of both gases before they are sent from the power plant enables delivery without booster compression. Resources used in the LCA analysis

for these pipelines include steel and concrete, as well as energy for manufacture and delivery. Accordingly, emissions associated with construction of pipelines include emissions from manufacturing and delivery of materials. We assume that the pipelines will not be demolished.

Emissions Allocation

A consistent way to compare the environmental performance of alternative plants is to report emissions per unit of production (e.g., per kilowatt-hour (kWh) output for the power generating plant). In the case of multi-product plants, emissions should be somehow allocated to the various products. Then these unit emissions can be compared with those from alternative systems for producing the same products. Unfortunately, there is no standardized or unified system that can be recommended to accomplish this allocation. Our approach is to regard hydrogen and fuel gas as two product fuel streams and allocate emissions according to the energy content of each stream. This allocation is applied to (1) all emissions associated with plant operation before separation of H_2 and CO_2, (2) solid waste collection and transportation, (3) plant construction and demolition, and (4) emissions associated with the construction of the CO_2 transportation line. We view CO_2 as a waste stream, which is to be stored underground. If CO_2 were viewed as a product, the allocation scheme would be more difficult. All emissions associated with operation of the combined cycle are allocated to electricity production (including gas and steam turbines, plant water treatment, and the cooling tower); these include the emissions already allocated to the fuel gas. All emissions associated with construction of the hydrogen transportation line are allocated to the hydrogen flow. This allocation scheme facilitates comparison of the environmental performance of the power production part of the co-product plant with the base-case IGCC plant that only produces electricity. Our previous studies have shown that collection of CO_2 from flue gas and its pressurization for transportation via a pipeline can require a significant amount of additional parasitic power. Thus, *a priori*, both the economic and the environmental performances of a multi-product cycle are expected to be worse than those of the cycle without CO_2 separation. Therefore, an additional comparison of the multi-product IGCC system with an IGCC cycle with separation of CO_2 and electricity-only generation [5] was included in the analysis. These comparisons were made on the per-kWh basis. Environmental performance of the hydrogen-generating part of the multi-product system was compared with the performance of a methane-steam reforming hydrogen-manufacturing process [11] on the per-Btu of generated hydrogen basis.

Emission Inventory Analysis

Bituminous coal and water are the major material inputs. Other fuels and electricity are used mostly for coal extraction and transportation and for solid waste transportation. Although the amounts of steel and concrete needed for plant construction are significant, the per-kWh (per-Btu) amounts, distributed over the 30 years of expected plant life, are several orders of magnitude lower than the amounts of coal and water used for production of electricity.

Emission inventory results for some components are presented in Figure 3. Contributions to emissions by each phase of the process are presented as percentages of the total for each emitted species. On a mass basis, CO_2 is the dominant gaseous emission for the base-case power plant. Most of this CO_2 is produced in the power cycle. In the multi-product plant, more than 90% of the potential CO_2 is captured. Coal extraction and transportation processes result in the next-largest emissions stream, although that stream is two orders of magnitude smaller than the

emissions from the power cycle; consequently, total CO_2 emissions from the multi-product cycle are significantly lower. CO_2 emissions are followed in magnitude by CO emissions, also released mainly in the power cycle. Methane released via coal mining represents the third-largest emission. NO_x emissions are associated mostly with coal extraction and transportation, while SO_x emissions are generated only from the power cycle. Almost all organic emissions identified in the inventory assessment are associated with fuel use for extraction of coal and transportation of coal, waste, and construction materials.

As expected, significant particulate matter emissions are associated with coal extraction and transportation and with the construction/ demolition processes. Note that when the construction and demolition particulates are levelized over the power plant life cycle, the amount (per kWh) is of the same order of magnitude as from extraction and transportation of coal, probably because the construction process includes all emissions associated with extraction of iron ore, development of cement and coke, and transportation of these materials, plus any particulates from the construction site itself. In this analysis, these emissions are distributed over the 30-yr power plant life, while in reality all these emissions are released to the air shed in about a two- to four-year period during power plant construction. Thus, the local impact of these emissions can be very significant. Slag, the most significant solid emission, is expected to have minor impacts, especially since it is a useful by-product.

APPLICATIONS OF LIFE-CYCLE IMPACT ASSESSMENT (LCIA)
IMPACT CATEGORIES

LCIA is a technical, quantitative, and/or qualitative process of characterizing and assessing the environmental effects of plant resource requirements and environmental loadings identified in inventory collection. Strictly speaking, it should address all human health, ecological, and resource depletion impacts. This assessment reports the inventory results as a distillation of inventory loadings and resource use assigned to specific impact categories.

A broad spectrum of impact categories has been developed in the practice of LCIA. The number of selected categories and their nature generally influence the amount of work required to perform the LCIA. On the basis of previous experience [6], 12 categories are selected as the most important for the evaluation of power cycles. These are identified below, aggregated into three broad impact groups:

Natural Environment - Acidification, eutrophication, smog, global climate changes, and ecotoxicological impacts (aquatic and terrestrial toxicity);

Human Health - Toxicological impacts, PM_{10} inhalation effects, and carcinogenic impacts; and

Natural Resources- Depletion of fuels and water.

Some products, resources, or emissions can be involved in more than one impact category. The same emission/product may contribute to two or more exclusive categories in a parallel or sequential manner, and the emission should be divided or allocated to the relevant categories to avoid double counting. It is also possible that the product or result of an effect in one impact category may be the starting point for another effect in another impact category. To deal with such complexities, LCIA procedure in this project was simplified by (1) accounting for primary

emission impacts only and (2) not distributing a particular product/emission among a number of different applicable impact categories, but rather assigning the full value of that product/emission to each applicable category, to determine the worst-case impact.

The relative significance of each environmental loading is represented by category indicators, which usually incorporate a spectrum of results ranging from technical values to subjective judgments. These indicators are the basis on which comparisons can be made, so the value of a comparison depends on the varying technical strength and relevance, as well as the degree and type of subjective judgment used to derive a particular indicator. Some indicators can be estimated as a total amount of a single material or emission, such as water use or PM_{10} emission. Other indicators can represent the total amount of different species. For example, land depletion resulting from landfilling of waste can be represented by the total space occupied by all types of landfilled solid waste. In many cases, data on individual chemicals or resources within an impact category must be combined, using so-called "equivalency factors." These equivalency factors express the relative hazard potential of different chemicals within an impact category, but they do not represent actual environmental impact. SETAC and other organizations have developed numerous equivalency factors and provided recommendations for development of new equivalency factors. A brief description is provided below for each impact category, together with the list of inventory items assigned to this category, as well as a basis for calculating category indicators with the relevant equivalency factors.

Acidification
Acidifying substances cause a large diversity of impacts on soil, groundwater, and surface water organisms, ecosystems, and materials (buildings). The most important acidifying compounds are SO_2, NO_x, and NH_3. Acidification potentials (APs) based on H^+ equivalents are used as equivalency factors to calculate the total indicator for acidification. The total indicator score is expressed in kilograms of SO_2 equivalents.

Eutrophication
This category includes all impacts caused by excessively high levels of macronutrients in the environment. Nitrogen (N) and phosphorus (P) are the most important eutrophicating elements. Eutrophication potentials (EPs) are used as equivalency factors to calculate the total indicator for eutrophication. The EPs reflect the potential contribution of a substance to biomass formation and are expressed in kilograms of PO_4^{3-} equivalents. Major contributors to this impact for both power cycles are ammonia and NO_x.

Smog or Photo-Oxidant Formation Impact
Photo-oxidants can be formed in the troposphere via photochemical oxidation of volatile organic compounds (VOCs) or carbon monoxide (CO) in the presence of NO_x and under the influence of UV light. Ozone is considered to be the most important oxidant. The Maximum Incremental Reactivity (MIR) scoring system, developed by W. Carter, is used to calculate the total indicator for the formation of photo-oxidants, converted to kilograms of ozone formed [3].

Global Climate Changes
Global warming is the impact of fossil fuel emissions on heat radiation absorption in the atmosphere. Major contributors are CO_2, methane, and N_2O. Global Warming Potentials

(GWPs) are used as equivalency factors, to convert all emissions into kilograms of CO_2-equivalent [3].

Ecotoxicological Impacts

These impacts are the effects of toxic substances on aquatic and terrestrial ecosystems. Only emissions to water and soil are taken into account in this category. Emissions to water are considered to be toxic only for aquatic ecosystems, and emissions to soil are considered to be toxic only for terrestrial ecosystems. Toxicity factors for these toxicity impact criteria were calculated using a combination of the toxicity, persistence, and bioaccumulation properties of the inventoried chemicals to assess their potential fate and environmental effects. Data used for terrestrial toxicity and aquatic toxicity were lowest rodent LD_{50} (mg/kg) and lowest fish LC_{50} (mg/L) [8,9].

Toxicological Impacts on Human Health

This impact category reflects the effects of toxic substances on humans. There are different ways for these substances to enter the human body (inhalation, water, food, etc.), but only the inhalation and water effects are evaluated here. Factors for these toxicity impact criteria were calculated using Toxic Equivalency Potentials (TEPs), which indicate the relative human health risk associated with the release of one pound of a chemical, compared to the risk posed by release of a reference chemical. In this risk scoring system, all releases of carcinogens are converted to pounds of benzene-equivalents; all releases of chemicals that cause non-cancer health effects are converted to pounds of toluene-equivalents [3].

PM_{10} Inhalation Impact

PM_{10} inhalation affects human health via chronic and nonchronic (short-term) respiratory diseases, increasing both human mortality and morbidity rates in exposed areas. The equivalency factor was estimated as the total weight of solid particulate matter released to the atmosphere.

Depletion of Fuel and Water

These categories characterize depletion of so-called abiotic resources. The basis for resource depletion equivalency factors is the inverse of sustainability, which can be expressed as the world annual production of a mineral or a fossil fuel divided by the world reserve base [3,8]. For example, the fossil fuel data, based on global reserves and production, were obtained from Ref. 10. The calculations include all types of fuel used in the power cycle, as well as in all other activities for manufacturing and transportation of all materials included in the inventory.

Depletion of Land

This impact category focuses only on the loss of land as a result of coal mining or other fuel development operations, and on the use of land for landfilling of waste. Because no specific place and type of coal mining were chosen, only use of land for waste landfills was evaluated in this project. The land-use equivalency factors for solid waste disposal are based on the estimated volume calculated using the specific gravity of each type of solid waste. Inventory data for solid waste are expressed in kg/kW (kg/Btu); multiplication of the weight and the inverse of the

specific gravity give an indicator of the waste volume per kilowatt, and thus, the landfill volume required per kilowatt of developed energy, or per Btu of generated hydrogen.

LIFE-CYCLE IMPACT ASSESSMENT (LCIA) RESULTS

A comparison of unweighted impact scores for all impact categories is presented in Tables 5 and 6. Table 5 contains data for electric energy generation in three power cycles – base-case IGCC cycle (column 1), multi-product IGCC cycle with separation of CO_2 (Column 2), and an electricity-generating IGCC cycle with CO_2 separation modeled by the IEA [5] (Column 3). Column 2 presents data for the combined-cycle part of the multi-product system. The last two columns in this table represent a shorthand way of comparing the electricity-generating part of the multi-product IGCC cycle with the base-case IGCC cycle and with the IEA IGCC cycle with CO_2 separation in terms of environmental impacts. If values in this column are substantially larger than one, the multi-product cycle has greater environmental impact than the base-case or IEA IGCC cycle. Values within 20% of unity indicate that the impact potentials of the two cycles are not distinguishable [13]. Results in the column Case B/Case A show that the combined cycle of the multi-product system has significantly higher environmental performance than the base case in such categories as eutrophication and toxicity (better reduction of acids and NO_x), GCC (more than 90% of CO_2 captured), and water use (steam-generating cycle significantly smaller than in the base case). On the other hand, its impact in such categories as PM_{10}, smog, air toxicity, land use, and resource depletion is much higher, because overall efficiency of the cycle is less due to the additional auxiliary power required for CO_2 pressurization. Results in the column B/C show that the performance of the multi-product plant for electricity generation is better than that of the IEA-developed IGCC cycle with CO_2 capture in 7 of 13 categories.

Table 6 compares the environmental performance of the hydrogen-generating part of the multi-product system with that of a methane-steam reforming hydrogen-generating process. Results in column 3 show that the multi-product system is superior to the methane-steam reforming process in almost all categories, except for land use and PM_{10} emissions. The higher impact of the multi-product system in the land use category occurs because the methane-steam reforming process generates minimal solid waste. PM_{10} emissions are mostly associated with coal mining and transportation, as well as with construction and demolition of facilities. In addition to the absence of PM_{10} emissions associated with coal processing and transportation, the methane-steam reforming facility is much smaller and accordingly requires fewer raw materials (steel, cement, and aggregates) and activities for construction and demolition. A significant difference in the resource depletion category can be explained by the fact that the indicator for this category is based on a ratio of annual production of fuel to its reserves. This ratio for coal is several orders of magnitude smaller than the ratio for natural gas, the main raw material for the methane-steam reforming process.

Figures 4 and 5 show the comparison of emission impact scores for the different processes in five major emission impact categories.

CONCLUSIONS

- This process design employs a Shell IGCC cycle in a "Vision 21" multi-product plant with low greenhouse impact. Hydrogen can be cogenerated with electricity and delivered to consumers at very high purities. The selection of a very high purity hydrogen product stream benefits the high-efficiency performance of fuel cells while still meeting the internal power needs of the IGCC and having a revenue stream from electricity sales. The introduction of "shift" to increase the hydrogen content of the gasifier product also benefits the CO_2 recovery, which has inherent cost advantages if it is largely removed prior to the combustion turbines.

- Based on emission inventory analysis, the most CO_2, CO, and SO_2 are generated in the IGCC cycle, methane emissions are mostly associated with coal mining, and particulate matter is mostly generated in construction and demolition of the plant and pipelines. Transportation and mining are responsible for NO_x emissions.

- Environmental performance of the electricity-generating part of the co-product system is similar to that of the IGCC-based cycle with CO_2 removal. However, the co-product plant has larger environmental impact than a base-case IGCC system without CO_2 removal in almost all impact categories, because of the higher auxiliary power requirement connected to CO_2 pressurization before its output from the power plant. Removal of CO_2 and deeper reduction of acid gas emissions makes the multi-product system better in the GCC, toxicity, and eutrophication categories.

ACKNOWLEDGMENT

REFERENCES

1. Barnthouse, L., et al., "Life Cycle Impact Assessment: The State-of-the-Art," 2nd Edition, A Report on the SETAC LCA Impact Assessment Workgroup, Pensacola, Fla., 1998.
2. *Evolution and Development of the Conceptual Framework and Methodology of Life-Cycle Impact Assessment*, SETAC Press, Jan. 1998.
3. Guinee, J.B., et al., "Life Cycle Assessment. An Operational Guide to the ISO Standard," Centre for Environmental Science, Leiden University, The Netherlands, Oct. 2000.
4. *Life-Cycle Advantage^{TM} Start-Up Guide, Version 1.0*, Battelle, Aug. 1997.
5. "Full Fuel Cycle Study on Power Generation Schemes Incorporating the Capture and Disposal of Carbon Dioxide," ETSU, United Kingdom, Oct. 1994.
6. Gorokhov, V., et al., "Life Cycle Assessment of Gasification-Based Power Cycles," Proceedings of the 2000 International Joint Power Generation Conference, Miami Beach, Fla., July 23-26, 2000.
7. Internet, URL: http://www.internationalfuelcells.com/commercial/features.shtml#perform.
8. Evers, D., et al., "Streamlined Life-Cycle Assessment of 1,2-Butanediol Produced from Petroleum Feedstocks versus Bio-Derived Feedstocks," National Risk Management Research Laboratory, Office of Research and Development, U.S. Environmental Protection Agency, Cincinnati, Ohio, Sept. 1997.

9. Davis, G.A., et al., "Chemical Hazard Evaluation for Management Strategies: A Method for Ranking and Scoring Chemicals by Potential Human Health and Environmental Impacts," Risk Reduction Engineering Laboratory, Office of Research and Development, U.S. Environmental Protection Agency, Cincinnati, Ohio, Sept. 1994.

10. *Annual Energy Review for 1998*, U.S. Department of Energy/Energy Information Agency, 1999.

11. "Hydrogen from Natural Gas Steam Reforming," Letter Report, prepared for DOE/NETL by Parsons Infrastructure and Technology Group, Feb. 2001.

Table 1. Comparison of Design Basis for Three Power Cycles

Process	Base Case	Co-Product Case	IEA Case
Gasification	Shell gasification with cold gas cleanup. Raw gas is produced at 1,844°F and 352 psia.		Texaco gasification with cold gas cleanup. Raw gas is produced at 788° F and 711 psia
Ash removal	This is a slagging gasifier with slag quench.		
Air separation	Cryogenic air separation with partial integration (N_2 used as diluent for combustion turbine)		
High-temperature gas cooling/particulate removal	Used to raise high-pressure, superheated steam	Also used for combustion turbine fuel gas preheat	Used to raise high-pressure, superheated steam
COS hydrolysis	Single stage to form H_2S and CO_2		Not applicable
Shift reaction	Not applicable	Two-stage shift to convert raw gas to high H_2 and CO_2 content	Three-stage shift to convert raw gas to high H_2 and CO_2 content
H_2S recovery	MDEA	Glycol used for improved selectivity (H_2S vs. CO_2)	Glycol/ether used
Acid gas treatment	Claus-SCOT using filtered raw gas as SCOT reagent	Claus-SCOT using H_2 product as reagent	Claus plant
CO_2 removal	Not applicable	Glycol	Glycol/ether
H_2 purification	Not applicable	Pressure Swing Adsorption	Not applicable
Combustion turbine fuel	Synthesis gas cleaned of sulfur and particulates	Residual gas rejected by PSA	Synthesis gas cleaned of sulfur and particulates
Steam cycle heat source	Gas turbine exhaust	Gas turbine exhaust and heat recovery from shift reaction	Gas turbine exhaust and heat recovery from shift reaction

Table 2. Comparison of Plant Performance for Three Power Cycles

Item	Base Case	Co-Product Case	IEA Case
Coal consumption, ton/day	3,171	3,171	4,823
Gas turbine power, MW	272.3	62.0	456
Steam cycle power, MW	188.8	91.5	354
Internal power consumption, MW	- 48.3	-77.4	-155
Net electricity, MW	412.8	76.1	646
H_2 production (equivalent MW)	0	423.2 – 100% effic. 275.1 – 65% effic. 194.7 – 46% effic.	0
CO_2 product, ton/day	0	6,612	11,767
CO_2 emissions, ton/day	7,412	800	1,384

Table 3. Coal Mining and Cleaning, Rail Transport and Delivery to IGCC

11-Coal Preparation	As-Received Basis, wt %			Raw Coal	Coal to train	Coal to pulverizer		Coal to gasifier
	Raw Coal wt%	Clean Coal wt%	Dry Coal wt%	ton/d	ton/d	ton/d	ton/d	lbs/hr
Ultimate Analysis				4967	3179.197	3171.00	2977.06	248,088.52
Moisture	10.10	11.12	5.33		353.527	352.62	158.68	13,223.12
Ash	26.19	9.70	10.33		308.382	307.59	307.59	25,632.25
Sulfur	3.68	2.51	2.67		79.798	79.59	79.59	6,632.68
MAF Values								
83.15 Carbon	48.984	63.751	67.904		2026.773	2021.548	2021.548	168,462.29
5.87 Hydrogen	3.458	4.501	4.794		143.081	142.712	142.712	11,892.65
1.63 Nitrogen	0.960	1.250	1.331		39.731	39.629	39.629	3,302.39
0.38 Chlorine	0.224	0.291	0.310		9.262	9.239	9.239	769.88
8.97 Oxygen	5.284	6.877	7.325		218.643	218.079	218.079	18,173.26
100	100.000	100.000	100.000		2437.490	3171.000	2977.062	248,088.52

Table 4.1 IGCC Major Process Streams

	1	2	3	4	5		6	7	8	
21 - Gasification	Coal feed	Dust from	Nitrogen for	Steam	Oxygen	TOTALin	Slag	Dust	Raw gas	TOTALout
22 - Heat Recovery	to gasifier	recycle	coal transport					to gasifier	product	
23 - Particulates	(pulverized)	Str #8						Str #2	(dust-free)	
Mass Flow lb/hr										
O2	18,173.26	0.00	151.29	0.00	201,606.00	219,930.55	0.00	0.00	2.89E-08	2.89E-08
N2	3,302.39	0.00	18,714.32	0.00	3,863.23	25,879.93	0.00	0.00	25,878.80	25,878.80
AR	0.00	0.00	105.23	0.00	7,737.82	7,843.05	0.00	0.00	7,843.05	7,843.05
H2	11,892.65	0.00	0.00	0.00	0.00	11,892.65	0.00	0.00	12,799.66	12,799.66
CO	0.00	0.00	0.00	0.00	0.00	0.00	0.00	0.00	375,401.00	375,401.00
CO2	0.00	0.00	0.00	0.00	0.00	0.00	0.00	0.00	22,016.03	22,016.03
H2O	13,223.12	0.00	0.00	7,214.38	0.00	20,437.50	0.00	0.00	8,314.22	8,314.22
CH4	0.00	0.00	0.00	0.00	0.00	0.00	0.00	0.00	140.52	140.52
H2S	0.00	0.00	0.00	0.00	0.00	0.00	0.00	0.00	6,438.24	6,438.24
CL2	769.88	0.00	0.00	0.00	0.00	769.88	0.00	0.00	1.20E-06	0.00
HCL	0.00	0.00	0.00	0.00	0.00	0.00	0.00	0.00	797.13	797.13
NH3	0.00	0.00	0.00	0.00	0.00	0.00	0.00	0.00	12.79	12.79
COS	0.00	0.00	0.00	0.00	0.00	0.00	0.00	0.00	1,061.33	1,061.33
CARBON	168,462.29	60.75	0.00	0.00	0.00	168,523.04	1,154.16	60.75	0.00	1,214.91
SULFUR	6,632.68	0.00	0.00	0.00	0.00	6,632.68	0.00	0.00	0.00	0.00
ASH	25,632.25	1,348.66	0.00	0.00	0.00	26,980.91	25,624.60	1,348.66	0.00	26,973.26
Total Flow lb/hr	248,088.52	1,409.41	18,970.83	7,214.38	213,207.00	**488,890.14**	26,778.77	1,409.41	460,703.00	**488,890.94**
Total Flow cuft/hr			10,148.1	9,289.4	99,340.37				1,915,340.00	
Temperature F	60.0	640.13	104.0	694.0	204.69		2,500.00	640.13	2,500.00	
Pressure psi	14.7	370.00	400.0	500.0	472.00		367.50	370.00	367.50	

Table 4.2 IGCC Major Process Streams (Continued)

24 - COS Hydrolysis
31 - Shift
41 - H2S Glycol
42 - CO2 Glycol

	8	9	10	11	12	13	14	15
	Raw gas to Hydrolysis	Hydrolysis Product	Shift Feed	Shift Product	H2S Glycol Feed	H2S Glycol Product	CO2 Glycol Clean-Gas	CO2 to Sequestration
Mass Flow lb/hr								
O2	2.89E-08	2.89E-08	2.89E-08	2.89E-08	2.89E-08	0	0	
N2	25,878.80	25,878.66	25,878.66	25,878.66	25,878.66	24,298.90	22,540.23	
AR	7,843.05	7,842.30	7,842.30	7,842.30	7,842.30	6,675.96	5,475.72	
H2	12,799.66	12,799.46	12,799.47	39,689.99	39,689.99	39,689.99	39,689.99	
CO	375,401.00	375,399.00	375,399.00	1,806.73	1,806.73	1,657.77	1,493.95	
CO2	22,016.03	22,772.42	22,772.58	609,777.00	609,777.00	240,935.45	58,778.41	550,999
H2O	8,314.22	1,143.78	1,143.76	1,245.04	1,245.04	31.17	14.99	trace
CH4	140.52	140.51	140.51	133.57	133.57	93.28	62.20	
H2S	6,438.24	6,945.58	6,945.58	6,945.57	6,945.57	89.87	0.14	<1% volume
CL2	1.19923E-06	0	0	0	0	0		
HCL	797.13	0.555	0.555	0.555	0.555	0.148	1.70E-02	
NH3	12.79	3.57E-02	3.570E-02	3.570E-02	3.570E-02	0	0	
COS	1,061.33	14.93	14.93	14.93	14.93	1.70E-02	0	
Glycol-C10H22O5	0	0	0	0	0	5.20E-02	1.30E-02	
Total Flow lbmol/hr	22,071.44	21,665.29	21,665.29	35,010.25	35,010.25	26,267.14	22,023.98	
Total Flow lb/hr	460,703.00	452,937.00	452,937.00	693,335.00	693,335.00	313,472.61	128,055.67	
Total Flow cuft/hr	1,915,340.00	395,716.00	468,999.00	471,273.00	393,819.47	322,464.01	268,406.05	
Temperature F	2500	100	457	100	15	35	19	100
Pressure psi	367.5	327.5	459	440	438	434	428	2100

Table 4.3 IGCC Major Process Streams (Continued)

43 - PSA 51 - Power	14 PSA Feed	16 Hydrogen	17 Turbine Feed	18 Air	19 Flue gas to HRSG
Mass Flow lb/hr					
O2	0	0	0	245,550.56	165,696.81
N2	22,540.23	2.25	22,537.95	803,694.99	826,232.57
AR	5,475.72	0.55	5,475.17	14,080.71	19,555.86
H2	39,689.99	29,767.52	9,922.51	0	0
CO	1,493.95	0.15	1,493.80	0	0
CO2	58,778.41	5.88	58,772.48	0	61,290.44
H2O	14.99	1.00E-03	14.99	0	88,827.63
CH4	62.20	6.00E-03	62.198	0	0
H2S	0.14	0	0.144	0	0
CL2	0	0	0	0	0
HCL	1.70E-02	0	1.70E-02	0	1.70E-02
SO2	0	0	0	0	0.256252
NOx	0	0	0		10ppm
Glycol-C10H22O5	1.30E-02	0	0	0	0
Total Flow lbmol/hr	22,023.98	14,766.75	7,257.25	36,716.24	41,485.74
Total Flow lb/hr	128,055.67	29,776.35	98,279.27	1,063,326.26	1,161,603.57
Total Flow cuft/hr	268,406.05	181,150.06	88,002.16		
Temperature F	19	100	100	70	1213
Pressure psi	428	500	500	14.7	14.9

Table 5. Comparison of Impact Scores for Three Power Cycles

Impact Category	Base Case Cycle * (Case A)	Multi-Product Cycle, Combined Part (Case B)	IEA IGCC Cycle with CO_2 Separation (Case C)	Case B/Case A	Case B/ Case C
Acidification	5.03E-04	3.19E-04	3.46E-04	0.63	0.92
Eutrophication	8.72E-01	9.43E-01	1.13E+00	1.08	0.84
Smog	8.52E-05	7.83E-05	1.08E-04	0.92	0.73
GCC	1.56E+00	4.90E-01	2.80E-01	0.31	1.75
Particulate Matter (PM_{10})	3.27E-04	3.31E-04	4.17E-04	1.01	0.79
Terrestrial Toxicity	8.27E-06	6.55E-07	1.07E-06	0.08	0.61
Human Toxicity (air)	1.11E-02	1.08E-02	1.05E-02	0.97	1.02
Human Toxicity (water)	2.16E-08	3.21E-08	4.26E-04	1.49	0.00
Carcinogenicity (air)	2.02E-08	1.69E-08	1.17E-08	0.84	1.45
Land Use	1.09E-01	1.06E-01	8.69E-02	0.97	1.22
Resource Depletion	5.66E-03	5.53E-03	3.64E-03	0.98	1.52
Water Use	1.43E+00	1.84E+00	3.56E+00	1.29	0.52

*A) Base-case IGCC cycle without H_2 and CO_2 separation; net power output – 412.8 MW.
  B) Multi-product system, combined cycle only; net power output – 110.3 MW.
  C) IEA IGCC cycle with separation of CO_2; net power output – 646 MW.

Table 6. Comparison of Impact Scores for Two Hydrogen Production Cases

Impact Category	Multi-Product Cycle, Hydrogen Part * (Case D)	H$_2$ Plant (Case E)	Case D/Case E
Acidification	5.50E-08	5.31E-07	0.10
Eutrophication	1.05E-05	4.14E-05	0.25
Smog	1.36E-08	4.21E-07	0.03
GCC	1.81E-05	1.15E-04	0.16
Particulate Matter (PM$_{10}$)	5.91E-08	1.33E-08	4.43
Terrestrial Toxicity	1.54E-10	1.41E-09	0.11
Human Toxicity (air)	1.84E-06	1.23E-05	0.15
Human Toxicity (water)	7.14E-15	3.93E-13	0.02
Carcinogenicity (air)	3.35E-12	2.39E-09	0.00
Land Use	1.79E-05	2.35E-06	7.64
Resource Depletion	9.40E-07	3.02E-05	0.03
Water Use	3.11E-04	3.93E-04	0.79

*D) Multi-product system, hydrogen cycle – 1.86E-06 MBtu/hr.
 E) Hydrogen production, natural gas steam reforming – 2.03E-06 MBtu/hr.

Figure 1. Shell-based Gasification Combined Cycle Plant with Hydrogen and Carbon Dioxide
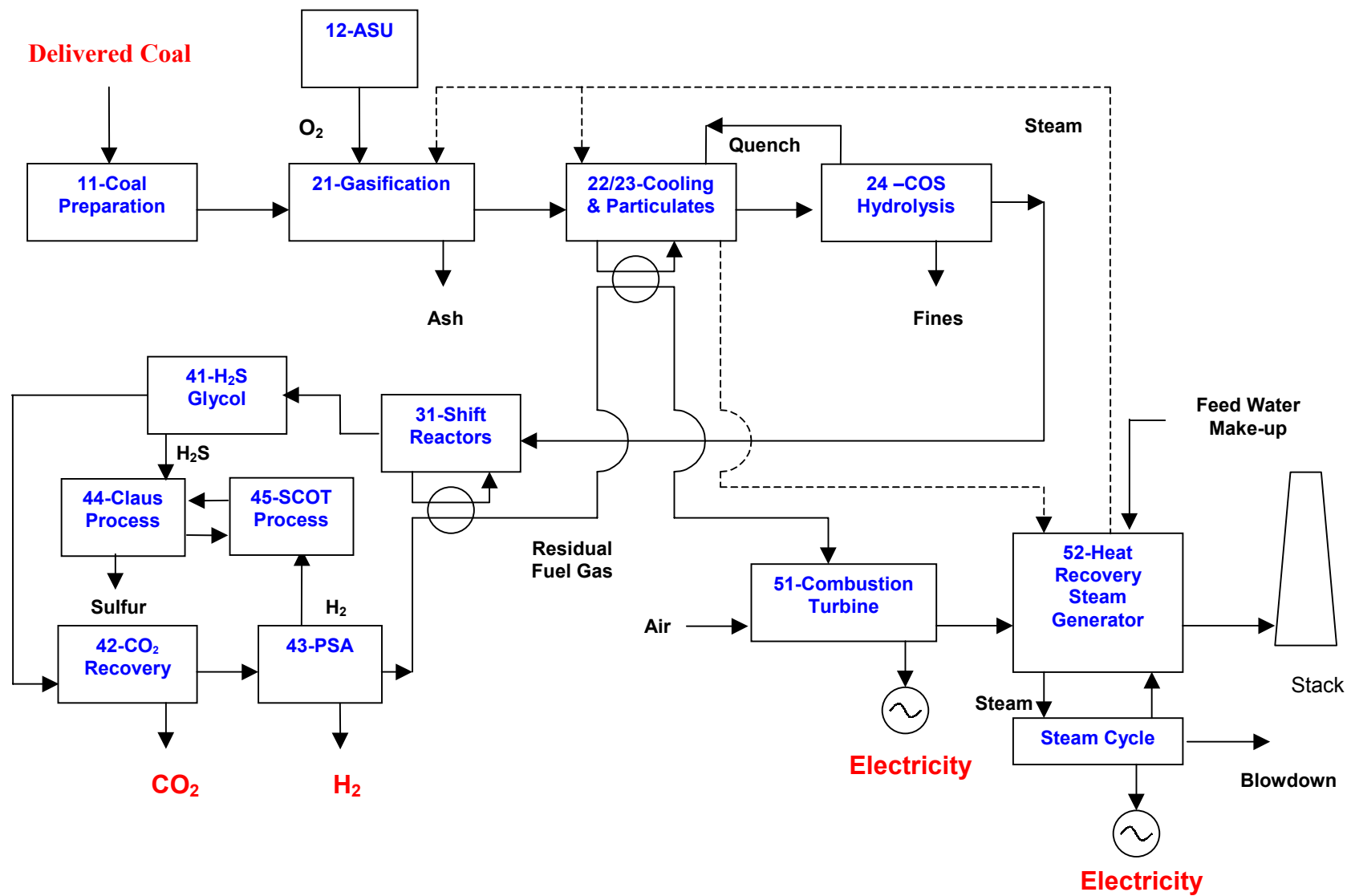
Fig. 2.Coal-fired IGCC-based Multi-product System

SYSTEM BOUNDARY

Energy	Construction of Power Plant	Electricity Generation → Electricity Output
Power Plant Construction and Operation Materials	Demolition of Power Plant	Hydrogen Generation → Hydrogen Output
Transportation	Construction of H_2 Pipeline	CO_2 Separation → CO_2 Output
	Construction of CO_2 Pipeline	Airborne Emissions → Air Shed
Transportation	Power Gener. Island	Solid Waste Collection and Transportation → Waste Landfill
Fuel Extraction and Processing	Coal Preparation	Waste Water Treatment → Water Shed
Energy	Water Treatment	
	Water Cooling System	

Raw Materials →

Fuel in Ground →

Emission Inventory Analysis
A - Base-case Gasification Power Plant
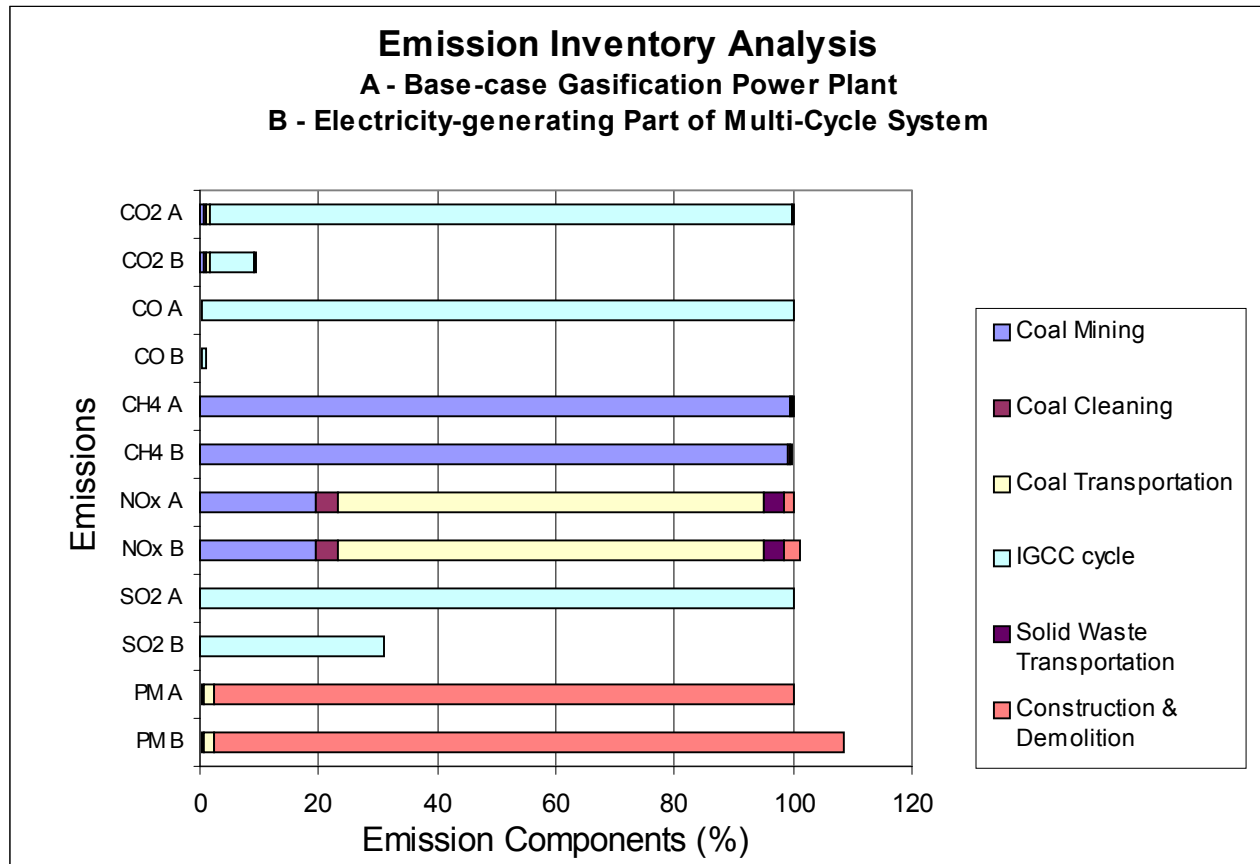**B - Electricity-generating Part of Multi-Cycle System**

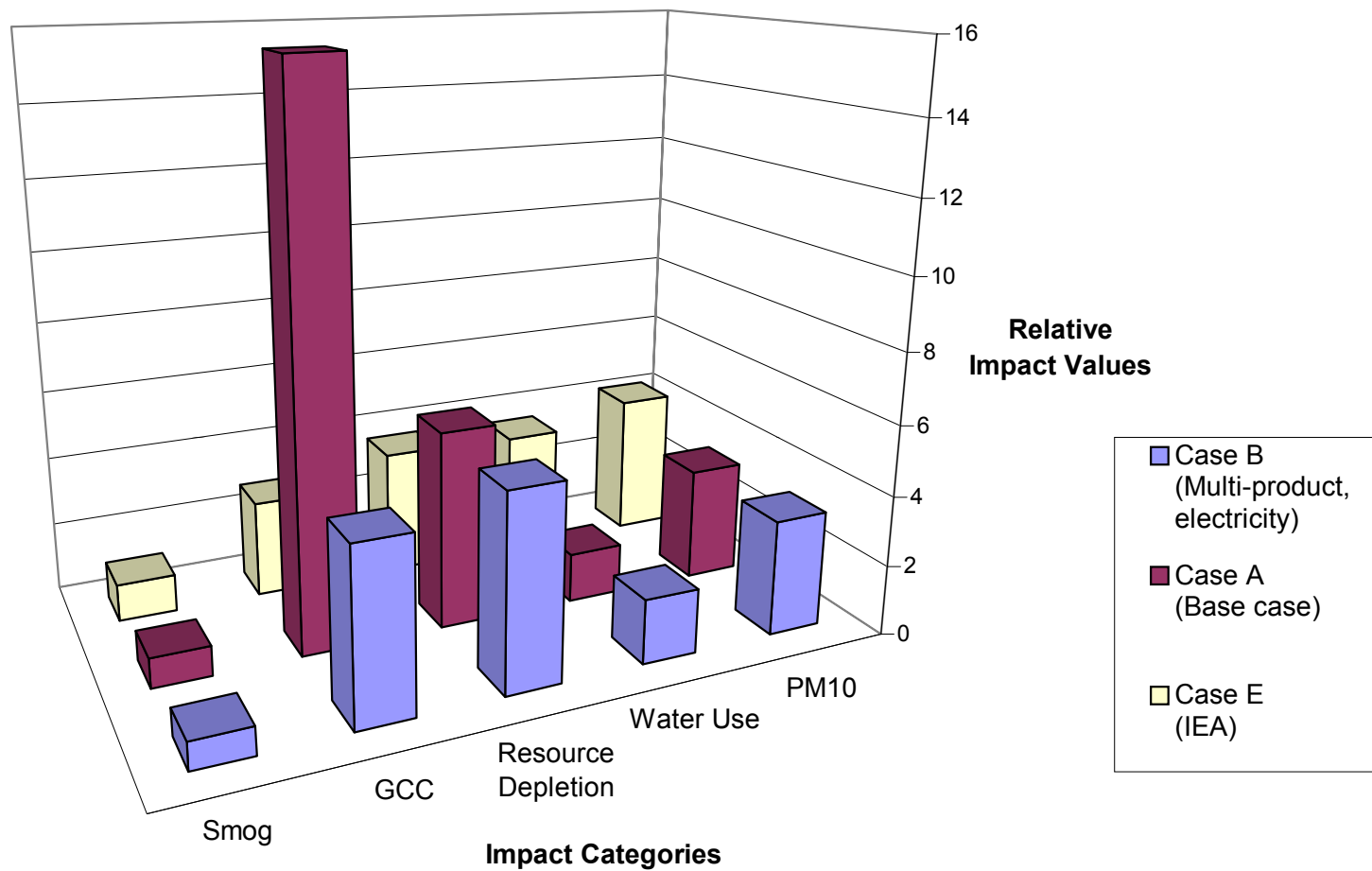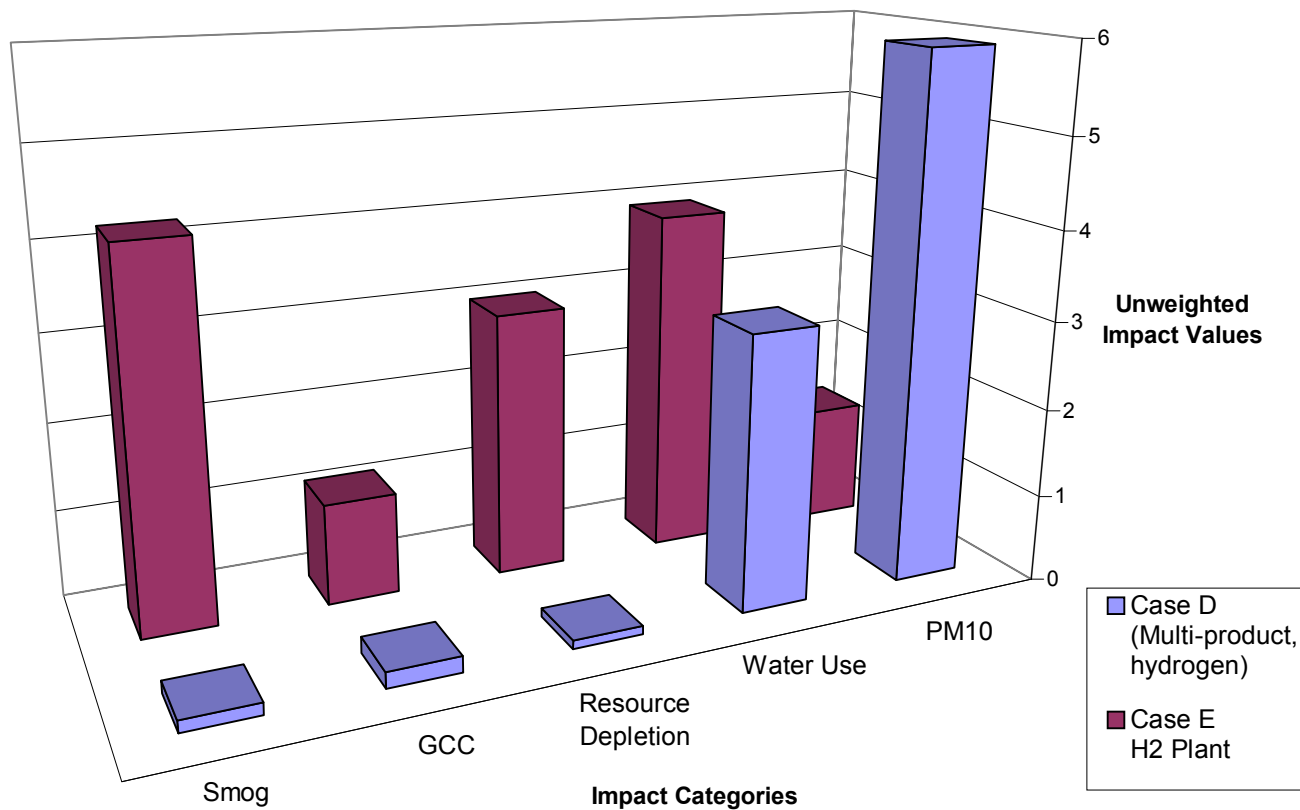Figure 4. Comparison of Selected Impact Scores for Three Power Cycles

**Figure 5. Comparison of Selected Impact Scores
for Two Hydrogen Cases**

NOVEL AMINE ENRICHED SOLID SORBENTS
FOR CARBON DIOXIDE CAPTURE

*Y. Soong[1] (*Soong@netl.doe.gov; *412-386-4925)*
*M. L. Gray[1] (*Gray@netl.doe.gov; *412-386-4826)*
*R. V. Siriwardane[1] (*Siriwardane@netl.doe.gov; *304-285-4513)*
*K. J. Champagne[1],(*Champagn@netl.doe.gov; *412-386-4589)*
[1]U.S. Department of Energy, National Energy Technology Laboratory,
P.O. Box 10940, Pittsburgh, PA 15236

R. W. Stevens, Jr[2]
P. Toochinda[2]
S. S. C. Chuang[2](Schuang@uakron.edu; 330-972-6993)
[2]Chemical Engineering Department, University of Akron,
Akron, OH 44325-3906

Introduction

Separation and capture of CO_2 have been identified as a high-priority research topic in several DOE's reports.[1,2] The costs of separation and capture, including compression to the required pressure for the sequestration step, are generally estimated to comprise about three-fourths of the total cost of ocean or geologic sequestration. An improvement of the separation and capture of CO_2 will reduce the total cost required for sequestration.

The goal of CO_2 separation and capture is to isolate CO_2 from its many sources in a form which is suitable for transport and sequestration. The most likely options for CO_2 separation and capture include chemical absorption, physical and chemical adsorption, low-temperature distillation, gas-separation membranes, mineralization/biomineralization, and vegetation.[1,2] The CO_2 absorption process using aqueous amine solutions have been extensively used for the removal of CO_2 from gas streams in many industries. This process based on the principles of chemical absorption of CO_2 via monoethanolamine (MEA) or diethanolamine (DEA) is considered to be a potential technique for capturing greenhouse gas emission from flue gas streams. Wet chemical stripping of CO_2 involves one or more reversible chemical reactions between CO_2 and another material such as MEA to produce a liquid species which, upon heating, breaks down to liberate CO_2, and regenerate the original material used to react with CO_2.[3] For example, the monoethanol amine process can be illustrated by the following reversible reaction:

$$C_2H_4OHNH_2 + CO_2 + H_2O \xrightleftharpoons[\text{Hot}]{\text{Cold}} C_2H_4OHNH_3^+ + HCO_3^-$$
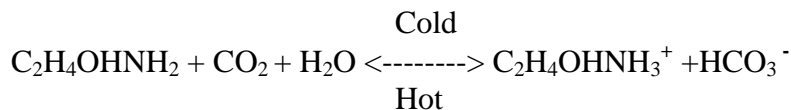
The amines (MEA and DEA) are utilized in the aqueous phase, typically containing 25-30 wt% amine. The amine solution enters the top of an absorption tower while the carbon dioxide containing gaseous stream is introduced at the bottom. While intimately contacting the gaseous stream in a

countercurrent fashion, the amine solution chemically absorbs the carbon dioxide from the gaseous stream. Desorption of the adsorbed carbon dioxide then proceeds via a thermal regeneration process. During desorption, carbon dioxide and water evolve from the amine solution and are separated by condensing the water vapor in a heat exchanger. Once regenerated, the amine solution is recycled back to the absorption tower for additional carbon dioxide absorption.

These processes are, in general, energy intensive. The amine solution has a limited lifetime due to degradation through oxidation of the amine. In addition, corrosion problems are usually observed for the aqueous amine process. Recently, several solid sorbents have been utilized to remove carbon dioxide from enclosed environments such as submarine, aircraft, spacecraft or enclosed pressurized chambers.[4,5] Leal et al., demonstrated the reversible adsorption of CO_2 on amine surface-bonded silica gel.[6] The porous support provides the amine with structural integrity and a surface for gas/solid contact. The ability to regenerate an adsorbent and the ease of its regeneration are also important consideration. The need for extreme conditions such as high temperatures or very low vacuums makes regeneration more complicated and costly.[4]

Objective

The objective of this research is to develop the novel amine enriched sorbents for the capture of CO_2 from flue gas streams. These novel CO_2 capture sorbents can be prepared by the chemical treatment of the surface oxide material with various amine compounds.[4-6]

Approach

The material tested in this study was a fly ash with 8% carbon content, namely, sample 59. The sample was first concentrated via the column agglomeration technique to enhance the concentration of carbon to about 52 %, namely, sample 95.[7] Subsequently, three different amine treatment procedures were applied to sample 95. The treated amine enriched samples were designated as 95A, 95B and 95C.

In order to understand the reaction of CO_2 on these amine-enriched solids and assess their relative CO_2 uptake capabilities, adsorption studies followed by a temperature-programmed-desorption (TPD) technique were conducted under ambient pressure and at temperatures between 30 and 120 °C. Figure 1 illustrates a schematic of the experimental system. All gas flows to the system were regulated with Brooks 5850 mass flow controllers. The 4-port valve allowed for ease of switching between He and 10% CO_2/He flows to the reactor system; moisture was added to either flow stream via a water saturator maintained at ambient temperature (partial pressure of $H_2O = 23.36$ mmHg). A sample charge of 100 mg was used in each experiment; approximately 15 mg was placed into a Spectra Tech diffuse reflectance infrared Fourier transform infrared spectroscopy (DRIFTS) reactor while the remaining sample was charged to a tubular reactor connected to the effluent of the DRIFTS. Separate temperature control systems existed on each reactor. Each reactor had a its own temperature control. The sample in the DRIFTS was examined in situ via a Nicolet Magna 560 infrared spectrometer (IR), allowing observation of CO_2 adsorbate formation/desorption on the sample surface. The gaseous effluent from the DRIFTS-tubular reactor was continuously analyzed by a Balzers QMG 112 mass spectrometer (MS), allowing determination of the CO_2 concentration

in the effluent stream. Capture capacities of the different amine-enriched samples were calculated by MS analysis of the CO_2 (m/e = 44) desorption profile.

Each sample was first exposed to He at a flow rate of 30 ml/min for 3 hours, prior to any further experiment, to clean the sample surface (confirmed by observing stable background signals of both IR and MS).   For the CO_2 absorption study, He flow was then replaced with 10% CO_2 in He at ambient conditions. The moisture content plays an important role in the CO_2 adsorption process; formation of CO_2-amine complexes take place only in its presence. Therefore, after the exposure of 10% CO_2 in He, the flow was redirected through an H_2O saturator; the $CO_2/H_2O/He$ flow over the surface of the sample was maintained for 30 minutes. The $CO_2/H_2O/He$ stream was then replaced by H_2O/He flow to expunge the system of gaseous CO_2.

For the TPD study, the H_2O/He flow was finally replaced with pure He flow to monitor desorption of adsorbed CO_2. Both reactors were heated, simultaneously, from 30 to 120°C at a rate of 10 °C/min and maintained at 120 °C for an additional 20 min. CO_2 desorption amounts were calculated by separate calibration factors that were obtained during each experiment. The calibration factors were obtained by pulsing 1 cc volumes of the 10% CO_2/He (4.089 μmol CO_2) directly to the MS using a 6-port valve. The CO_2 pulse profile (m/e = 44) was integrated and a calibration factor was calculated, equating areas to moles of CO_2. Using this calibration factor, the integrated CO_2 desorption curve could be converted into moles of CO_2 eluded.

Sample regeneration was also assessed via reusing a sample following its adsorption/desorption techniques. Following the TPD, the sample was cooled to ambient temperature and its surface was again cleaned via He flow for 3 h. This was followed by conducting the adsorption and desorption techniques, described above, again.

Results and Discussion

The detail chemical analyses of the amine-enriched sorbents along with the untreated samples are illustrated in Table 1. A significant increase of nitrogen contents from 0.6 to 0.73% was observed on the treated samples.   In addition, the oxygen contents also increase to a great extent from 0.77 to as high as 2.81 % on the enriched amine samples. The increase of the nitrogen contents of the treated samples suggested that some nitrogen-contained species were attached and/or bonded to the treated samples. This implies the presence of amine species on the treated samples.

The typical DRIFTS and TPD results obtained from sample 95C are illustrated in Figures 2 and 3, respectively.   Exposure of the surface to dry CO_2/He flow did not lead to any observable surface CO_2-amine complex formations; only gaseous CO_2 (centered around 2350 cm^{-1}) was observed. When the CO_2/He flow was switched to the $CO_2/H_2O/He$, two distinct bands, 1148 cm^{-1} and 1087 cm^{-1}, were formed shortly thereafter. These bands were assigned tentatively to bidentate carbonate and monodentate carbonate, respectively. It is speculated that the amine chemically absorbs CO_2 and water upon contact with a gaseous stream, thereby forming the amine complexes.   The $CO_2/H_2O/He$ stream was then switched to only He flow until the removal of gaseous CO_2 was completed. For the TPD study, the pure He flow was utilized to monitor desorption of adsorbed CO_2. Figure 3 illustrates that the desorption spectrum of the N_2 (or CO), CO_2, O_2 and H_2O as a function of temperature ramping. Two desorption peaks centered 40 and 110 °C from CO_2

desorption spectra along with the corresponding peaks from H_2O spectra centered around 60 and 120 °C might correlate to the decomposition of CO_2-amine complexes, monodentate carbonate and bidentate carbonate, respectively. The amounts of desorbed CO_2 were calculated by the separate calibration factors obtained for each experiment. The results illustrated in Figure 2 also confirmed that the absorption of CO_2 does not take place in the absence of water and that once flow is switched to He only, the absorbed species can desorb at room temperature. To prevent the desorption of amine-CO_2 complexes during the purging of gaseous CO_2, the $CO_2/H_2O/He$ stream was replaced with H_2O/He instead of only He at the completion of the absorption phase. This proved to be effective method to maintain adsorbates while purging the gaseous CO_2. This finding led to the procedure described above where the TPD is conducted under only He but H_2O/He is used to purge CO_2. It is believed that the presence of moisture is beneficial to the long term stability of the subject material as the carbon dioxide retaining complex is believed to require the presence of a water molecule.[4] These procedures (using H_2O/He instead of He only during the purging of gaseous CO_2) were applied to all samples. To further investigate the stability of the surface amine species, a repeated experiment was conducted on sample 95C. The amounts of desorbed CO_2 from all samples tested are tabulated in Table 1. Samples 59 and 95 showed some CO_2 capture capability and were probably in the forms of physical/chemical adsorption of CO_2. However, the treated samples 95A, 95B and 95C showed significant enhancement of the CO_2 capture capability. The sample 95C showed more than double the amount of CO_2 released compared to the untreated sample. A repeated experiment was conducted on sample 95C. It was seen that its uptake capability was only slightly degraded after being heated to 120 °C (140.6 μmol/g after regeneration vs. 174.5 μmol/g fresh). More importantly, the repeated run for 95C still showed good CO_2 capture results. This suggested that the sample 95C could be regenerated.

In addition to desorption of CO_2, species with m/e of 28 (CO or N_2) and 32 (O_2) were observed in the reactor effluent (Figure 3). If the m/e = 28 profile represents N_2, this profile would be indicative of surface amine decomposition. It is also reasonable that this profile may be representative of CO, which would result if the complexed CO_2 species decomposed to CO and O on the surface. The fates and origins of m/e of 28 and 32 are still under investigation.

In summary, the amine-enriched samples chemically adsorb CO_2 and water upon contact with a gaseous stream, thereby forming the amine complexes. The temperature gradients drive the reaction between the carbon dioxide, water, and amine in the reverse direction, thereby regenerating the amine and releasing the absorbed carbon dioxide and water.

Conclusions

The untreated materials showed some capability of capture/release of CO_2. The results of the samples being modified by various treatments indicated that the amine-enriched sorbents have the potential of capturing/releasing CO_2 and the amine surface is sufficiently stable to withstand regeneration.

References

1. DOE Report DOE/ER-30194, A Research Needs Assessment for the Capture, Utilization and Disposal of Carbon Dioxide from Fossil Fuel-Fired Power Plants," 1993.

2. DOE Report DOE/SC/FE-1, Carbon Sequestration Research & Development," 1999.

3. Blauwhoff, P. M. M., Versteeg, G. F. and Van Swaaij. W. P. M., *Chem. Eng. Scie*.,**1984**. 39 (92), 207.

4. Zinnen; H. A., Oroskar; A. R., Chang; C-H., U.S. Patent 4,810,266 (1989)

5. Birbara; P. J., and Nalette; T. A., U.S. Patent 5492683 (1996)

6. Leal, O; Bolivar, C; Ovalles, C; Garcia, J. J., Espidel, Y., *Inorganica Chimica Acta,* **1995,** 240, 183-189.

7. Gray, M. L., Champagne, K. J., and Soong. Y., Proceedings the 1999 International Ash Utilization Symposium, pp. 603-608, October 18-20, 1999, Lexington, Kentucky

Table 1: TPD CO$_2$ Desorption Results of Amine-Enriched Sorbents

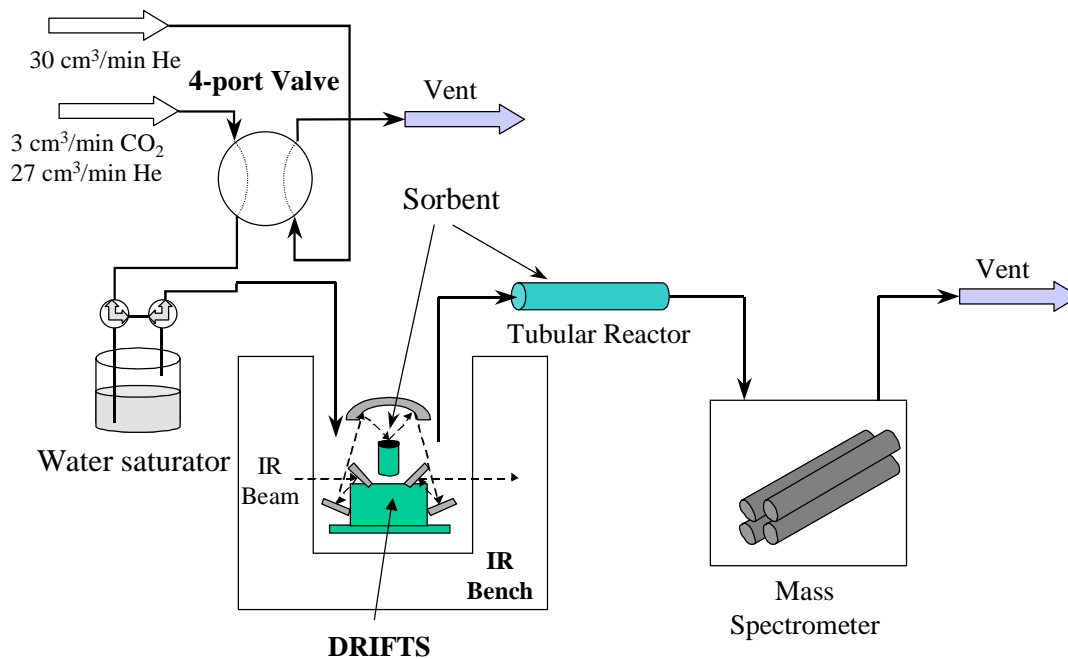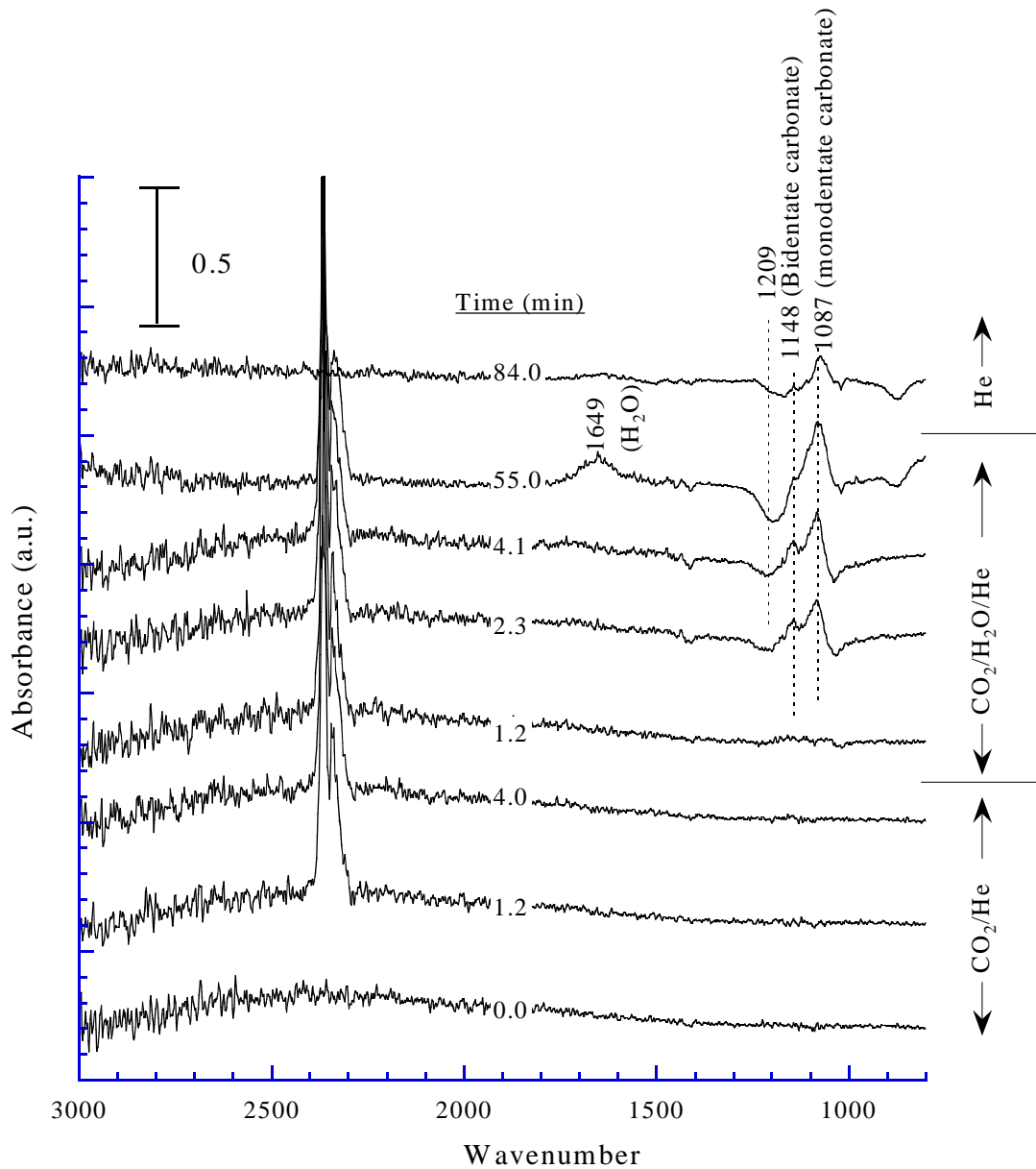| Sample #	Treatment methods	N, %	O, %	CO2 released, μmol/g sample
59 (7% carbon)	none	0.21	0.61	24.4
95 (52% carbon)	none	0.6	0.77	72.9
95A	A	0.73	2.81	81.1
95B	B	0.66	1.78	117.9
95C	C	0.65	2.28	174.5
95C (after regeneration)	C	0.65	2.28	140.6

Figure 1.   Schematic of experimental system.

Figure 2. IR analysis of CO_2 adsorption over 95C at ambient temperature. Feed gas composition to the system are shown between brackets at right; times indicated are relative to points of feed composition changes.
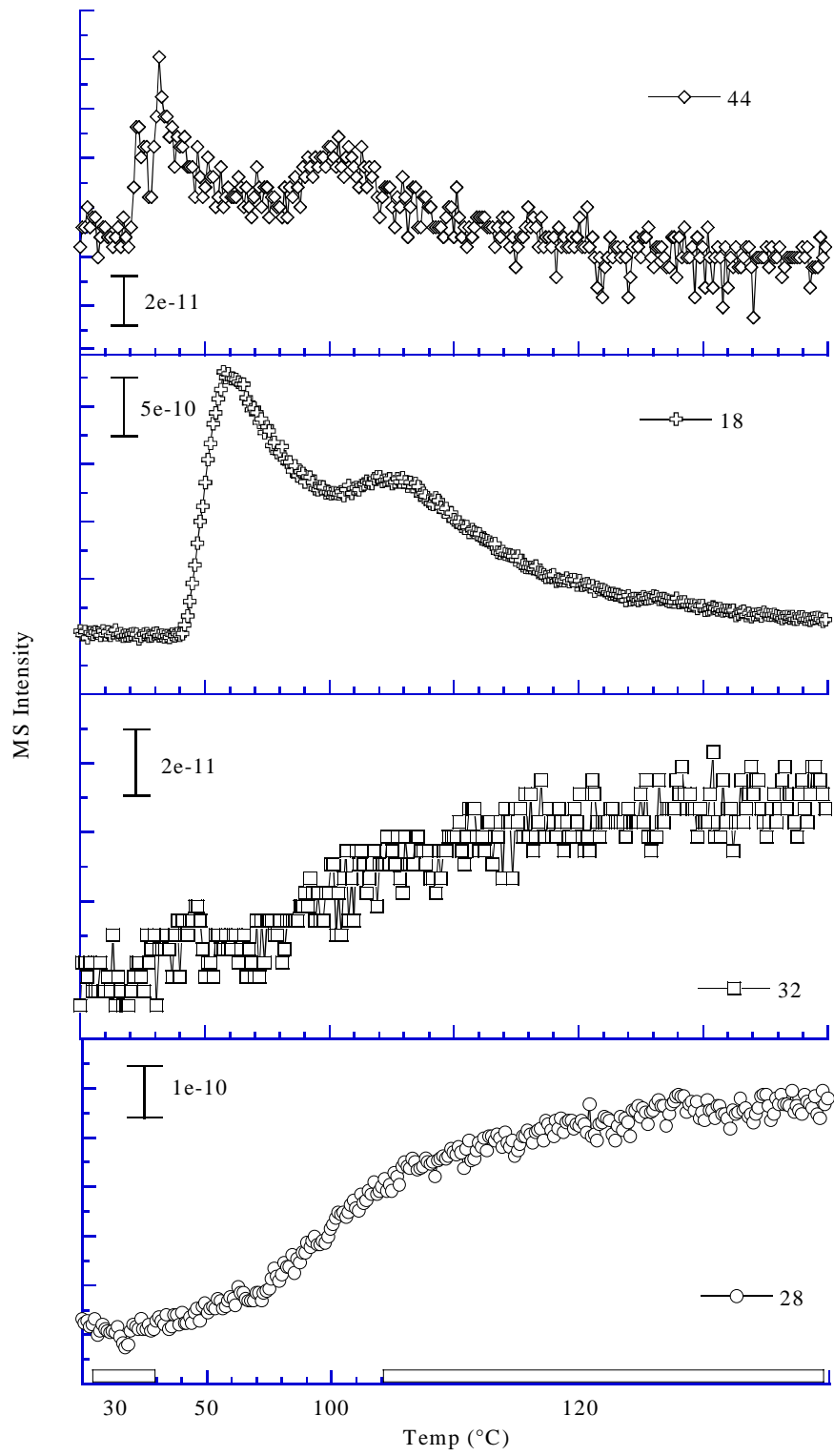
Figure 3.   MS analysis of the CO_2 TPD over 95C in He flow.

Recovery of Carbon Dioxide in Advanced Fossil Energy Conversion Processes Using a Membrane Reactor

Ashok S. Damle *
Research Triangle Institute
P.O. Box 12194
Research Triangle Park, NC 27709
Phone: (919) 541-6146   Fax: (919) 541-6965
E-mail: adamle@rti.org

Thomas P. Dorchak
National Energy Technology Laboratory
P.O. Box 880, Mail Stop C04
Morgantown, WV 26507-0880
Phone: (304) 285-4305   E-mail: tdorch@netl.doe.gov

Abstract

Increased awareness of the global warming trend has led to worldwide concerns regarding "greenhouse gas" emissions, with CO_2 being the single greatest contributor to global warming. Fossil fuels (i.e., coal, oil, and natural gas) currently supply over 85% of the world's energy needs, and their utilization is the major source of the anthropogenic greenhouse gas emissions of CO_2. Advanced coal gasification power plants offer many new opportunities for integrating CO_2 capture. Converting the fuel values to hydrogen by fuel reforming reactions allows CO_2 capture prior to combustion increasing overall power generation efficiency and reducing the cost of CO_2 capture. By conducting fuel reforming with simultaneous hydrogen separation in a catalytic membrane reactor unit, equilibrium-limited reforming reaction is driven to completion with conversion of the fossil fuel energy values to the equivalent of hydrogen fuel. The fuel carbon content is recovered in a compressed, sequestration-ready CO_2 form.

This paper describes development of a membrane reactor process for hydrogen generation by fuel reforming based on palladium-silver alloy/ceramic composite membrane. By utilizing a thin yet structurally stable palladium/ceramic composite membrane hydrogen flux is increased while reducing costs. Electroless plating technique is used to prepare palladium-silver alloy films of about 2 to 3 micron thickness on commercially available tubular alumina substrates. The observed hydrogen flux rates are of the order of 1 gmole/m^2-sec at 500-600 ^{o}C temperature and 40 psi pressure differential. The membrane reactor concept may be used to produce hydrogen by fuel reforming for stationary power generation as well as transportation applications. Adjustment of H$_2$:CO ratio involved in production of liquid fuels/chemicals from synthesis gas is also possible with this concept. This paper presents the results of experimental evaluation and model simulations of the composite membrane performance both as a hydrogen separation unit and as a membrane reactor for fuel reforming.

* To whom all correspondences should be addressed.

Introduction

Increased awareness of the global warming trend has led to worldwide concerns regarding "greenhouse gas" emissions, as evidenced by the recent signing of Framework Convention in Climate Change treaty. Greenhouse gases include CO_2, CH_4, and N_2O and are mostly associated with the production and utilization of fossil fuels, with CO_2 being the single greatest contributor to global warming. Fossil fuels (i.e., coal, oil, and natural gas) currently supply over 85% of the world's energy needs, and their utilization is the major source of the anthropogenic greenhouse gas emissions of CO_2 (Herzog et al., 1997). Primary alternatives to fossil fuels, such as nuclear power and renewable solar energy, must overcome obstacles of public acceptance and exorbitant costs. Near-term approaches based on improving energy efficiency and switching from coal to oil or natural gas have limited impact potential. For sustained fossil fuel utilization to meet the world's energy demands while addressing long-term mitigation of concerns over global climate change, it is necessary to develop cost-effective means to capture and sequester the resulting CO_2. The conventional technology for CO_2 recovery from dilute flue gas after fossil fuel combustion incurs substantial energy penalty. For coal-based power plants, the energy penalty is as much as 27% to 37%, depending on the CO_2 removal process and operating conditions (Herzog and Drake, 1993.) For natural gas-based power plants, the 15% to 24% penalty is lower due to lower fuel carbon content (Herzog and Drake, 1993).

Advanced coal gasification power plants offer many new opportunities for integrating CO_2 capture, for example in an integrated gasification combined cycle (IGCC) power plant (Doctor et al., 1994, 1996). An additional advantage of an IGCC power plant is that its energy conversion is more efficient than coal-fired power plants. IGCC plants first gasify the fuel to produce a pressurized synthesis gas (mainly CO and H_2). After particulate and sulfur contaminants are removed, the synthesis gas is burned in a gas turbine to produce electricity. Additional power is produced using the steam generated during heat recovery from the gas turbine exhaust.

If CO_2 were captured prior to combustion it would require treatment of substantially smaller gas volumes and thus could be less expensive than capture after combustion. CO_2 can be recovered before fuel combustion by reacting the synthesis gas (clean coal gas) with steam in a water gas shift (WGS) reactor to produce CO_2 and additional H_2 by WGS reaction: $(CO + H_2O \Leftrightarrow CO_2 + H_2)$. The CO_2 and H_2 are then separated, the hydrogen is combusted to produce power, and the CO_2 stream is available for disposal. The overall schematic of an IGCC process with CO_2 recovery before combustion is shown in Figure 1. The energy penalty associated with CO_2 capture in such advanced coal power plants, however, is still high at 13% to 17% (Herzog and Drake, 1993).

Available technologies for CO_2 removal from synthesis gas streams include low temperature absorption by amines, glycol, and chilled methanol; hot potassium carbonate process; reaction with calcium oxide; and separation by low temperature polymeric membranes (Doctor et al., 1994). All low temperature processes require gas cooling and heat recovery leading to energy losses. In addition, significant energy is also required (lost) for regeneration in solvent- and reagent-based systems. The major challenge regarding CO_2 capture technology is to reduce the overall costs by lowering both the energy penalty and the capital cost requirements.
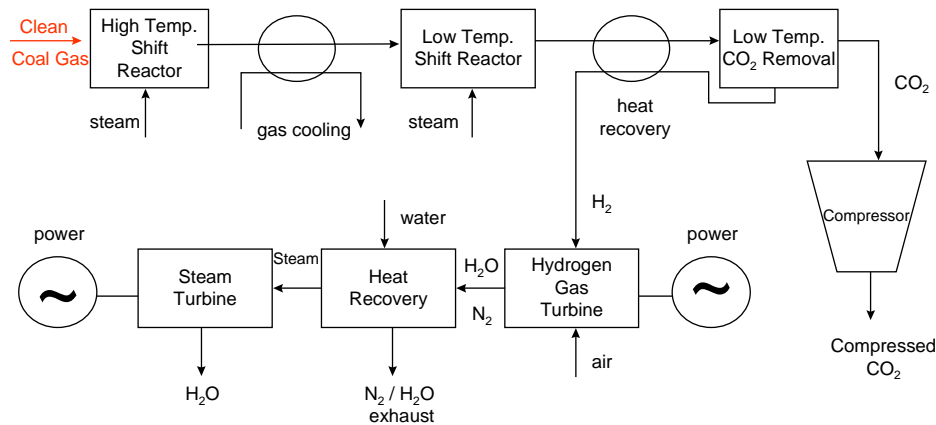
Figure 1. IGCC Process with Conventional CO_2 Recovery before Fuel Combustion

Project Concept

CO_2 capture in an advanced coal power plant, as shown in Figure 1, involves an equilibrium-limited and kinetically inhibited WGS reaction that typically requires two stages with inter-stage cooling. It also requires a separate CO_2 removal step. Additional improvements and cost reductions are possible by combining the WGS reaction and gas separation steps in one high-temperature unit and eliminating the parasitic CO_2 removal step. By continually removing a reaction product in a membrane reactor, thermodynamic and kinetic limitations to the WGS reaction are removed, leading to complete conversion of CO to H_2 (without lowering the gas temperature) as well as simultaneous separation of products. Separation of hydrogen in a membrane reactor will essentially replace the two-step shift reaction units as well as the separate CO_2 removal process by a single unit. Generation of a high purity hydrogen fuel stream will allow utilization of highly efficient alternative power generation technologies, such as PEM fuel cells. A possible schematic for PEM fuel cell power generation coupled with early heat recovery steam generation and steam turbine power generation is shown in Figure 2.
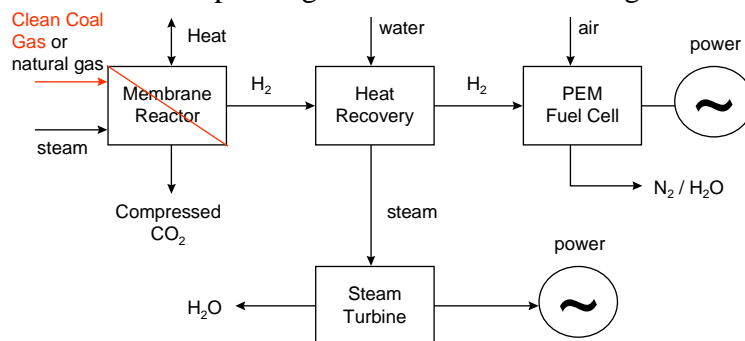
Figure 2. Schematic of Membrane Reactor Process with PEM Fuel Cell

The membrane reactor concept can also be used for power generation from other fossil fuels, such as oil and natural gas. Hydrocarbon liquid fuels, such as diesel oil or gasoline are first vaporized and then reformed with steam to produce synthesis gas containing CO and H_2 similar to coal gas. The CO in synthesis gas is then converted to H_2 by the membrane reactor. In case of

natural gas, the membrane reactor may allow one-step steam reforming with hydrogen separation leaving behind a compressed CO_2-rich stream.

For the membrane reactor concept, a hydrogen- (or CO_2) selective membrane capable of operating in a high-temperature, high-pressure environment is needed. Micro-porous inorganic membranes based upon Knudsen diffusion separation exhibit low separation factors (e.g., $H_2:CO_2$ separation factor of 4.7). Moreover, the separation ability of the commercially available 4 nm pore size gamma-alumina membranes depends upon the stability of the membrane pore size, which is adversely affected by the action of steam (Damle et al, 1995). The dense ceramic membranes based on inorganic perovskite oxides need considerably high temperatures, greater than 800 ^{o}C, to achieve practical hydrogen flux rates. Palladium-based dense membranes are known for their high hydrogen selectivity and permeability over other gases. Although palladium alloy tubes have been available for several decades, they are expensive for commercial applications due to the thickness needed for structural stability. The tubular membranes also exhibit low hydrogen flux rates due to their thickness. In order to be suitable for the target application, a hydrogen separation membrane must have adequate selectivity and flux rate and must be stable in the reducing coal gas or fuel reforming environment containing steam and hydrogen sulfide. The membrane module must also be economically competitive.

Project Objectives

The overall objective of the U.S. DOE sponsored program at RTI is to develop an inorganic composite palladium-based membrane reactor module that is structurally stable under the fuel reforming WGS reaction conditions with a high selectivity and flux rate for hydrogen permeation through the membrane. For membrane structural stability, the emphasis is on developing sulfur resistant palladium-silver alloy composite membranes. To maximize flux rates and to minimize cost, thin yet durable composite membranes with commercially available substrates are desirable. Another objective of this program is to demonstrate simultaneous WGS reaction with CO_2/H_2 separation using the membrane reactor at a bench scale in Phase II efforts and at a pilot scale at a host site in Phase III efforts. A membrane reactor must be able to carry out the WGS or fuel-reforming reaction to its desired conversion level while permeating all of the hydrogen produced in the reactor. Thus, the development of this technology must take into account reaction kinetics and reforming operating conditions in addition to the membrane permeation characteristics. Requirements for successful development and demonstration of the membrane reactor process through Phase III program are: (1) hydrogen-selective membrane reactor unit, (2) synthesis gas reforming with CO_2/hydrogen separation, (3) power generation unit (PEM fuel cell or hydrogen turbine), and (4) integration of all components.

Technical Approach

A number of recent studies have been directed toward synthesizing palladium-ceramic composite membranes to reduce the palladium-layer thickness while providing the structural integrity. Several approaches have been used to produce the thin-film membranes: physical vapor deposition (PVD), chemical vapor deposition (CVD), electroplating, compression cladding, sputtering, spray pyrolysis, and electroless plating. Of these methods, CVD and electroless

deposition methods have been considered as most promising. In our efforts, the electroless plating method is preferred over CVD for several reasons. Electroless deposition provides thin metal and metal-alloy films that have excellent adhesion properties; the deposition rate is high, and it can be easily controlled. Further, this is an auto-catalytic process that does not require any expensive setup. On the other hand, the CVD process requires appropriate stable organo-metallic precursors which may be expensive. The CVD process does provide film that has fair adhesion properties, and the deposition rate is high, but the rate cannot be controlled. It would also be difficult to deposit two species simultaneously for fabrication of palladium alloy membranes. Furthermore, CVD requires expensive and elaborate setup. The challenge in synthesizing composite membranes is to obtain uniform, defect-free coating, as even small pinholes would be detrimental to the hydrogen selectivity.

Pure palladium metal becomes brittle in presence of hydrogen and is prone to distortions during thermal cycling due to the dimensional changes caused by transformations between the α-phase palladium, which is stable at low temperatures, and the β-phase palladium, which is stable at high temperatures. Alloying elements such as Ag stabilizes the β-phase against the α-phase, substantially reducing metal embrittlement. Pd-Ag alloy also exhibits greater permeability for hydrogen than pure palladium at similar conditions. An alloy with 23% Ag and 77% Pd has been shown to have the maximum permeability as well as dimensional stability (Shu et al., 1993; Uemiya et al., 1991). Although, theoretically palladium is stable in reducing hydrogen environment at low levels of H_2S below 100 ppm (Krishnan et al., 1993), it must be protected against system upsets in the upstream desulfurization process. Platinum has been shown to be highly resistant to H_2S attack with a surface penetration of only 30 nm in the presence of 1.2% H_2S at 600 ^oC (Damle, 1995).

The focus in these efforts has therefore been on developing thin palladium-silver alloy composite membranes with a thin protective noble metal coating. Commercially available ceramic (alumina) micro- and ultra-filtration membranes are used as substrates for deposition of hydrogen-selective layers. By reducing the thickness of the palladium membrane, the hydrogen flux rate is increased while decreasing the cost of the membrane.

The electroless plating technique for palladium has been well known and involves pretreatment of the substrate, sensitization and activation of the substrate surface, and electroless plating with palladium deposition which is a combination of cathodic deposition of metal and the anodic oxidation of reductant:

Anodic Reaction: $\quad\quad\quad N_2H_4 + 4\,OH^- \;\rightarrow\; N_2 + 4\,H_2O + 4\,e^-$

Cathodic Reaction: $\quad\quad 2\,Pd[NH_3]_4^{2+} + 4\,e^- \;\rightarrow\; 2\,Pd^0 + 8\,NH_3$

Autocatalytic Reaction: $\quad 2\,Pd[NH_3]_4^{2+} + N_2H_4 + 4\,OH^- \;\rightarrow\; 2\,Pd^0 + N_2 + 4\,H_2O + 8\,NH_3$
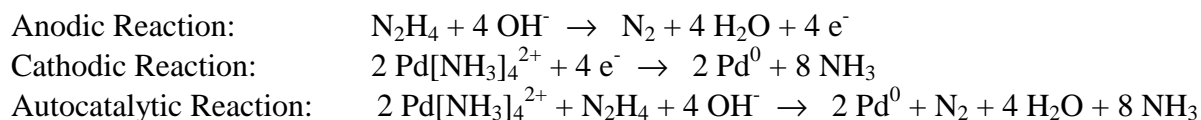
Each of the three steps is critical for uniform deposition of the palladium metal film. The sensitization and activation process, involving adsorption of Sn^{2+} ions on the substrate followed by substitution by Pd, produces finely divided palladium metal nuclei on the substrate that initiate the autocatalytic plating process. A similar reaction scheme can also be used for depositing other metals, such as silver, which is also of interest here.

The WGS reaction ($CO + H_2O \Leftrightarrow CO_2 + H_2$) is well known and is usually carried out in two stages: a high temperature (up to 550 ^{o}C) stage e.g. over Fe or sulfur tolerant Co-Mo based catalysts and a low temperature (175 - 205 ^{o}C) stage over copper based catalysts (Newsome, 1980). The reaction is mildly exothermic and lower temperature favors conversion of CO. Since the equilibrium limitation is removed in a membrane reactor, the reaction can be carried out at a single high/intermediate temperature. The palladium composite membrane module can be used as a reactor/separator by packing appropriate catalyst pellets on the reactant side of the module. The key issue in such membrane reactor design is matching the hydrogen flux rates with the rate of the reaction. The reactant space velocity in the membrane module is dictated by the reaction kinetics and needed conversion. The hydrogen flux rate is determined by the hydrogen partial pressure gradient across the membrane and the membrane surface area.

The natural gas reforming reaction ($CH_4 + H_2O \Leftrightarrow CO + 3H_2$) is also well studied, especially for hydrogen production, and is typically carried out over Ni-based catalyst at 400 psig and 750 ^{o}C. This reaction is endothermic and is also yield limited. WGS reaction is subsequently carried out to increase hydrogen yield. The use of membrane reactor may allow one-step reforming to produce hydrogen. In this program only commercially available catalysts will be utilized.

Results

In this program, the efforts to-date have been focussed on establishing procedures for depositing thin, uniform, defect-free palladium-silver alloy films on porous substrates. Bulk of the work so far has been conducted with commercially available porous alumina micro- and ultra-filtration membrane substrates. Techniques were developed to deposit metal alloy films on porous substrates by electroless plating process assuring uniform defect-free dense metal alloy films. A technique has also been demonstrated for deposition of a uniform ultrathin (~20 nm) platinum layer on the membrane to provide resistance to low levels of H_2S typically present in syngas following desulfurization. The overall membrane synthesis process is amenable for easy scale up and process automation and for plating longer tubes and multi-channel monolithic elements.

Membrane characterization studies have been conducted with short 2" long tubular sections as well as with 10" long tubular elements of 10 mm OD and 7 mm ID. Composite membranes were analyzed by scanning electron microscopy (SEM) and energy dispersive X-ray elemental analysis (EDAX) techniques to determine membrane thickness, structure, integrity, and elemental composition. The plating technique allows varying film thickness and composition by depositing multiple metal layer films and alloy films from 1 to 5 micron thickness have been synthesized. The metal films are annealed in flowing inert gas atmosphere (nitrogen or argon) to homogenize the film to assure uniform composition throughout the film cross-section. Figure 3 shows an example of a three-layer 1.5 μm metal composite film, prior to annealing, whereas, Figure 4

shows an example of an annealed homogenized metal/ceramic composite film. Both figures show excellent adhesion of the metal films to the porous ceramic substrates.

Pd—
Ag—
Pd—

Ceramic

000005 15KV X20.0K 1.50um

000003 15KV X20.0K 1.50um
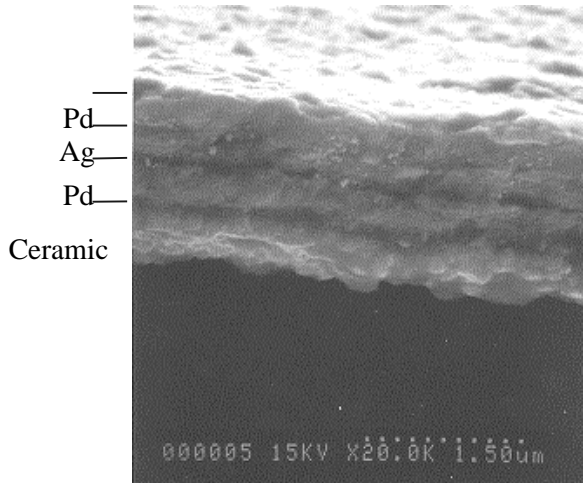
Figure 3. Metal Film Before Annealing   **Figure 4. Metal Film After Annealing**
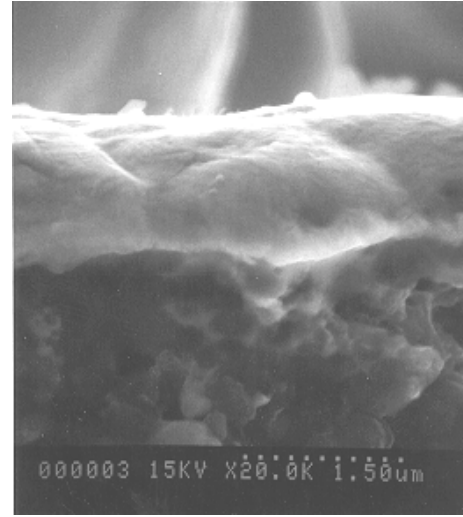
The permeation characteristics of the composite membranes were determined by single pure component permeation as well as mixed gas permeation testing at various temperatures and trans-membrane pressure differentials. Figure 5 schematically shows the tubular membrane test apparatus used for permeation testing.
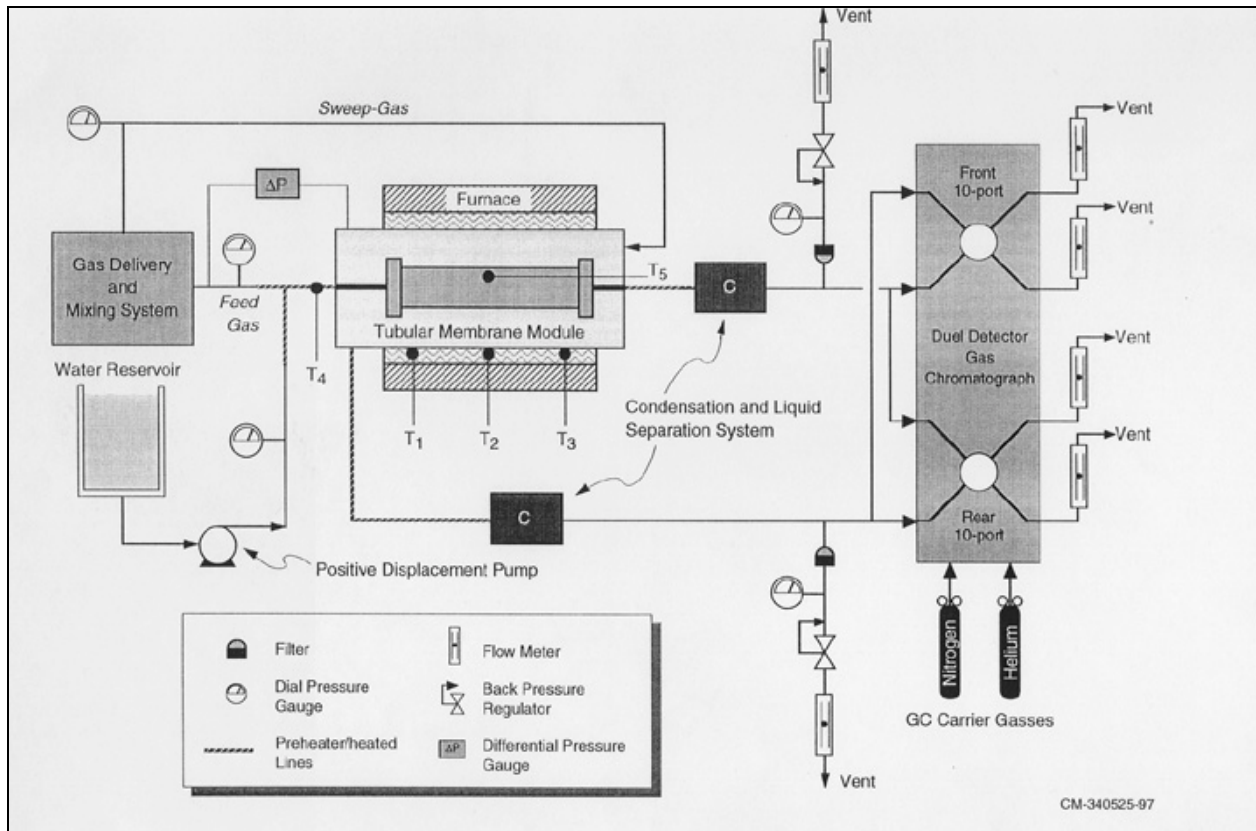
Figure 5. Schematic of Tubular Membrane Test Apparatus

The permeation test system consists of a gas mixing and delivery manifold, a controlled temperature furnace, a gas chromatograph (GC) equipped with gas sampling valves, and an integrator to analyze the GC data. The gas delivery system allows multi-component feed gases for mixed permeation and selectivity testing. The tubular furnace comprises of cylindrical heating elements capable of controlling temperature up to 800 ^{o}C. Back-pressure regulators (BPRs) control the feed and permeate side pressures independently at the desired levels. GC samples can be drawn from both the feed exhaust and sweep lines.

For sealing the ceramic tubes, in-situ-formed graphite ferrules were used with Swagelok metal reducing unions bored to allow close fitting with the 10 mm OD ceramic tubes. The leak rate at the graphite seals was found to be variable and was found to permit nitrogen leak rate from 0 to 10 cc/min. The leak rate was found to decrease with temperature as expected due to increasing gas viscosity with temperature. Although, this leak rate was more than two to three orders of magnitude smaller compared to the observed hydrogen permeation rates, it contributed to 100% of the observed nitrogen permeation rate thus affecting the mixed gas selectivity measurements.

The observed hydrogen permeation rate depends upon the film thickness, the substrate pore size, alloy composition, and the operating conditions of temperature and hydrogen partial pressure differential. Figure 6 shows typical observed annealed membrane flux rates.

Figure 6. Hydrogen Flux with Temperature, Membrane L21

The observed hydrogen permeances range from 16 to 80 gmoles/m^2-min at 500-600 ^{o}C temperature and 40 psi hydrogen partial pressure differential. The observed hydrogen to nitrogen

selectivity of these membranes range from 150 to 10,000 in mixed gas experiments, primarily influenced by leak rate at the seals .

Recently, porous stainless steel substrates in both flat and tubular geometry were evaluated for depositing metal films. SEM scan of the composite membrane cross-section (Figure 7) shows excellen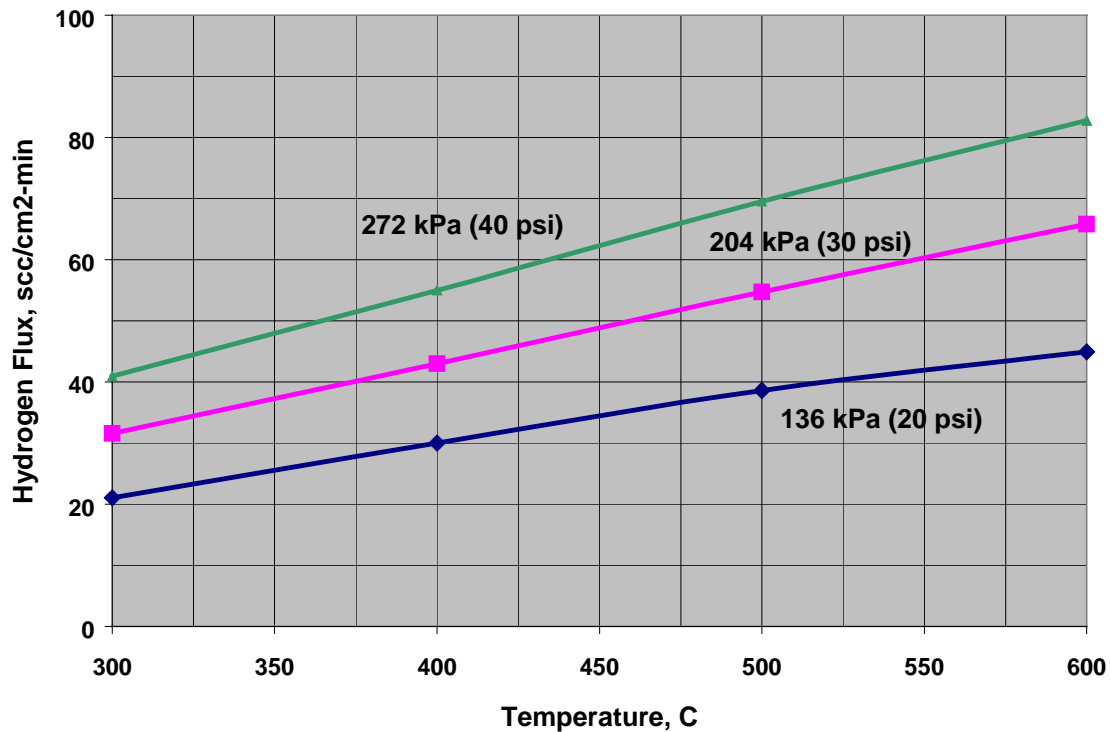t adhesion and complete surface coverage by the metal film as well as cohesion between different layers in spite of the surface roughness of the steel substrate. Tubular sintered metal composite membrane samples are currently being prepared for hydrogen permeation evaluation. Metal substrates have an obvious structural advantage over ceramic substrates. For using ceramic substrates for gas separation application, effective sealing technique is essential. The ongoing program, in collaboration with ORNL scientists, has indicated feasibility of a brazing technique to join ceramic tubes to metal tubes allowing metal fittings to house ceramic elements.

Figure 7. 3-Layer Plating on Porous Stainless Steel Substrate

Simple, one-dimensional model simulations of the membrane reactor concept were conducted to determine the effect of simultaneous hydrogen separation on CO conversion in the WGS reaction. Figure 8 schematically shows the one-dimensional membrane reactor.
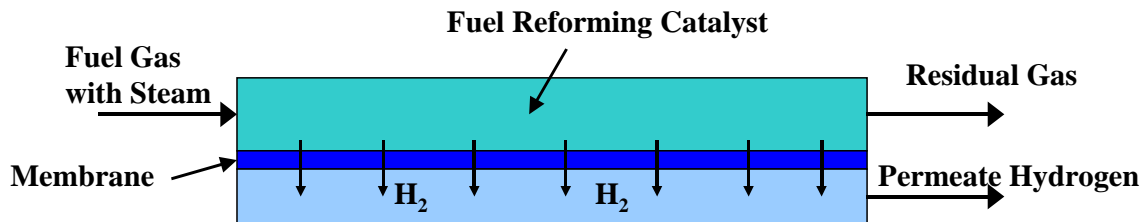
Figure 8. Schematic of a One-Dimensional Membrane Reactor Model

The basic assumptions of this simple model are: 1) temperature and total pressure are constant on both permeate and feed sides; 2) reaction kinetics is faster than the hydrogen permeation flux rates allowing the feed side to be in dynamic equilibrium; and 3) hydrogen flux is determined by the local driving force. One target application of the membrane reactor concept is to convert synthesis gas derived from coal gasification to hydrogen for power generation by PEM fuel cells. Gas composition typical of a coal gas generated by an oxygen blown gasifier was used as the dry feed gas composition in the model simulations (H_2 – 36%, CO – 47%, and CO_2 – 17%.) Model simulations were conducted at steam to CO mole ratios of 1:1, 1.5:1, and 2:1 to determine the effect of steam to CO ratio on CO conversion and the membrane area requirements. A feed gas pressure of 20 atm and the permeate hydrogen pressure of 1 atm was assumed with an effective pressure ratio of 20. Predicted CO conversions and total hydrogen recovery are shown in Figure 9 as a function of stage cut fraction for steam to CO ratio of 1:1. As seen from this figure, CO conversion continues to increase as more and more hydrogen is withdrawn from the membrane

reactor. The eventual CO conversion and hydrogen recovery are essentially limited only by the hydrogen partial pressure in the residual gas which must be greater than the permeate pressure for hydrogen permeation. Typical target overall hydrogen recovery would be about 80% with the residual gas heating value used for the reactor. The model simulations also indicate the feasibility of using low steam to CO ratio provided carbon formation is avoided by utilization of appropriate catalysts.
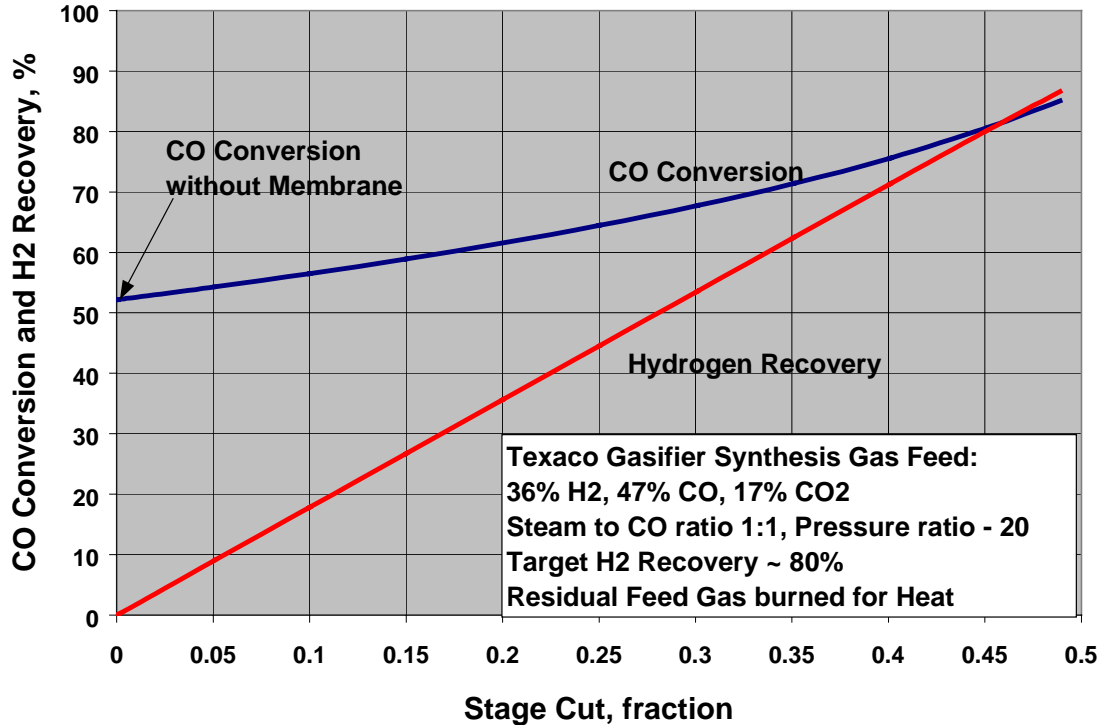
Figure 9. Increase in Equilibrium Conversion with Hydrogen Separation

Based on the observed hydrogen permeation rates the membrane area required was estimated at about 100 cm^2/kW equivalent hydrogen generation (1 g/min). For a 100 kW equivalent unit the estimated module area is about 1 m^2. Due to the thin metal film in the composite membrane, the cost of the ceramic substrate is expected to constitute bulk of the composite membrane cost. Inexpensive ceramic substrates are therefore being investigated.

Based on a preliminary techno-economic analysis four possible applications have been identified for the membrane reactor concept:

- Distributed power generation – Reforming of fuel gas to hydrogen with power generation by PEM fuel cells (~ 50-500 kW)
- On-board fuel reforming for automobiles (~50 kW)
- Hydrogen separation and H$_2$:CO ratio adjustment for liquid transportation fuels production – Vision 21 Energyplex
- Portable power generation – Micro-channel reactor/PEM fuel cells (~ 20-200 W)

Potential Benefits

The membrane reactor technology will have a substantial impact on the new generation of advanced fossil fuel power plants and has the potential to capture all of the carbon content before combustion cost effectively. This technology would also fit very well in the Vision 21 energyplex concept. An important application of the proposed membrane reactor concept is in "distributed power generation" complexes for large facilities such as shopping centers or apartment complexes. Power generation systems such as PEM fuel cells are attractive for distributed power generation. The palladium-based membrane reactor concept is especially well-suited for these applications since it can provide the high-purity hydrogen needed for PEM fuel cells while capturing all carbon as compressed CO_2. Stationary power applications in the <50 kWe range are a good fit with steam reforming of natural gas coupled with palladium membranes for hydrogen separation and PEM fuel cells power generation. Table 1 summarizes the total market potential for fuel cell distributed power systems (EPRI Report TR-1006645, August 1996). The potential for CO_2 capture by a membrane reactor process is approximately 270 tons CO_2/year in a 50 kW plant. About 4800 small-scale generators with a cumulative power of 9512 MW were operating in 1996-97 with an approximate capacity growth of 250 MW. For the new capacity growth alone, the potential impact of the proposed technology is estimated to be 1.6×10^6 tons of CO_2 /yr.

Table 1. Potential Applications of Fuel Cell Distributed Power Systems

Size Range	# of Potential Applications
<15kW	935,000
15-20kW	99,000
20-30kW	131,000
30-40kW	67,000
40-60kW	64,000
60-100kW	62,000
100-500kW	85,000
500-1000kW	8,000
>1000kW	5,000

In spite of energy conservation measures, the demand for energy continues to rise. In U.S. alone, energy consumption is estimated to increase from 91 quads in 1995 to 111 quads in 2015 or almost 1 quad/year (Winslow, 1997) with a corresponding increase in CO_2 emissions of almost 200 million tons/year. Coal based energy use is expected to increase from 20 quads in 1995 to 24 quads in 2015 or about 0.2 quad/year. About a third of the total energy increase and almost all of the coal energy increase is expected for power generation. Utilization of advanced power generation with CO_2 recovery prior to combustion using the proposed membrane reactor process will reduce the increase in CO_2 emissions as well as costs of CO_2 capture significantly.

The demand for transportation fuels is expected to increase from 17 million bbls/day in 1995 to 21 million bbls/day in 2015 (Winslow, 1997) or about 0.44 quads/year resulting in about 90 million tons/yr. increase in CO_2 emission. Due to declining oil production, it will be necessary to develop advanced Pioneer plants for producing transportation fuels from coal. The proposed

membrane reactor can be effectively used to process part of the synthesis gas to adjust the H_2:CO ratio, simultaneously capturing carbon content of the processed gas as compressed CO_2.

Hydrogen is an important high-volume feedstock in the chemical industry, e.g. in ammonia synthesis in fertilizer industry, and for hydro-cracking and hydrogenation processes in petrochemical industry. Commercial production of hydrogen by steam reforming of hydrocarbons, most commonly natural gas, is a significant contributor to CO_2 greenhouse gas emissions. Thus, the membrane reactor concept will be directly applicable for commercial hydrogen production.

Future Activities

The planned future activities in the current DOE Phase II program include experimental demonstration of the membrane reactor process with a single tube element of 50 cm^2 surface area using simulated coal gas composition as feed gas. The experiments will determine the effect of steam to CO ratio and stage cut fraction on the CO conversion and hydrogen recovery and will compare the results to the model simulations similar to those shown in Figure 9. Tubular sintered porous metal substrates will also be evaluated for hydrogen permeation characteristics.

Acknowledgement

References

1. Damle, A.S., G.N. Krishnan, A. Sanjurjo, B.J. Wood, and K.H. Lau, "Thermal and Chemical Degradation of Inorganic Membrane Materials," Final Report Submitted to U.S. DOE, May 1995.
2. Doctor, R.D., J.C. Molburg, P.R. Thimmapuram, G.F. Berry, and C.D. Livengood, "Gasification Combined Cycle: Carbon Dioxide Recovery, Transport, and Disposal," ANL/ESD-24, Argonne National Laboratory, Argonne, IL, September 1994.
3. Doctor, R.D., J.C. Molburg, and P.R. Thimmapuram, "KRW Oxygen-Blown Gasification Combined Cycle: Carbon Dioxide Recovery, Transport, and Disposal," ANL/ESD-34, Argonne National Laboratory, Argonne, IL, 1996.
4. EPRI Report TR-1006645, August 1996
5. Herzog, H., E. Drake, and E. Adams, "CO2 Capture, Reuse, and Storage Technologies for Mitigating Global Climate Change," Final Report, DOE Order No. DE-AF22-96PC01257, January 1997.
6. Herzog, H.J. and E.M. Drake, "Long-Term Advanced CO2 Capture Options," IEA/93/0E6, IEA Greenhouse Gas R&D Programme, Cheltenham, UK, 1993.
7. Krishnan, G.N., A. Sanjurjo, B.J. Wood, and K.H. Lau, "Thermal and Chemical Degradation of Inorganic Membrane Materials," Topical Report Submitted to U.S. DOE, December, 1993.
8. Newsome, D.S., Catal. Rev. Sci. Eng., 21(2): 275-318, 1980.

9. Shu, J., B.P.A. Grandjean, E. Ghali, and S. Kaliaguine, "Simultaneous Deposition of Pd and Ag on Porous Stainless Steel by Electroless Plating," J. Membrane Science., 77: 185-195, 1993.

10. Uemiya, S., N. Sato, H. Ando, Y. Kude, T. Matsuda, and E. Kikuchi, J. Membrane Sci., 56: 303, 1991a.; Uemiya, S., T. Matsuda, and E. Kikuchi, J. Membrane Sci., 56: 315, 1991b.

11. Winslow, J., Presentation at the U.S. DOE Coal Liquefaction Workshop, Pittsburgh, PA, Sept. 1997.

Study of Regenerable Sorbents for CO_2 Capture

James S. Hoffman (jhoffman@netl.doe.gov; 412-386-5740)
Henry W. Pennline (pennline@netl.doe.gov; 412-386-6013)
National Energy Technology Laboratory
U.S. Department of Energy
P.O. Box 10940
Pittsburgh, PA 15236

Introduction

Carbon dioxide (CO_2) is a greenhouse gas that is customarily released to the environment during the usage of fossil fuels, including electric power generation. With the projected increase in consumption and demand for fossil fuels, CO_2 emissions will correspondingly increase in the absence of any capture/sequestration strategy. In view that CO_2 is a greenhouse gas with the potential to contribute to global climate warming, existing and improved technologies to mitigate the release of CO_2 to the environment are being considered as a prudent precaution against global warming. Industry, if mandated to remove CO_2 from gases emitted to the atmosphere, will certainly require improved and novel technologies for the removal of CO_2.

Carbon dioxide can be removed from flue gas and waste gas streams produced from carbon usage by various methods, that include absorption with a solvent, membrane separation, cryogenic fractionation, and adsorption using molecular sieves [Herzog et al., 1997]. Capture of CO_2 from each of these processes is costly. Another technique for removal of carbon dioxide is dry scrubbing or chemical absorption of CO_2 with a solid sorbent. The development of dry, regenerable scrubbing processes for CO_2 capture is the focus of the current study.

Objective

The objective of the study is to identify and evaluate novel sorbents that potentially could be utilized in a dry, regenerable scrubbing process for the capture of CO_2 from gaseous streams. Of particular interest are sorbents containing alkali- and alkaline-earth metals distributed onto a substrate support. Specifically, potassium carbonate and calcium oxide are the subjects of the experimental investigations. The chemical reactions for CO_2 capture using these compounds are shown in reactions 1 and 2. The forward reaction path depicts absorption of CO_2, whereas regeneration is expressed as the reverse reaction path.

$$K_2CO_3 + CO_2 + H_2O \iff 2KHCO_3 \qquad (1)$$

$$CaO + CO_2 \iff CaCO_3 \qquad (2)$$

The use of alkali- or alkaline-earth metals for CO_2 capture has been previously reported in the literature. Work by Japanese researchers encompassed the potential use of potassium, sodium, and

lithium compounds as CO_2 sorbents [Hayashi et al., 1998]. Potassium carbonate was emphasized as a good candidate while utilizing an activated carbon as the substrate material. Earlier studies by the same researchers [Hayashi et al., 1995; Hirano et al., 1995] examined the use of other substrate materials, including silica gel and alumina.

The use of potassium carbonate, in addition to other alkali-metal materials, was studied by the space agency (NASA) as a regenerative means by which to absorb CO_2 and H_2O [Onischak et al., 1978]. The intent was to develop portable life support systems to scrub breathing air during human space travel. Japan, in conjunction with development of the space station with NASA, also pursued regenerable solid sorbents for space travel using a solid amine [Otsuji et al., 1987]. Some of the yet earlier space work considered molecular sieves, clathrates, and zeolites for regenerable solid sorbents for CO_2 capture [Martin, 1969; Trusch, 1967; Remus et al., 1969].

In other work, silver was used to capture CO_2 [Nalette et al., 1992]. The unsupported solid sorbent was composed of silver carbonate in a combination of alkali metal silicate (sodium and/or potassium), alkali metal carbonate (cesium, potassium and/or sodium), and an alkaline earth metal salt (nitrates and chlorides of calcium, magnesium, and/or barium). An example was cited for a sorbent comprised of calcium nitrate, sodium silicate, potassium carbonate, and silver carbonate. The same authors also investigated amine compounds on solid supports for CO_2 sorbents [Bibara et al., 1999].

The use of calcium, an alkaline earth metal, for CO_2 capture in a dry, regenerable sorbent process, has been proposed in prior studies. The carbonation reaction is employed in the CO_2 Acceptor Process developed several decades ago for coal gasification [Curran et al., 1967]. A summary of the process [Elliott, 1981] describes the gasification of coal by steam. The energy required for gasification is partially supplied by the exothermic carbonation reaction of dolomitic lime.

Of more recent notable interest is a series of papers by several investigators [Siliban et al., 1995; Siliban et al., 1996; Han et al., 1997]. The effects of temperature, pressure, and reactive gas composition on the gas-solid reaction was examined in an electrobalance reactor. Multicyle tests were conducted to demonstrate the durability of the material. Some degradation of the material was observed during multicycle tests. Calcined dolomite, a mixture of $CaCO_3$ and $MgCO_3$, proved to be superior in performance to calcined $CaCO_3$. It should be noted that these studies were conducted using fine, unsupported, powdered materials and are therefore much smaller than the sorbents under consideration in the current study.

Approach

Prior to the experimentation, a thermodynamic analysis was conducted for some proposed alkali- and alkaline-earth sorbents of interest. Enthalpy and free energy changes were calculated for both absorption and regeneration reactions. Equilibrium constants were formulated over a range of temperatures. Results for alkali-based sorbents are generally favorable in that the forward (CO_2 absorption) reaction rate is typically much larger than the reverse reaction. Thermodynamic analysis identified ranges of temperature for absorption and regeneration to be thermodynamically feasible.

The approach undertaken in the study was to investigate sorbents using two reactor systems; a thermogravimetric analyzer (TGA) and a packed-bed reactor. For the TGA system, change in sample weight was recorded as the sorbent was exposed to gases under conditions representative of absorption and regeneration. The extent of chemical reaction was linked to sample weight change, from which kinetic rate parameters could be estimated. In the packed-bed reactor system, process gases were flowed through a stationary bed of sorbent. The effluent from the reactor was fed to continuous emission monitors (CEM), facilitating on-line measurement of gas composition, including CO_2, and thus the breakthrough curve.

Project Description

Experiments were performed using a microbalance assembly consisting of a Cahn TG-131 Thermogravimetric Analyzer (TGA). Gas composition that approximately simulates flue gas was created by blending high purity gases using mass flow controllers (Brooks model 5850E controller and Brooks model 5878 instrument readout). Carbon dioxide of stock gas grade (99.99%) was supplied by gas cylinder and pressure regulator, and a house supply of dry nitrogen was utilized. The gas stream was humidified using a sparger vessel. Gas relative humidity was verified using a Vaisala HMP-36 humidity/temperature probe and a Vaisala HMI-32 instrument readout. Moisture-laden gas streams were heat-traced with electrical heating tapes and controlled by variable autotransformers (Variac). A heated section had one heating tape with one thermocouple mounted on the external surface. The electrical power to the tape was manually governed by Variac setting to achieve a temperature readout in excess of the dew point to prevent condensation. A circulating bath (Haake) of ethylene glycol/water was used to provide fine temperature control of the gas mixture prior to the gas entering the reactor.

Approximately 200 mg of sample was placed in a quartz cylindrical sample pan. Slotted apertures in the bottom and side wall of the sample pan help mitigate gas diffusional resistance. Sample temperature was measured and controlled with a type K thermocouple placed immediately below the suspended sample pan. Total gas flow rate was held constant at 140 cc/min. For the typical baseline condition during CO_2 absorption, the gas inlet composition (vol%) was typically 10% CO_2, 10% H_2O, and 80% N_2, at a TGA reactor temperature of 60°C.

After charging the sorbent to the TGA, the sample was preconditioned and dried in nitrogen by elevating the reactor temperature to 150°C for approximately 4 hours. This preheating near the thermal regeneration temperature assured that the initial chemical state of the sample contained only reactant material (potassium carbonate) and no product material (potassium bicarbonate). The sample was then cooled to the desired absorption temperature and allowed to come to steady state, both thermally and gravimetrically.

The sample was then preconditioned with humidified gas by switching the sparger in-line, whereby nitrogen was flowed through the heated reservoir of water in the sparger. The ability of the sparger to achieve saturation of the nitrogen gas was verified with a sampling probe measuring relative humidity and gas temperature. The humidity probe was independently calibrated against several standards including saturated salt solutions.

Once the sample achieved steady state under humidified conditions, carbon dioxide was added to the water/nitrogen mixture. Nitrogen gas flows were adjusted so that the sample was exposed to the same level of moisture (10%) and total flow rate (140 cc/min) prior to the introduction of CO_2. The CO_2 absorption stage was allowed to proceed until a steady-state weight gain was achieved.

The sequence of gas switching was then reversed. First CO_2 was turned off, eventually followed by a termination of the humidification. The motivation for observing the sample during CO_2 isolation was to verify what fraction of the weight gain during absorption was indeed permanent weight gain by chemical reaction to form bicarbonate. Some of the weight gain was due to physical sorption of CO_2, most likely onto the alumina substrate. Once the sample was exposed to a gas lacking carbon dioxide (i.e., moist N_2), sorbed CO_2 would then desorb from the substrate, resulting in sample weight loss. This difference in the initial and final sample weight under humidified conditions represented chemical CO_2 uptake by the sorbent, from which an overall sorbent utilization was calculated based on the metal loading and theoretical weight gain due to bicarbonate formation.

Experiments were conducted at larger scale in a packed-bed reactor to supplement the information obtained during TGA testing. The reactor is comprised of a quartz tube measuring 40 mm internal diameter by 450 mm length. Sorbent sample was placed on a fritted filter in the center of the quartz tube, and then positioned at the center of a 400 mm clam-shell furnace. The furnace has a heating zone of 300 mm length and is controlled by a linear programmable controller. Bed temperature was measured and controlled through the use of a dual type J thermocouple located in the sample bed. A sample charge of 75 grams of sorbent resulted in a bed height of about 3 inches, and the thermocouple was positioned at approximately the 1-inch bed height, corresponding to the bottom third of the inventory. Secondary temperature controls for heater tapes along the gas inlet path served to control the temperatures of several gas mixing chambers and a water humidification chamber. A superficial gas contact time of 3.7 seconds was provided based on total gas flowrate (1.5 liter/min at STP) and sample bulk density. Gas composition was blended from gas cylinders using thermal mass flow controllers, and water was metered using a variable flow dispensing pump. The packed-bed system is configured with gas analyzers for continuous monitoring of flue gas components (SO_2, NO_2, O_2, hydrocarbons, etc.), but for the current study, only a CO_2 gas analyzer was required to monitor gas composition. The process gas is passed through a Perma Pure drying tube to remove moisture prior to the stream entering the gas analysis train.

The experimental procedure and test conditions employed for the packed-bed tests were similar to those used for the TGA tests. Gas composition and reactor temperatures were chosen to replicate the TGA test conditions. For the typical baseline condition during CO_2 absorption, the gas inlet composition (vol%) was typically 10% CO_2, 10% H_2O, and 80% N_2, at a reactor temperature of 60°C. Once the sample was charged to the system, it was dried under nitrogen, then humidified, and then exposed to CO_2 during the absorption step. Once CO_2 breakthrough was complete and the exit gas reached the inlet CO_2 level, the reactor was isolated (i.e., gas bypass) and the gas analyzer was recalibrated. The reactor was then brought back on-line and thermal regeneration was initiated by raising the bed temperature. However, the rate of temperature ramping was much slower in the packed-bed tests, due to larger thermal inertia, as compared to the TGA tests. Therefore, it is difficult to assign a singular temperature for the condition of regeneration, although a target

regeneration temperature of 150°C was eventually achieved. Due to limited sample quantity, the same sample was used repetitively and was not removed from the reactor after each test, but instead remained within the reactor as the sample was cycled between absorption and regeneration for various test conditions. Baseline conditions were re-tested periodically to check for degradation in system performance.

Results

Results using a potassium carbonate sorbent have been previously reported [Hoffman and Pennline, 2000], and major findings are summarized here. The experimental description for the current study, with few minor exceptions, remains unchanged from the previous investigation.

Thermodynamic analysis identified ranges of temperature for absorption and regeneration to be thermodynamically feasible. Potassium carbonate is applicable for CO_2 capture at low absorption temperatures (less than 145°C), while calcium oxide is applicable for much higher absorption temperatures (less than 860°C).

Experiments were conducted in both a TGA reactor and a packed-bed reactor using sorbent fabricated from potassium carbonate supported on a high surface area activated alumina. Sorbent batches with potassium loadings (as potassium carbonate) of 12.2 and 17.1 weight percent were prepared for experimental evaluation. Chemical analyses indicated approximately one-third of the surface area was lost upon impregnation of the metal, but the potassium loading is uniform across the cross-section of the sorbent sample as determined by XPS analysis.

TGA experiments were typically conducted using a gas composition (vol%) of 10% CO_2, 10% H_2O, with balance N_2. TGA results indicate CO_2 capture is favored at low absorption temperature (50-60°C), with sorbent utilization strongly decreasing with higher absorption temperature (80-100°C). Higher potassium loading on the sorbent did not provide additional benefit for CO_2 capture, as evidenced by lower sorbent utilization for the higher loaded sorbent. The sorbent was thermally regenerated at 150°C, which is consistent with the predicted temperature based on thermodynamic analysis.

Packed-bed results provided the additional benefit of measuring changes in exit gas composition (CO_2) as well as changes in bed temperature due to exothermic reaction. Breakthrough of CO_2 through the bed was strongly influenced by higher inlet CO_2 levels. The onset of bed temperature rise was noted to coincide with the breakthrough of CO_2, with earlier CO_2 breakthrough characterized by earlier temperature rise within the bed. Minor differences in the breakthrough curve were noted for absorption temperatures ranging between 60-100°C. Moisture difference was found to have little influence on the breakthrough curve. Sorption of moisture onto the sample, in the absence of CO_2, did not result in bed temperature rise. Absorption after multi-cycling of the sorbent between absorption and regeneration results in equivalent CO_2 breakthrough curves and thus indicates that negligible sorbent degradation is occurring.

The alumina substrate, when tested individually, does exhibit an affinity to sorb CO_2. In the TGA tests, some of the CO_2 is presumably desorbed (as observed as sample weight loss) as the sample is

exposed to nitrogen following CO_2 absorption. In the packed-bed tests, the CO_2 breakthrough curve for the substrate occurs in approximately half the time as for the sorbent (alumina plus potassium carbonate). In addition, a temperature rise does occur for the substrate when exposed to CO_2, indicating that the substrate does participate in the capture of CO_2.

More recently, the TGA data was analyzed in greater detail in an attempt to extract kinetic rate information. The effect of temperature on the reaction rate was studied, and an apparent activation energy was determined. Chemical reaction is assumed to be the rate limiting step, and diffusion is assumed to be a minor resistance. Derivatives of the weight/time data were calculated, from which the maximum and average derivatives were then related to reaction rate law expressions. Data was fitted to a first order Arrhenius rate law, and the regression line coefficients were used to calculate the overall activation energy and preexponential term. It must be noted that some limitations in the data did periodically make interpretation of the results difficult. For the reaction of CO_2 absorption using potassium carbonate, the activation energy was estimated at approximately 4 kcal/mole and the preexponential term was approximately 10^{-3}/hr. A comparison was made to an analogous gas-solid absorption reaction that has previously been investigated at NETL [Yeh et al., 1987]. The reaction of SO_2 with an alumina supported copper oxide sorbent has been used in regenerable processes to remove SO_2 from flue gas. The copper oxide absorption reaction has a similar activation energy (approximately 5 kcal/mole), but the preexponential term (approximately 10^{+4}/hr) is vastly larger by many orders of magnitude than the CO_2 absorption reaction. Hence the CO_2 absorption reaction appears considerably slow in comparison to an SO_2 removal system. Although the reactions have different optimal reaction temperatures and process conditions, concentration levels, etc., the comparison does yield qualitative insight into the slow nature of the CO_2 absorption reaction using the potassium carbonate sorbent.

For the next phase of the investigation, sorbents composed of calcium deposited on silica were prepared. For the substrate support, silica was selected based on the thermodynamically-predicted high operating temperatures required for absorption and regeneration. Sintering expected to occur for activated alumina at elevated temperature would be eliminated with silica.

The silica, Type XS 16080 from Norton Chemical [Koradia, 2000], consists of 1/8" diameter cylindrical pellets. The original extrudates were cleaved with a razor blade to yield pellets whose length approximated its diameter, and thus a similar aspect ratio. The silica has a medium surface area (117 m^2/g) with a packing density of 40.5 lbs/ft^3 and a crush strength of 14.4 lbs. The total pore volume was 0.8 cc/g and the median pore diameter was 393 Angstroms.

Calcium nitrate tetrahydrate [ACS reagent grade, 99% $Ca(NO_3)_2 \bullet 4H_2O$] from Aldrich Chemical was used to deposit the calcium onto the silica. Acetone [ACS reagent grade, 99.6%] from Mallinckrodt Chemical was the solution medium in which the wet impregnation occurred. Calcination of the impregnated silica at 400°C under nitrogen for 48 hours converted the calcium nitrate tetrahydrate into calcium oxide on the silica.

Six batches of sorbent were prepared for use in this study. For a batch, silica was added to a specific solution, soaked for 18 hours, dried at 100-110°C for approximately three hours, and then calcined. Properties of the sorbent batches and of the silica substrate itself, are listed in Table 1.

Samples were routinely dried at temperatures in excess of 100°C prior to performing the chemical analysis. In Table 1, samples not calcined are designated as "uncal", whereas calcined samples are denoted as "cal". Silica substrate (with no calcium impregnation) is designated as "Sub", and impregnated sorbent batches as "B#". Analysis for metals were conducted using two sample preparation methods. For the microwave digestion technique, high-temperature fusion of the sample matrix with a low-melting salt is conducted followed by dissolution with a dilute acid. The hot plate digestion technique follows ASTM Method PS 52-96. For both methods, the resulting solution is analyzed using ICP emission spectroscopy on a Perkin Elmer Optima 3000 spectrometer. The former preparation method allows both calcium and silicon to be dissolved from the sample matrix for analysis. The latter method assures better dissolution of the calcium from the matrix, but silicon is not recovered.

Results in Table 1 are given in terms of pure metal content as determined by analysis, as well as the calculated loading of each metal compound assumed in its oxidized state. A check on the material balance of analysis for the sample is calculated by summing the levels of the calcium oxide and silica loadings, the only two predominant compounds assumed present. Higher levels of impregnated calcium (up to 9 wt% Ca) were achieved by raising the calcium nitrate tetrahydrate concentration in the starting absorbing solution, but a point of diminishing return was obvious in the trend of the data. There is generally good agreement in calcium content when the results of the two sample preparation techniques are compared, lending confidence to the calcium determination. For most of the samples, the material balance is within 10% for the summed total analysis.

Materials will be additionally characterized for BET surface area, pore volume, and average pore radius. To check on the uniformity of the impregnation of calcium within the pellet, representative samples will be analyzed with x-ray photoelectron spectroscopy (XPS) and scanning electron microscopy (SEM). In order to image the cross section of the calcium-containing pellet, the pellets will be cleaved both radially and longitudinally in half with a razor blade to produce a relatively smooth cross section to image.

Preliminary SEM photos taken of the sorbent cross sections have yielded favorable results with respect to calcium distribution. The inner region of the pellet definitely contains calcium, and therefore internal calcium voids are not present. The distribution of calcium is fairly uniform across the majority of the cross section, both longitudinally and radially. For some of the samples, particularly those having higher overall calcium deposition, an outer shell of high calcium loading can be observed, suggesting an impedance to experimentally attaining even higher calcium deposition uniformly throughout the entire pellet. When comparing uncalcined and calcined samples, no apparent differences are noted due to the calcination step. In some of the samples, hairline fractures are evident throughout the cross section of the pellet.

Application

For a dry, regenerable sorbent system, the process consists of two major steps: an absorption step where CO_2 is removed from a gaseous stream by the action of the sorbent; and a regeneration step where the sorbent is rejuvenated and a concentrated stream of CO_2 is off-gased. In the first step, the reaction of the active chemical by itself or on a support occurs in the gas phase to form a

bicarbonate/carbonate that is the product of the CO_2 removal reaction. In the second step, the sorbent is regenerated by chemically treating it or by heating it to the decomposition temperature so that CO_2 is produced in a concentrated stream. The sorbent is then recycled back to begin another cycle

For a conceptual commercial system employing continuous integrated absorption and regeneration operation, the process is cyclic but different than switching between two static reactors in tandem or parallel. It is envisioned that in the first step, carbon dioxide is captured by a moving-bed of sorbent. The absorption reactor design is unique in that a cross-flow moving-bed configuration is utilized. Carbon dioxide-laden gas flows horizontally through the reactor where the sorbent removes CO_2. Similarly, the sorbent flows continuously vertically through the reactor. The sorbent is then transported to the regenerator. In the regenerator, the sorbent is thermally or chemically regenerated in a moving-bed or fluidized-bed mode. The sorbent flows continuously through the reactor and is transported back to the absorber where another sorbent cycle begins.

This dry, regenerable sorbent process can be installed on new facilities or retrofitted into an existing producer of CO_2-containing gas, for example, a utility or industrial boiler. Depending on the optimum temperature of CO_2 absorption with the sorbent, the absorber could be placed anywhere along the gas stream that may have been or will be treated with another scrubbing process to remove other pollutants. With respect to new advanced power systems, for example, Integrated Gasification Combined Cycle, High Performance Power Systems, Pressurized Fluid Bed Combustors, Vision 21 Systems, etc., the process can be installed at appropriate locations.

A dry, regenerable sorbent process can offer certain processing advantages. Utilization of a cross-flow, moving-bed absorber, as compared to fluidized bed or other reactor configurations, presents the potential advantages of high levels of CO_2 removals, high sorbent utilization, low pressure drop, and low sorbent attrition. Additional economic advantages over commercially available CO_2 wet scrubbing technologies [Bartoo, 1984] exist. The contacting of the CO_2-laden gas with a solid bed of material is better since less vessel volume is needed for the processing; temperature control could be better; a massive quantity of water is not required in the capture step; and overall energy consumption would be less since pressure drop would be less for gas/solid contact as compared to commercial gas/liquid contact design. Also, the land area required for installation of the proposed technology is less since wet scrubbing systems, if retrofitted onto existing power plants, would require land area almost as vast as the power plant itself [DOE, 1993].

Future Activities

Parametric experiments using a calcium-based sorbent will be continued in both the TGA and the packed-bed apparatus. Optimal process parameters for absorption and regeneration will be identified, and kinetic rate information extracted. An existing numerical model of a moving-bed absorber will be modified to incorporate the kinetic information of the alkali/alkaline earth sorbents tested to date. Additionally, a systems analysis will be pursued to help identify key parameters affecting performance as well as guide future research efforts to enhance technical performance and/or reduce costs.

Disclaimer

References

Bartoo, R. (1984). Removing Acid Gas by the Benfield Process. Chem. Eng. Prog., 80, 35-39, 1984.

Bibara, P.; Filburn, T.; and T. Nalette (1992). Regenerable Solid Amine Sorbent. US Patent No. 5,876,488, 1999.

Curran, G.P.; Fink, C.E.; and E. Gorin (1967). CO_2 Acceptor Gasification Process: Studies of Acceptor Properties, Advances in Chemistry, 69, Fuel Gasification, ed. by Schorda, F.C., American Chemical Society, Washington, 141-165, 1967.

Elliott, M.A. (1981). Chemistry of Coal Utilization. Second Supplementary Volume, Prepared Under the Guidance of the Committee on Chemistry of Coal Utilization, ed. by Elliott, M.A., John Wiley & Sons, New York, 1642-1648, 1981.

Final Report DOE/ER-30194 (1993). The Capture, Utilization and Disposal of Carbon Dioxide from Fossil Fuel-Fired Power Plants. DOE Contract No. DE-FG02-92ER30194.A000, July 1993.

Han, C.; and D.P. Harrison (1997). Multicycle Performance of a Single-Step Process for H_2 Production. Sep. Sci. Tech., 32, 681-697, 1997.

Hayashi, H.; Taniuchi, J.; Furuyashiki, N; Sugiyama, S.; Hirano, S.; Shigemoto, N.; and T. Nonaka (1998). Efficient Recovery of Carbon Dioxide from Flue Gases of Coal-Fired Power Plants by Cyclic Fixed-Bed Operations over K2CO3-on-Carbon. Ind. Eng. Chem. Res., 37, 185-191, 1998.

Hayashi, H.; Hirano, S.; Shigemoto, N.; and Yamada, S. (1995). Characterization of Potassium Carbonate Supported on Porous Materials and Application for the Recovery of Carbon Dioxide

from Flue Gases under Moist Conditions. Nippon Kagaku Kaishi, 1006-1012, 1995.

Herzog, H.; Drake, E.; and E. Adams (1997). CO_2 Capture, Reuse, and Storage Technologies for Mitigating Global Climate Change, Final Report DOE Contract No. DE-AF22-96PC01257, January 1997.

Hirano, S.; Shigemoto, N.; Yamada, S.; and H. Hayashi (1995). Cyclic Fixed-Bed Operations over K_2CO_3-on-Carbon for the Recovery of Carbon Dioxide under Moist Conditions. Bull. Chem. Soc. Jpn., 68, 1030-1035, 1995.

Hoffman, J.S., and Pennline, H.W (2000). Investigation of CO_2 Capture Using Regenerable Sorbents. Proceedings of the Seventeenth Annual International Pittsburgh Coal Conference, Paper No. 12-1, September, 2000, Pittsburgh, Pennsylvania.

Koradia, P. (2000). Material Properties and Identification of XS 16080 Silica. Cover Letter from P. Koradia of Norton Chemical Process Product Corporation, Catalytic Products, P.O. Box 350, Akron OH, to S. Hedges of U.S. DOE/NETL, April 19, 2000.

Martin, R; (1969). Regenerable Sorbers and Portable Life Support. NASA Spec. Publ., NASA SP-234, 379-389, 1969.

Nalette, T.; Bibara, P.; and J. Aylward (1992). Preparation of high capacity unsupported regenerable CO_2 sorbent. US Patent No. 5,079,209, 1992.

Onischak, J.; and B. Baker (1978). Development of a Prototype Regenerable Carbon Dioxide Absorber for Portable Life Support Systems. J. Eng. Ind., 100(3), 383-385, 1978.

Otsuji, K.; Hirao, M.; and S. Satoh (1987). A Regenerable Carbon Dioxide Removal and Oxygen Recovery System for the Japanese Experiment Module. Acta Astronaut., 15(1), 45-54, 1987.

Remus, G.; Nuccio, P.; and R. Honegger (1969). Carbon Dioxide Removal System of the Regenerable Solid Adsorbent Type. U.S. Govt. Res. Develop. Rep., 69(18), 39, 1969.

Siliban, A.; and D.P. Harrison (1995). High Temperature Capture of CO_2: Characteristics of the Reversible Reaction Between CaO(s) and CO_2(g). Chem. Eng. Comm., 137, 177-190, 1995.

Siliban, A.; Narcida, M.; and D.P. Harrison (1996). Characteristics of the Reversible Reaction Between CO_2(g) and Calcined Dolomite. Chem. Eng. Comm., 147, 149-162, 1996.

Trusch, R. (1967). Carbon Dioxide Control in Spacecraft by Regenerable Solid Adsorbents. Space Congr., 4th, Cocoa Beach, Fla, 1-31-1-56, 1967.

Yeh, J.T.; Strakey, J.P.; and J.I. Joubert (1987). SO_2 Absorption and Regeneration Kinetics Employing Supported Copper Oxide. U.S. DOE, Pittsburgh Energy Technology Center, Internal Communication (unpublished), 1987.

Table 1. Elemental Analysis of Ca-Loaded Silica Samples

Sample	Solution Mix			Silica (g)	Ca (wt%)		Si (wt%)	CaO (wt%)		SiO$_2$ (wt%)	Total (wt%)
	Ca(NO$_3$)$_2$•4H$_2$O (g)	Acetone (ml)	Conc (g/ml)		Micro wave	Hot Plate	Micro wave	Micro wave	Hot Plate	Micro wave	Micro wave
uncal-Sub	-	-	-	12	0		47.4	0		101.4	101.4
uncal-B1	8	50	0.16	12	1.92		44.5	2.69		95.2	97.9
uncal-B2	16	50	0.32	12	3.07		42.1	4.29		90.0	94.3
uncal-B3	24	50	0.48	12	4.06		40.0	5.68		85.6	91.3
uncal-B4	32	50	0.64	12	4.83		37.4	6.76		80.0	86.8
uncal-Sub	-	-	-	12	0		46.4	0		99.2	99.2
uncal-B6	25	25	1.00	12	5.80		30.5	8.11		65.2	73.3
uncal-B5	40	25	1.60	12	7.33		29.5	10.3		63.1	73.4
cal-Sub	-	-	-	12	0	0	47.9	0	0	102.4	102.4
cal-B1	8	50	0.16	12	1.70	2.09	40.7	2.38	2.92	87.0	89.4
cal-B2	16	50	0.32	12	3.13	3.41	41.0	4.38	4.77	87.7	92.1
cal-B3	24	50	0.48	12	4.64	4.68	44.4	6.49	6.55	95.0	101.5
cal-B4	32	50	0.64	12	5.68	5.73	43.7	7.95	8.02	93.5	101.5
cal-Sub	-	-	-	12	0		47.5	0		101.6	101.6
cal-B6	25	25	1.00	12	7.49		39.9	10.5		85.3	95.8
cal-B5	40	25	1.60	12	8.92		37.1	12.5		79.3	91.8

11

Assessing the Thermodynamic Feasibility of the Conversion of Methane Hydrate into Carbon Dioxide Hydrate in Porous Media

Duane H. Smith (dsmith@netl.doe.gov; 304-285-4069), U.S. Department of Energy, National Energy Technology Laboratory, Morgantown, WV 26507-0880

Kal Seshadri (kal.seshadri@netl.doe.gov; 304-285-4680), Parsons Infrastructure and Technology Group, Morgantown, WV 26505

Joseph W. Wilder (wilder@math.wvu.edu; 304-293-2011), U.S. Department of Energy, National Energy Technology Laboratory, Morgantown, WV 26507-0880 (Permanent Address: Dept of Mathematics, P. O. Box 6310, West Virginia University, Morgantown, WV, 26506-6310)

Abstract

Concerns about the potential effects of rising carbon dioxide levels in the atmosphere have stimulated interest in a number of carbon dioxide sequestration studies. One suggestion is the sequestration of carbon dioxide as clathrate hydrates by injection of carbon dioxide into methane hydrate. Energy-supply research estimates indicate that natural gas hydrates in arctic and sub-seafloor formations contain more energy than all other fossil fuel deposits combined. The simultaneous sequestration of carbon dioxide and the production of methane by injection of carbon dioxide into deposits of natural gas hydrates, if possible, represents a potentially efficient and cost effective option for the sequestration of carbon dioxide.

Data in the literature show that the conversion of bulk methane hydrate into carbon dioxide hydrate is thermodynamically favored. These results are not directly applicable to naturally occurring hydrates, because the hydrates in these locations are embedded in sediments. The thermodynamics of any potential conversion of CH_4 hydrate to CO_2 hydrate will therefore be affected by the size of the pores in which the conversion of CH_4 hydrate to CO_2 hydrate would take place. We have developed a model that is able to explain and predict equilibria in porous media for any pore size distribution. This model can be used to calculate the heats of dissociation for these hydrates in porous media as a function of pore size and temperature. These results allow for an assessment of the thermodynamic feasibility of converting CH_4 hydrate to CO_2 hydrate in porous media involving various size pores. We have used this model to derive a simple, explicit relation for the hydrate formation conditions in porous media, as well as the enthalpy of dissociation for these hydrates.

Introduction

The build up of carbon dioxide in the atmosphere due to anthropogenic emissions has become of great scientific and popular interest due to the potential of this gas to play an important role in greenhouse effects, and its reported potential to induce global warming on the order of $2 - 5$ K over the next century (Ravkin, 1992). As a result of these concerns, various researchers have suggested the sequestration of CO_2 to remove it from the atmosphere. One set of potential sequestration scenarios involves the injection of CO_2 into the earth's oceans. One obvious drawback to these scenarios is that due to its solubility in water the injected CO_2 will dissolve, with unknown ecological effects. This potential dissolution of CO_2 could be reduced/prolonged by some extent if the conditions were such that CO_2 hydrates could be formed and were stable. Gas hydrates are crystalline structures, belonging to a group of solids known as clathrates, which involve a lattice made up of hydrogen-bonded water molecules containing cavities occupied by guest gas molecules. Gas hydrates form under low temperature – high pressure conditions, both above and below the freezing point of water. Under proper conditions, the lattice is stabilized by van der Waals forces through the occupation of specific cavities within the lattice by certain types of guest molecules. The type of guest molecule(s) present determines which of three known crystal structures the lattice assumes (Sloan, 1997).

It has been suggested (Komai et al., 1997) that the injection of CO_2 into methane hydrate could result in the simultaneous sequestration of the CO_2 and the liberation of methane (which could be used as a clean fuel). Since much of the worlds naturally occurring methane hydrates are in sediments below the ocean floors or in permafrost regions, it is necessary to consider the effects of porous media on the formation of these hydrates separately, as well as for mixtures. In this work we examine empirical relations based on experimental data for bulk hydrates that have been presented in the literature (Holder et al., 1988; Kamath, 1983; Sloan, 1997). It is demonstrated that such relations can be derived from the standard thermodynamic models that have been applied to predict hydrate formation conditions. In addition, a simple relation is presented that allows for the prediction of the equilibrium conditions in porous media and,

subsequently, the enthalpy of dissociation of these hydrates. In this work we shall only consider hydrate equilibria above 273.15 K (where the equilibria involve liquid water), though similar relations can be derived for temperatures below the water ice-point.

Empirical Fits to Bulk Hydrate Data

Kamath (1983) has noted that the equilibrium pressures for single component hydrates are well fit by simple relations of the form

$$\ln\left(P_{eq}\right) = \frac{a}{T} + b.\tag{1}$$

This simple form is often refered to as an Antione equation (Reid and Sherwood, 1966), and is analogous to the vapor-pressure equations derived from the Clapeyron equation

$$\frac{d\left(\ln P_{vp}\right)}{d\left(1/T\right)} = \frac{-\Delta H_v}{R\Delta Z_v},\tag{2}$$

where ΔH_v is the enthalpy of vaporization, and ΔZ_v is the difference between the gas and liquid compressibility factors. Reduction of eq (2) to a form analogous to eq. (1) results from the assumption that the ratio $\Delta H_v/\Delta Z_v$ is constant. The analogy between hydrate equilibrium pressures and vapor pressures is certainly not perfect, though the seeming agreement between experimental data and linear fits of this type are suggestive that this relation should be derivable from the statistical thermodynamic equations used to predict hydrate formation. Figure 1 shows graphical representations of the correlations given in Table 1 for methane and carbon dioxide hydrates using eq. (1). While this relation has been remarked on by several authors (see for example Sloan, 1997; and Holder, 1988), no explanation for its validity based on a statistical thermodynamic model has been presented in the literature.

Table 1: Correlations for fitting experimental equilibrium pressures for methane and CO$_2$ hydrates to $\ln(P_{eq}) \approx \dfrac{a}{T} + b$ where P_{eq} is in atm and T (> 273.15) is in K.

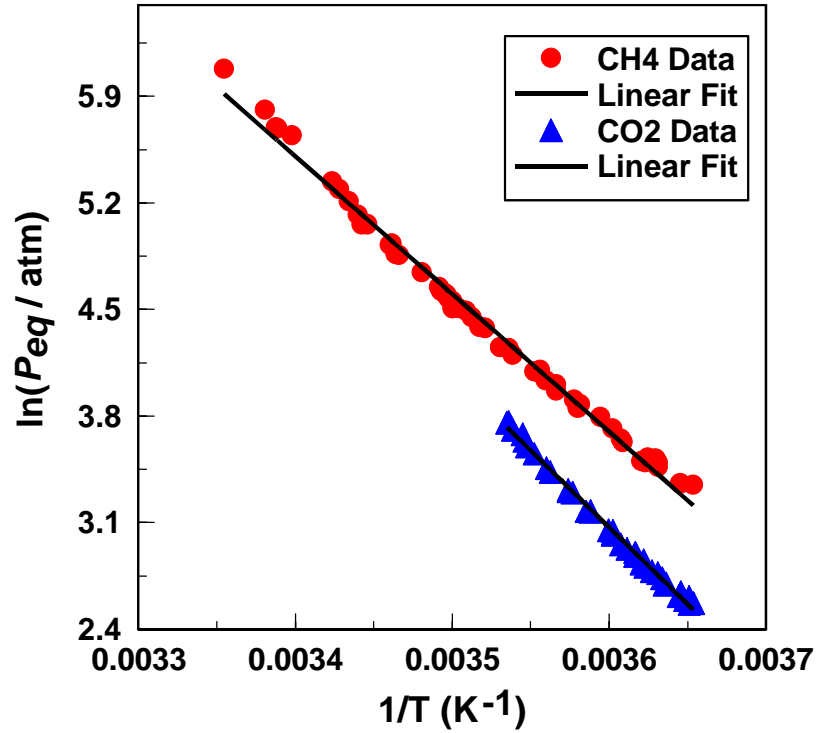|	a	b
Methane	-8995	36.09
Carbon Dioxide	-10091	39.39

Figure 1: Shown are experimental equilibrium pressures for methane (●) and carbon dioxide (▲) hydrate formation, as well as linear correlations using eq. (1) and the parameters given in Table 1.

Modeling Hydrate Formation in the Bulk

Munck et al. (1988) presented a single equation involving T_f and P_f (the temperature and pressure under which the hydrate forms) that can be used to predict hydrate formation conditions. In the case of hydrates formed from single component gases, this equation takes the form

$$\frac{\Delta\mu_W^0}{RT_0} - \int_{T_0}^{T_f}\frac{\Delta H_w}{RT^2}dT + \int_0^{P_f}\frac{\Delta V_w}{R\bar{T}}dP - \ln(\gamma_w X_w) + \sum_i \eta_i \ln(1 - Y_i) = 0 \tag{3}$$

In eq (3), $\bar{T} = (T_0 + T)/2$, T_0 is the temperature of the standard reference state (T = 273.15 K, P = 0), $\Delta\mu_W^0$ is the chemical potential difference for the reference state, η_i is the ratio of the number of cavities of type i to the number of water molecules in the hydrate lattice, and Y_i denotes the probability of a cavity of type i being occupied by the guest molecule, and is given in terms of the fugacity of the hydrate guest in the gaseous state (f_i) and the Langmuir adsorption constant (C_i) by $Y_i = \frac{C_i f_i}{1 + C_i f_i}$. Additionally,

$\Delta H_W = \Delta H_W^0 + \int_{T_0}^{T}\Delta C_p(T')dT'$, where ΔH_W^0 is a reference enthalpy difference between the empty hydrate lattice and the pure water phase at the reference temperature, $\Delta C_p(T')$ is assumed constant and equal to ΔC_p^0 (the reference heat capacity difference), and ΔV_W is the volume difference between the empty hydrate and pure liquid water (at T_0), and is assumed constant. In the present model the temperature dependence of the Langmuir constants is accounted for by using the form presented by Munck et al (1988),

$C_i = \frac{A_i}{T}\exp(B_i/T)$, where A_i and B_i are experimentally fit parameters, and are dependent on which guest molecule is present. The analysis we will describe below could be applied to any of the various forms of this model (all of which are based on that presented by van der Waals and Platteeau (1959)), but the one given above has several advantageous characteristics that facilitate the objectives of this work. As noted earlier,

5

we shall only consider equilibria involving liquid water, though the analysis that will be presented can also be applied to equilibria involving ice.

While eq. (3) can be solved numerically for the equilibrium pressure (given any choice of temperature) by an iterative procedure, it is not possible to solve for the pressure as a function of temperature, explicitly. Our goal is to find an accurate approximation of the true solution that allows such an explicit form to be determined. We begin by a consideration of the terms involving either the pressure or fugacity of the gas. The first such term on the left-hand side of eq. (3) is due to the affect of the volume difference between the empty hydrate lattice and the normal state of the water, namely

$\int_{0}^{P_f} \dfrac{\Delta V_w}{R\overline{\overline{T}}} dP = \dfrac{\Delta V_w}{R\overline{\overline{T}}} P_f$. Due to the relatively small volume change when hydrates form

from water, the magnitude of this term is small compared to others in eq. (3). As a result of this, we consider $\ln f$ to be given by $\ln f \approx \ln f^0 + \ln f^1$ where the second contribution (assumed small) is due to this term, and $\ln f^0$ can be found by ignoring this term in eq. (3). The other terms involving the pressure are those related to the cage occupancies

$$\sum_{i} \eta_i \ln(1 - Y_i) = \eta_s \ln(1 - Y_s) + \eta_1 \ln(1 - Y_l), \tag{4}$$

 where on the right hand side we have used a subscript "s" to denote quantities for the "small" cages, and "l" for those in "large" cages. Using the form for Y_i given above, each term of eq. (4) can be rewritten using

$$\begin{aligned} \eta_i \ln(1 - Y_i) &= -\eta_i \ln(1 + C_i f) \\ &= -\eta_i \ln\left[C_i f\left(1 + \frac{1}{C_i f}\right)\right] \\ &= -\eta_i \left\{ \ln(C_i f) + \ln\left(1 + \frac{1}{C_i f}\right)\right\} \end{aligned} \tag{5}$$

Clearly, if $C_i f$ is large enough, $\ln(1 + C_i f) \approx \ln(C_i f)$. If this approximation is not adequate but $C_i f$ is still larger than unity, one can use a Taylor series expansion of the second logarithm in the last line of eq. (5) to arrive at

$$\eta_i \ln(1 - Y_i) \approx -\eta_i \left\{ \ln(C_i f) + \frac{1}{C_i f} - \frac{1}{2}\left(\frac{1}{C_i f}\right)^2 + \ldots \right\}. \tag{6}$$

To demonstrate the validity of using $\ln(1 + C_i f) \approx \ln(C_i f)$, we shall consider its

application to methane hydrates. The experimental temperatures and pressures found in

Sloan (1997), as well as the second virial coefficient (used to convert these pressures to

fugacities) have been used to construct Figure 2 where the percent error in approximating

$\ln(1 + C_i f)$ as $\ln(C_i f)$ for both the small and large cages over the temperature range

from 273.7 K to 298.1 K is shown. Clearly, this approximation is extremely good for the

large

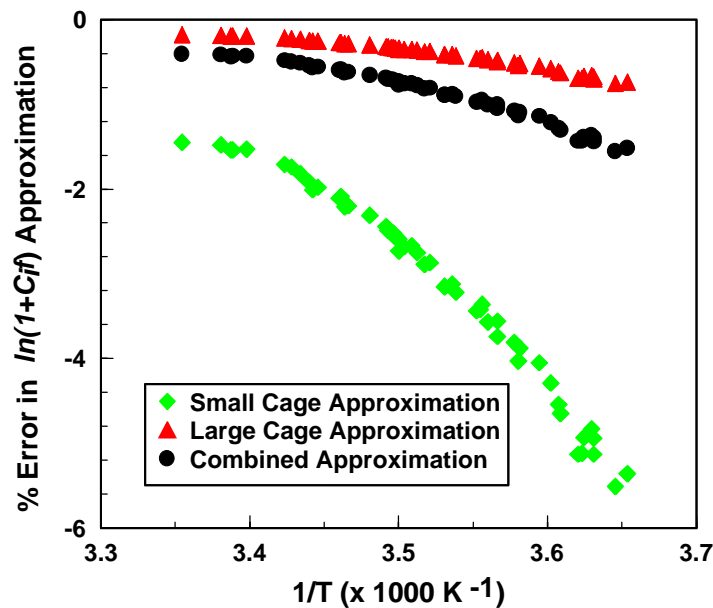**Figure 2:** Shown are the percent errors in approximating $\ln(1 + C_i f)$ as $\ln(C_i f)$ in both
the large (▲) and small (◆)cages in methane hydrates, as well as the error (●) in
using these approximations to compute the sum of the terms as appears in eq.
(7).

cages, and has a maximum error of 5.5 % for the small. Applying this approximation for

both terms in (3) yields

$$\eta_s \ln(1 - Y_s) + \eta_1 \ln(1 - Y_l) \approx (\eta_s + \eta_1) \ln f + \eta_s \ln C_s + \eta_l \ln C_l. \tag{7}$$

The error resulting from using the approximations for both cages (as in eq. (7)) is also shown in Figure 2, and is less than 1.6%. Using (7) in (3) leads to

$$
\begin{aligned}
\ln f &\approx \frac{1}{\eta_s + \eta_l} \left\{ \frac{\Delta\mu_W^0}{RT_0} - \int_{T_0}^{T_f} \frac{\Delta H_w}{RT^2} dT + \int_0^{P_f} \frac{\Delta V_w}{R\overline{T}} dP - \eta_s \ln C_s - \eta_l \ln C_l - \ln(\gamma_w X_w) \right\} \\
&\approx \frac{1}{\eta_s + \eta_l} \left\{ \frac{\Delta\mu_W^0}{RT_0} + \left(\frac{\Delta H_w^0 - T_0 \Delta C_P^0}{R} \right) \left(\frac{1}{T_f} - \frac{1}{T_0} \right) - \frac{\Delta C_P^0}{R} \ln\left(\frac{T_f}{T_0} \right) + \frac{\Delta V_w}{R\overline{\overline{T}}} P_f \\
&\qquad\qquad\qquad - \eta_s \ln C_s - \eta_l \ln C_l - \ln(\gamma_w X_w) \right\}
\end{aligned}
\tag{8}
$$

The second equality in eq. (8) follows from carrying out the indicated integrations. For hydrocarbons such as methane (where the gas solubility in water is very small), the last term on the right hand side of eq. (8) can be neglected (Munck, 1988). As mentioned above, we compute $\ln f$ as $\ln f \approx \ln f^0 + \ln f^1$, where the second term is small compared to the first, and is due to the affect of the term involving P_f on the RHS of (8). Neglecting this term, the zeroeth order term of $\ln f$ for a gas hydrate such as that involving methane is found to be

$$
\begin{aligned}
\ln f^0 &\approx \frac{1}{\eta_s + \eta_l} \left\{ \frac{\Delta\mu_W^0}{RT_0} + \left(\frac{\Delta H_w^0 - T_0 \Delta C_P^0}{R} \right) \left(\frac{1}{T_f} - \frac{1}{T_0} \right) - \frac{\Delta C_P^0}{R} \ln\left(\frac{T_f}{T_0} \right) - \eta_s \ln C_s - \eta_l \ln C_l \right\} \\
&\approx \frac{1}{\eta_s + \eta_l} \left\{ \left(\frac{\Delta H_w^0}{R} - \eta_s(T_0 + B_s) - \eta_l(T_0 + B_l) \right) \frac{1}{T_f} + \right. \\
&\qquad\qquad \left. \left(\frac{\Delta\mu_W^0 - \Delta H_w^0}{RT_0} - \eta_s[\ln(A_S/T_0) - 1] - \eta_l[\ln(A_l/T_0) - 1] \right) \right\} \\
&\approx \frac{\alpha}{T_f} + \beta
\end{aligned}
\tag{9}
$$

The second relation in (9) follows from using the above given form for the Langmuir constants and expanding the logarithm in the third term on the right of the first line of eq.

(9) in terms of a power series in T_f/T_0 and truncating after the first nonzero term. This last approximation is done only to show how the Antione type relation comes about, and is not necessary to simplify the calculations. Figure 3 shows predictions using eq. (9) (with the parameter values given in Table 2) for methane hydrate (dotted trace), as well as the experimental data (Sloan, 1997). Even without including the correction for the volume change on hydrate formation the maximum error is less than 4%.
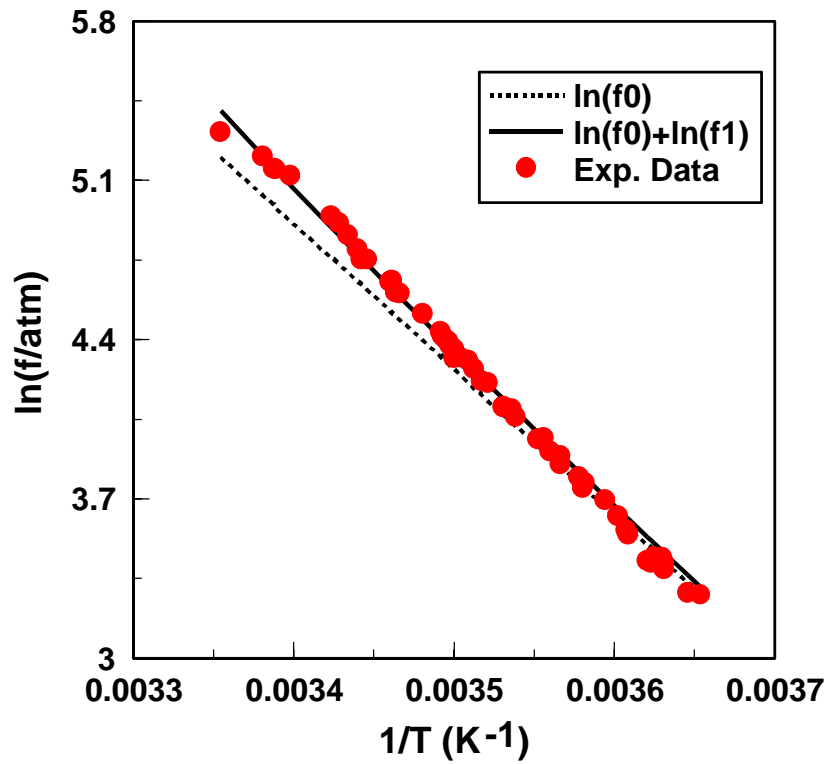
Figure 3: Shown are experimental data (●) for methane hydrate formation, as well as approximations using eq. (9) (⋯) and eq. (10) (━).

Table 2: Parameter values for bulk hydrate formation from liquid water

Property	Unit	Bulk Value for Methane	Bulk Value for CO_2
$\Delta\mu_w^0$	J/mol	1264	1264
$\left(\Delta H_W^0\right)_{liq}$	J/mol	-4858	-4858
ΔC_p^0	J/mol·K	39.16	39.16
ΔV_w	cm³/mol	3.0	3.0
σ_{hw}	J/m²	0.0267	0.0267
A_i	K/atm	0.0007228 (small cavity)	0.0002474 (small cavity)
		0.02335 (large cavity)	0.04246 (large cavity)
B_i	K	3187 (small cavity)	3410 (small cavity)
		2653 (large cavity)	2813 (large cavity)

The correction term that must be applied can be estimated by assuming that the pressure in $\dfrac{\Delta V_w}{R\overline{\overline{T}}}P_f$ can be approximated by f_0. Since the overall magnitude of this term is less than 4% of the remaining terms, the error in approximating P_f by f_0 will be very small. Therefore, using α and β defined by eq. (9) we find that

$$\ln f \approx \frac{\alpha}{T_f} + \beta + \frac{\Delta V}{(\eta_s + \eta_l)R\overline{\overline{T}}} e^{\alpha/T_f + \beta} . \tag{10}$$

Eq. (10) is shown graphically in Figure 3 as the solid trace. This approximation has a maximum error on the order of 1% over the temperature range shown. As can be seen from the difference between the results of using eq. (9) and eq. (10) in Figure 3, the third term on the right hand side of eq. (10) essentially results in a change in the slope of $\ln f$. Unfortunately, because this term is not truly linear in $1/T$ but only appears so on the scale of ln f, the dominant part of this correction can not be obtained from a Taylor series

expansion about the point $1/T_0$. It can, however be approximated by a straight line with only a small error, accounting for the high quality fit that can be attained using an Antione type equation for methane hydrates. A similar equation can be derived for CO_2 hydrates, though the higher gas solubility and the need to include the other terms in eq. (6) result in the need for a slight modification of the methods used to arrive at the resulting equation. These equations will not be given here since they lend no new insight into this approximation and will not be used below.

Modeling Hydrate Formation in Porous Media

To consider hydrate formation in porous media, eq. (3) must be modified to include the effect of the relevant interface on the activity of the water. Making the necessary modifications, eq. (3) becomes (Henry et al, 1999; Clark et al, 1999)

$$\frac{\Delta\mu_W^0}{RT_0} - \int_{T_0}^{T_f}\frac{\Delta H_w}{RT^2}dT + \int_0^{P_f}\frac{\Delta V_w}{R\overline{T}}dP - \ln(\gamma_w X_w) + \sum_i \eta_i \ln(1-Y_i) + V_L\frac{2\cos(\theta)\sigma_{hw}}{RT_f r} = 0. \quad (11)$$

In eq. (11), V_L is the molar volume of water in the pure water state, θ is the wetting angle between the pure water phase and the hydrate, σ_{hw} is the surface tension between the water and hydrate phases, and r is the radius of the pores in the porous medium. If the same analysis is performed on this equation as that described above, we arrive at (for methane and similar hydrates)

$$\ln f^0 \approx \frac{1}{\eta_s + \eta_l}\left\{\left[\left(\frac{\Delta H_w^0}{R} - \eta_s(T_0 + B_s) - \eta_l(T_0 + B_l)\right)\frac{1}{T_f} + \left(\frac{2V_L\cos(\theta)\sigma_{hw}}{R}\right)\frac{1}{T_f r}\right.\right.$$
$$\left.\left.\left(\frac{\Delta\mu_W^0 - \Delta H_w^0}{RT_0} - \eta_s[\ln(A_S/T_0)-1] - \eta_l[\ln(A_l/T_0)-1]\right)\right]\right\}. \quad (12)$$
$$\approx \frac{\alpha}{T_f} + \frac{\gamma}{T_f r} + \beta$$

Since at any given temperature the fugacity in a porous medium should be higher than that in the bulk, the magnitude of $C_i f$ will be larger, making the approximations used in

eq. (4) to compute $\ln f^0$ even more valid in the porous medium. Computing the correction due to the volume change and calculating the total fugacity we find

$$\ln f \approx \frac{\alpha}{T_f} + \frac{\gamma}{T_f r} + \beta + \frac{\Delta V e^{\alpha/T_f + \gamma/T_f r + \beta}}{(\eta_s + \eta_l) R \overline{T}}. \tag{13}$$

Since the last term in eq. (13) should be a small correction, eq. (12) suggests that the logarithm of the gas fugacity for simple hydrates in porous media should be very close to a bilinear function of *1/T* and *1/r*. The form of (12) is called bilinear since for a fixed value of 1/T the function is linear in 1/r, while for any fixed value of 1/r it is linear in 1/T. The complete surface, however, does have a very small amount of curvature due to the overall nonlinearity of its functional form, though it is so small as to be difficult to see in Figure 4, where eq. (13) has been used to generate the surface for methane hydrate formation in porous media.
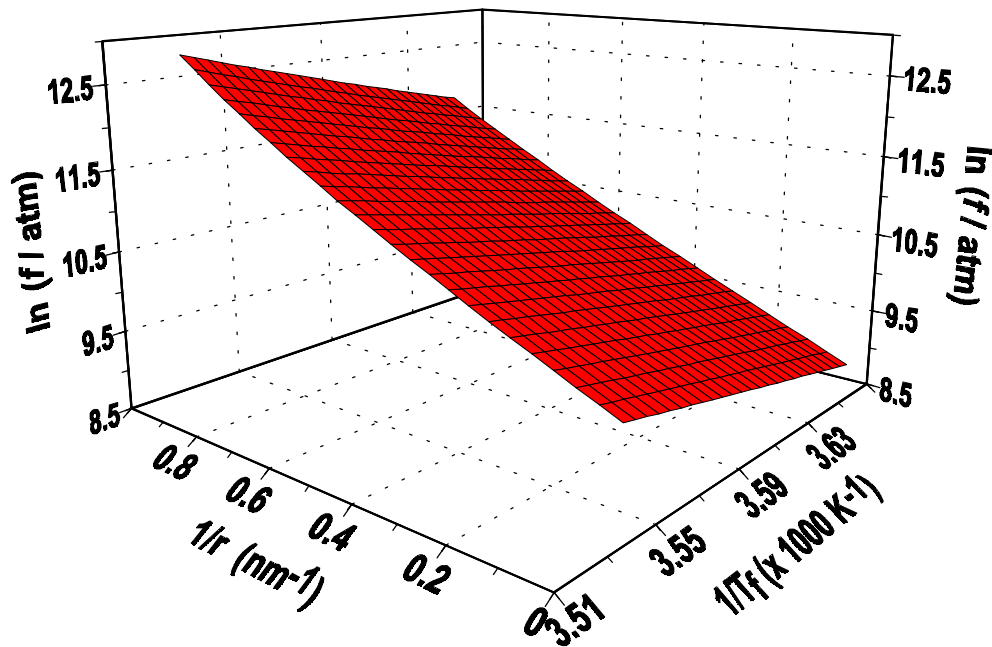

Figure 4:   Shown is the surface representing predicted methane hydrate formation conditions in porous media using eq. (13).

Of primary interest to this work is the effect of the porous medium on the enthalpy of dissociation of the hydrates. While it has been shown that the sequestration of CO_2 by injection of CO_2 into methane hydrate is thermodynamically favored in the bulk (Komai et al., 1997), it has not been established that this holds for porous media. Using eq. (13) and the Clausius-Clapeyron equation

$$\frac{d(\ln(f))}{d(1/T)} = -\Delta H \Big/ R \;,\tag{14}$$

it is possible to estimate the change in enthalpy due to the porous media. Using eq. (13) in eq. (14) yields

$$\Delta H \approx -R\left\{\alpha + \frac{\gamma}{r} + \frac{2\Delta V}{R(\eta_s + \eta_l)}\left[\left(\frac{T_f}{T_0 + T_f}\right)^2 + \alpha + \frac{\gamma}{r}\right]e^{\alpha/T_f + \gamma/T_f r + \beta}\right\}.\tag{15}$$

Since γ only depends on the hydrate lattice structure (and not on the gas species occupying the cages), it is the same for both methane and carbon dioxide hydrates which both form Structure I hydrates. As a result, it can be calculated based on well established quantities, and one only needs values of α and β (which are different for each gas) to estimate the dissociation enthalpies for various hydrates. While these can be calculated using relations similar to eq. (9), they can also be found by fitting (10) to the experimental data for the formation of bulk hydrates. This has been done for methane and CO2 hydrates, with the results given in Table 3. The slight difference (approximately 4%) between the optimal values for methane shown in Table 3 obtained from fitting the data and the ones obtained using eq. (9) with the model parameters given in Table 2 is due to not having optimal values of the model parameters. The large R^2 values shown in Table 3 for both methane and carbon dioxide indicate the quality of the fits obtained with the functional form given in (10).

The results of using (15) to calculate values of the enthalpies of formation for methane and CO_2 hydrates in porous media are shown in Figure 5. The values of α and β from Table 3 for each gas have been used, along with the value of γ calculated using the parameters in Table 2, to construct these surfaces. We note that the calculated bulk

Table 3: Correlations for fitting experimental equilibrium fugacities for methane and CO2 hydrates to $\ln f \approx \dfrac{\alpha}{T_f} + \beta + \dfrac{\Delta V}{R\bar{T}} e^{\alpha/T_f + \beta}$ where f is in atm and T is in K.

	α	β	R^2
Methane	-6705	27.73	0.9972
Carbon Dioxide	-8482	33.43	0.9978

Enthalpies are in good agreement with values reported in the literature. For example, the experimental value for the enthalpy of dissociation of bulk methane hydrate to liquid water has been reported by Handa (1986) to be 54.19 KJ/mol, while that obtained from eq. (15) is 57.38 KJ/mol, a difference of less than 6%. As can be seen in Figure 5, there is a significant decrease in the difference between the enthalpies of dissociation for methane and CO_2 hydrates as 1/r increases (corresponding to smaller pore sizes in the sediment).
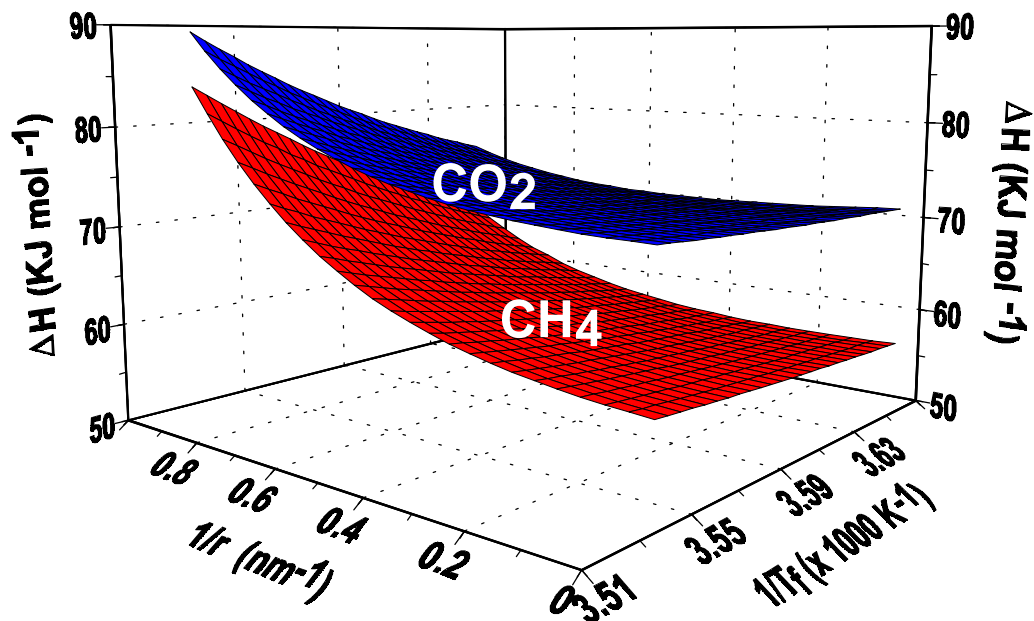

Figure 5: Shown are surfaces representing predicted enthalpies of dissociation for methane and CO_2 hydrates in porous media using eq. (15).

This degrease indicates that the replacement of methane by CO_2 in the hydrate lattice is less thermodynamically favored as the value of 1/r increases. This change may be experimentally detectable for sediments with very small pore sizes such as clays, and may manifest by taking a longer time for the displacement to take place in porous media as opposed to the bulk.

Future Activities

This work has considered the effect of porous media on the equilibrium of single component hydrates. We have shown that a relatively simple functional form allows for the estimation of both the equilibrium fugacity and the enthalpy of dissociation of the gas hydrates. If actual experimental replacement studies involving the injection of CO_2 into methane hydrate deposits are done in porous media, the gas involved in the equilibrium with the hydrate will not be made up of one component, but will be a mixture of carbon dioxide and methane. Future work will address such mixtures and the prediction of the resulting formation enthalpies.

References

Clarke, M.A.; Pooladi-Darvish, M.; Bishnoi, P.R. *Ind. Eng. Chem. Res*. 1999, 38, 2485.

Handa, Y.P. *J. Chem. Thermodynm.* 1986, 18, 915.

Henry, P.; Thomas, M.; Clennell, M.B. *J. Geophys. Res.* 1999, 104, 23005.

Holder, G.D.; Zetts, S.P.; Prodhan, N. *Reviews in Chem. Eng.* 1988, 5, 1.

Kamath, V.A. University of Pittsburgh, Ph.D. Dissertation, 1984, Univ. Microfilms No. 8417404.

Komai, T.; Yamamoto, Y.; and Ikegami, S.; *Preprints, Am. Chem. Soc. Div. Fuel. Chem.* 1997, 42 (2), 568.

Munck, J.; Skjoid-Jorgensen, S.; Rasmussen, P. *Chem. Eng. Sci*. 1988, 43, 2661.

Ravkin, A.; *Global Warming: understanding the forecast*. New York: Abbeville Press, 1992.

Reid, R.C; and Sherwood, T.K.; *The Properties of Gases and Liquids*. New York: McGraw Hill, 1966, 646pp.

Sloan, E.D. *Clathrate Hydrates of Natural Gases,* 2nd ed.; Marcel Dekker: New York, 1997.

van der Waals, J.H.; Platteeuw, J.C. *Adv. In Chem. Phys.* 1959, 2, 1.

CO$_2$ Mineral Sequestration Studies in US

Philip Goldberg[1], Zhong-Ying Chen[2], William O'Connor [3],
Richard Walters[3], and Hans Ziock[4]

[1]National Energy Technology Laboratory, P.O. Box 10940, Pittsburgh, PA 15236, goldberg@netl.doe.gov, (412)386-5806
[2]Science Applications International Corporation, 1710 Goodridge Dr. McLean, VA, zhong-ying.chen@saic.com, (703)676-7328
[3]Albany Research Center, Albany, OR oconner@arc.doe.gov, walters@alrc.doe, (541)967-5834
[4] Los Alamos National Laboratory, Los Alamos, NM, ksl@lanl.gov, ziock@lanl.gov, (505)667-7265

Abstract

Carbon sequestration by reacting naturally occurring Mg and Ca containing minerals with CO$_2$ to form carbonates has many unique advantages. Most notably is the fact that carbonates have a lower energy state than CO$_2$, which is why mineral carbonation is thermodynamically favorable and occurs naturally (e.g., the weathering of rock over geologic time periods). Secondly, the raw materials such as magnesium based minerals are abundant. Finally, the produced carbonates are unarguably stable and thus re-release of CO$_2$ into the atmosphere is not an issue. However, conventional carbonation pathways are slow under ambient temperatures and pressures. The significant challenge being addressed by this effort is to identify an industrially and environmentally viable carbonation route that will allow mineral sequestration to be implemented with acceptable economics.

Under the sponsorship of the U.S. Dept of Energy, a team of researchers from the National Energy Technology Laboratory, Albany Research Center, the Los Alamos National Laboratory, and Arizona State University was formed in the summer 1998 to investigate and improve the carbonation process. This paper discusses significant progress achieved by the team in searching for faster reaction methods using: magnesium silicates, supercritical CO$_2$, water, and additives; in searching for pretreatment methods to enhance mineral reactivity; and in analyzing the structural changes to identify reaction paths and potential barriers. The paper also discusses plans to construct larger scale operating units (up to several MWe) in order to validate the method as a viable sequestration tool at industrially relevant scales.

Keywords: carbon sequestration, global climate change, mineral carbonation, olivine, serpentine.

Introduction

Fossil fuels, which account for 80 - 85% of the total of world energy use today are an important energy source. Fossil fuels have many advantages including abundant supply, high energy density, ease of use and storage, existing infrastructure, and most importantly, their low cost. The use of this important energy source is facing a challenge due to the vast amounts of CO_2 released into the atmosphere as a result of combustion. The level of CO_2 in the atmosphere has increased by roughly 30% since the industrial revolution, with much of this rise being attributed to the increased use of fossil fuels such as coal, oil and natural gas ([1,2]). Since 1800, the CO_2 content of the atmosphere has risen from a stable level of 280 ppm to above 365 ppm today. While the observation that the atmospheric CO_2 level has increased significantly is generally not at issue, the consequences arising from this increase are the subject of vigorous debate. Given that CO_2 is a greenhouse gas, such large and increasing atmospheric CO_2 levels will have climatic consequences. Unless action is taken, the emissions of CO_2 will continue to increase as the world economy grows, resulting in exponential growth of the level of atmospheric CO_2. We are not likely to fully understand the actual consequences of increased levels of atmospheric CO_2 for some time. Should action be required, source control would likely be favored since it would be much more difficult and more expensive to retract dispersed CO_2 from the atmosphere than to gather it from large concentrated sources. Consequently, the USDOE is actively pursuing solutions that offer the potential to reduce atmospheric CO_2 emissions.

Historically, per capita energy consumption and wealth, as reflected by Gross Domestic Product (GDP), are nearly proportional. The U.S., followed closely by other highly industrialized nations, has a relatively high per capita energy consumption which is roughly equivalent to five times the global average. It is important to note that it is the U.S.'s high per capita energy consumption that is directly responsible for its high standard of living. As the standard of living continues to rise globally and in developing countries in particular, it is not difficult to imagine that in the not too distant future the world will be using energy (and emitting CO_2) at many times today's rate. Over the 30-year period ending in 2020, projections made by the U.S. Energy Information Agency indicate global increase in energy use will increase worldwide emissions of CO_2 to 38×10^9 tons per year or an increase of 80% compared to 1990 levels ([3]).

Given the public mandate to maintain economic growth, fossil fuels will remain a dominant energy source over the next century, as no alternative energy supply is poised to significantly replace fossil energy without causing other major problems. Therefore, developing effective CO_2 sequestration is one of the critical components in addressing global climate change. Note that improving the efficiency of energy production and utilization, and developing renewable energy sources will certainly play a very important role in reducing CO_2 emissions, however these measures alone cannot address the greenhouse emissions issue mainly because world energy consumption will increase significantly as the living standard improves in many parts of the world.

The Department of Energy is conducting various CO_2 sequestration and recycling studies including underground storage (seabed- or land-based), ocean sequestration, biomass utilization, and using CO_2 as feed material to produce various environmentally benign products (**4**). Challenges to any solution include technical feasibility, economic viability, environmental soundness and long term sustainability. A balanced research portfolio exploring a number of both short and long term mitigation methods is therefore essential to ensure appropriate technology for individual circumstances. This paper focuses on research on one method of CO_2 sequestration: permanent CO_2 fixation as environmentally benign carbonate minerals. The Mineral Sequestration Program is being managed by the National Energy Technology Laboratory (NETL) and is supported by USDOE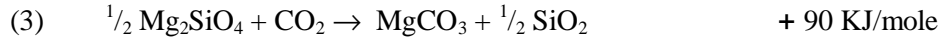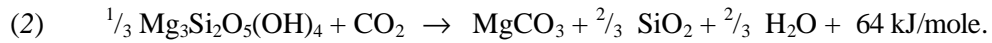/Fossil Energy's Power Systems Advanced Research and Advanced Metallurgical Processes programs. The activities of the working group are being coordinated by the CUS program. Related work is also being supported by internal funding at Los Alamos National Laboratory.

What is Mineral Sequestration

Mineral sequestration involves the reaction of CO_2 with minerals to form geologically stable carbonates, i.e. mineral carbonation. This idea was first proposed by Seifritz (**6**) in 1990. There have been several methods suggested to achieve carbonation: an aqueous scheme by Kojima (**7**); an underground injection scheme by Gunter *et al*. (**8**); the processes via mineral derived $Mg(OH)_2$ suggested by Lackner *et al*. (**9**); and most recently, the carbonic acid process using olivine and serpentine directly proposed by O'Connor *et al* (**10**).

Mineral carbonation reactions are known to geologists and occur spontaneously on geological time scales. For example, the reaction of CO_2 with common mineral silicates to form carbonates like magnesite or calcite is exothermic and thermodynamically favored. For illustrative purposes, general and specific global mineral carbonation reaction pathways are shown below. The family of reactions represented by Reaction 1 has the potential to convert naturally occurring silicate minerals to geologically stable carbonate minerals and silica. This process emulates natural chemical transformations such as weathering of rocks to form carbonates over geologic time periods. Reaction 2 illustrates the transformation of the common silicate mineral serpentine, $Mg_3Si_2O_5(OH)_4$, and CO_2 into magnesite, $MgCO_3$, silica and water. Using this ideal case, one ton of serpentine can dispose of approximately one-half ton of CO_2. Reaction 3 illustrates the transformation of forsterite, which is the end member of the common silicate mineral olivine. One ton of olivine can dispose of approximately two-thirds of a ton of CO_2. Again, the reaction is exothermic and releases 90 KJ/mole of CO_2.

(1) $(Mg, Ca)_x Si_y O_{x+2y+z} H_{2z} + xCO_2 \rightarrow x(Mg,Ca)CO_3 + ySiO_2 + zH_2O$

3

(2) $\frac{1}{3}$ Mg$_3$Si$_2$O$_5$(OH)$_4$ + CO$_2$ → MgCO$_3$ + $\frac{2}{3}$ SiO$_2$ + $\frac{2}{3}$ H$_2$O + 64 kJ/mole.

(3) $\frac{1}{2}$ Mg$_2$SiO$_4$ + CO$_2$ → MgCO$_3$ + $\frac{1}{2}$ SiO$_2$ + 90 KJ/mole
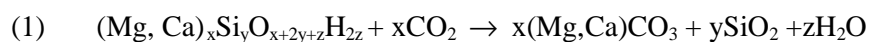
A conceptual illustration of the process is presented in Figure 1. As illustrated, CO$_2$ from one or more power plants is transported to a carbonation reactor, combined with crushed olivine or serpentine from a nearby mine and held at the appropriate reaction conditions until the desired degree of carbonation is reached. Then products of the reaction, which might be a slurry of carbonated minerals and residues in aqueous CO$_2$, are separated. The CO$_2$ is recycled, useful materials are collected and the carbonated materials and residue are returned to the mine site.

There are adequate mineral deposits to support mineral sequestration. The tonnage of silicate mineral necessary to carbonate 100% of the CO$_2$ emissions from a single 500 MW coal-fired power plant can be estimated based on the following assumptions: 1) a mean magnesium oxide (MgO) content in the magnesium silicate ore mineral of 40 weight percent (wt pct); 2) 90% ore recovery; 3) 80% efficiency of the carbonation reaction; and 4) stoichiometry of equation 1. Based on these assumptions, a single 500 MW power plant, generating approximately 10,000 tons/day of CO$_2$, would require just over 30,000 tons/day of magnesium silicate ore. Several ultramafic complexes in North America contain sufficient quantity of magnesium silicate mineral to provide raw materials for the mineral carbonation of all annual CO$_2$ emissions for many years (**14**).

Figure 1. Illustration of Mineral Sequestration Concept

Mineral Sequestration Concept
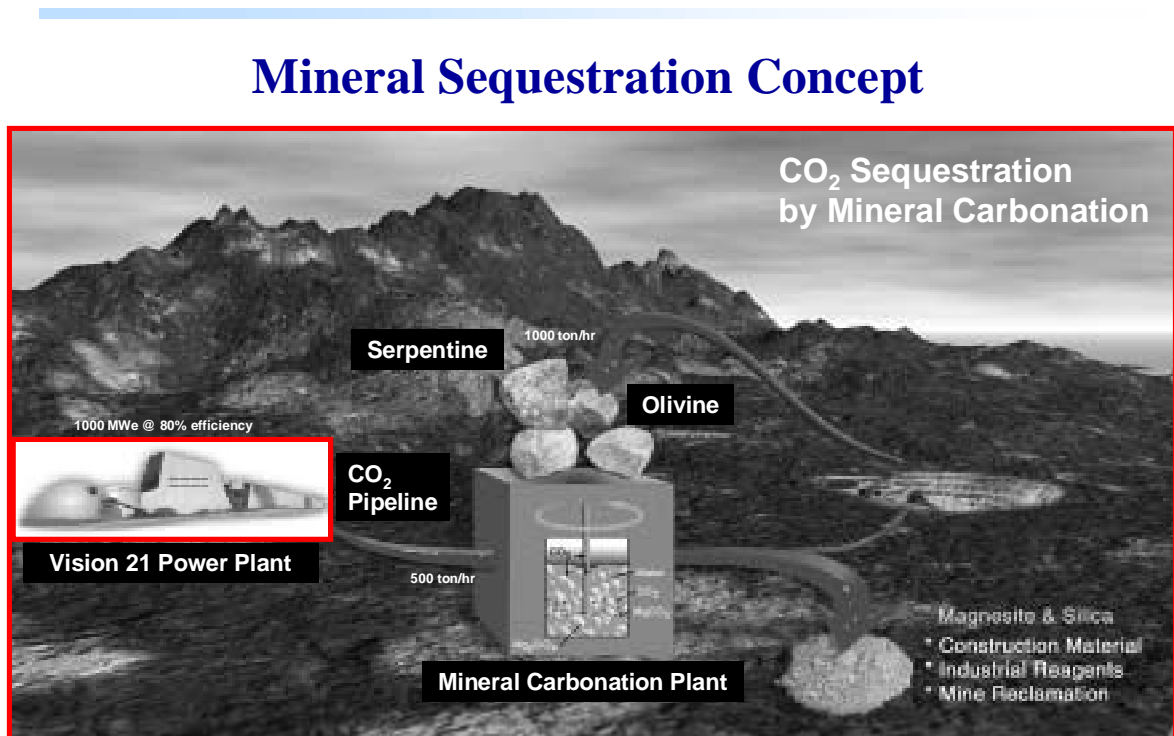
Courtesy of Albany Research Center

Advantages of Mineral Sequestration

The major advantages of CO_2 sequestration by mineral carbonation are:

Long Term Stability - Mineral carbonation is a natural process that is known to produce environmentally safe and stable material over geological time frames. The production of mineral carbonates insures a permanent fixation rather than temporary storage of the CO_2, thereby guaranteeing no legacy issues for future generations.

Vast Capacity - Raw materials for binding the CO_2 exist in vast quantities across the globe. Readily accessible deposits exist in quantities that far exceed even the most optimistic estimate of coal reserves ($\sim$10,000 $\times$ 10^9 tons) (**5**).

Potential to be Economically Viable - The overall process is exothermic and, hence, has the potential to be economically viable. In addition, its potential to produce value-added by-products during the carbonation process may further compensate its costs.

At a single site and scale that is consistent with current industrial practice, the process can handle the output of one to several large power plants. It is directly applicable to advanced power plants such as zero-emissions Vision 21 system configurations being developed by DOE's Fossil Energy Program or to existing power plants, thereby providing an additional degree of flexibility for future implementation (**5**).

Technical Challenges and Program Goals

The major technical challenge now hindering the use of minerals to sequester CO_2 is their slow reaction rate. Weathering of rock is extremely slow. The highest priority is given to identifying faster reaction pathways. Second, the optimized process has to be economical. Although many carbonation reactions are exothermic, it is generally very difficult to recover the low-grade heat while the long reaction time and demanding reaction conditions contribute to process expense. Clearly, the environmental impact from mining minerals and carbonation processes must be considered. The program goals are specifically designed to address these challenges, including

i.   identifying favored technical processes**,**
ii.   determining the economic feasibility of each sequestration process identified, and
iii.   determining the potential environmental impacts of each process.

Rapid Progress

Although the program only has about two years of history, the working team consisting of Albany Research Center (ARC), the Los Alamos National Laboratory, the Arizona State University, and the National Energy Technology Laboratory has made significant progress.

In striving to accelerate overall reaction rates, the team has identified one very promising reaction pathway and succeeded in achieving dramatically shortened carbonation reaction times employing magnesium silicates such as olivine and serpentine.

For example, research at the Albany Research Center (*10,13*) has focused upon the direct carbonation of olivine. When the program first started, it took 24 hours to reach 40-50% completion of carbonation of olivine. The reaction required temperatures of 150-250 C, pressures of 85-125 bar, and mineral particles in the 75-100 micron size range. Careful control of solution chemistry yielded olivine conversions of 90% in 24 hrs and 83% within 6 hrs. The most recent results show further modifications of the same basic reaction can achieve 65% conversion in 1 hour and 83% conversion in 3 hours.

While the potential to utilize olivine to sequester CO_2 is clearly significant, there is approximately an order of magnitude more serpentine than olivine. Consequently, finding a way to use serpentine to scrub CO_2 will have greater practical impact than using olivine. Both minerals are valuable feedstocks and progress has been made in direct carbonation using serpentine also. When the program started, tests conducted at Los Alamos National Laboratory only achieved 25% conversion using 100 micron serpentine particles with CO_2 even at a very high pressure of 340 bars. Independently, researchers at ARC developed a successful carbonation process for serpentine that utilizes mineral heat pretreatment and carbonation in carbonic acid in aqueous solution. A recent literature review indicated that weak carbonic acid treatments had also been suggested for Mg extraction in the prior literature (*12*). Carbonation tests performed at ARC employing heat pretreated serpentine have resulted in up to 83 % conversion in 30 minutes under 115 bars (*13*)

Because the high pressure requirement of the carbonation reaction will certainly lead to high process costs, the team is modifying solution chemistry to allow reaction to proceed at a lower pressure and temperature. The research is guided by the idea that the concentration of HCO_3^- in the solution is critical to the reaction rate. The high CO_2 pressure will lead increased CO_2 absorption in the solution and thus enhance the HCO_3^- concentration. Adding bicarbonate such as sodium bicarbonate in the solution will significantly increase the HCO_3^- concentration even at a relatively lower CO_2 pressure. Indeed, by increasing sodium bicarbonate concentration the carbonation reaction of serpentine can reach 62% completion under 50 bars.

To support laboratory carbonation tests, researchers at Arizona State are employing an Environmental-cell dynamic high- resolution transmission electron microscopy to directly image dehydroxylation of $Mg(OH)_2$, an important step in $Mg(OH)_2$ carbonation reactions. They are extending this technique to study the solid gas reaction path using serpentine to provide insights into pretreatment and reaction issues.

In the process development area, the team has completed a feasibility study of a process originally proposed by Los Alamos National Laboratory (*9, 11*). This process uses HCl

solution reacting with serpentine to produce $Mg(OH)_2$ which is subsequently used to sequester CO_2. Although the study found the process energy intensive and inappropriate for CO_2 sequestration, the analyses of individual steps were useful for developing new processes. Los Alamos National Laboratory is currently pursuing reaction mechanisms that may allow the heat treatment step for serpentine to be bypassed.

Progress has also been made in identifying sources of alternative minerals that can be used for CO_2 sequestration. In addition to natural olivine and serpentine deposits, researchers at NETL are engaged in a study of using waste streams such as coal ash rich in calcium and magnesium as a potential mineral source to sequester CO_2.
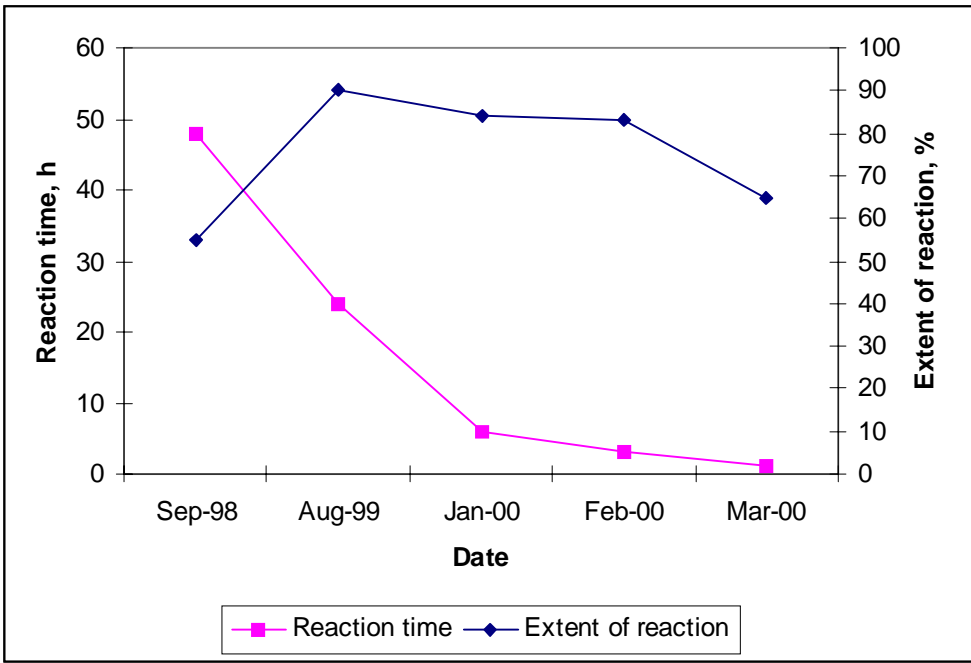
Figure 2. Reaction time of carbonic acid mineral carbonation has been reduced from 48 hrs to 1 hour over the period from Sept. 1998 to March 2000 at the Albany Research Center.

Scale-up Plan for Next Several Years

Most of the past work has been summarized in a paper presented at Globe-Ex conference (*15*). Recently, the mineral sequestration team conducted an extensive review of its approach and achievement and drafted a scale-up plan. Our projective goal is to build a validated knowledge base necessary to construct a demonstration plant capable of effectively sequestering 5.5 ton/h CO_2 (for a 10 MWe plant) in a time frame of around six

years. There are several stages of efforts to achieve such a goal. The team has identified critical issues at each stage. Table 1 listed a four-stage plan and critical issues to be addressed.

Table 1. Experimental Stages Employed to Address Critical Issues

Stage	Operational Scale	Major Issues
Laboratory	Batch operation using gram quantities	-Kinetics/Mechanisms/Feedstocks -Role of impurities -Pretreatment options
Bench	Continuous operation at 5 lb/hr mineral input	-Evaluation of multiple concepts -Semi-integrated pre- & post -processing -Materials issues -Heat transfer, solid & liquid flow effects
Engineering Development	Continuous operation at 500 lb/hr mineral input	-System integration -Concept validation -Relevant reliability, efficiency & cost data
Demonstration	Continuous operation at 5 tons/hr mineral input	-Site Issues -Relevant reliability, efficiency and cost data -Byproduct Handling

The critical issues can be further illustrated in their relation to the processing steps as shown in Figure 3.

Even with progress made so far, to develop an economical method to sequester CO_2 with minerals is still a challenging task, because the process is still relatively slow, and most reactions require high pressure and moderately elevated temperature. The number one priority is still to develop faster reaction conditions that require a lower pressure. In order to achieve this goal, the team is not only testing at different conditions, but also working to improve fundamental understanding of reaction paths. At the same time for scale-up purpose, a system study has been initiated at the Albany Research Center and the National Energy Technology Laboratory to evaluate a potential realization using conceptual designs and known reaction conditions. Issues to be addressed in the system study include capital and operating costs, and environmental impacts. The study will also prioritize future research needs.
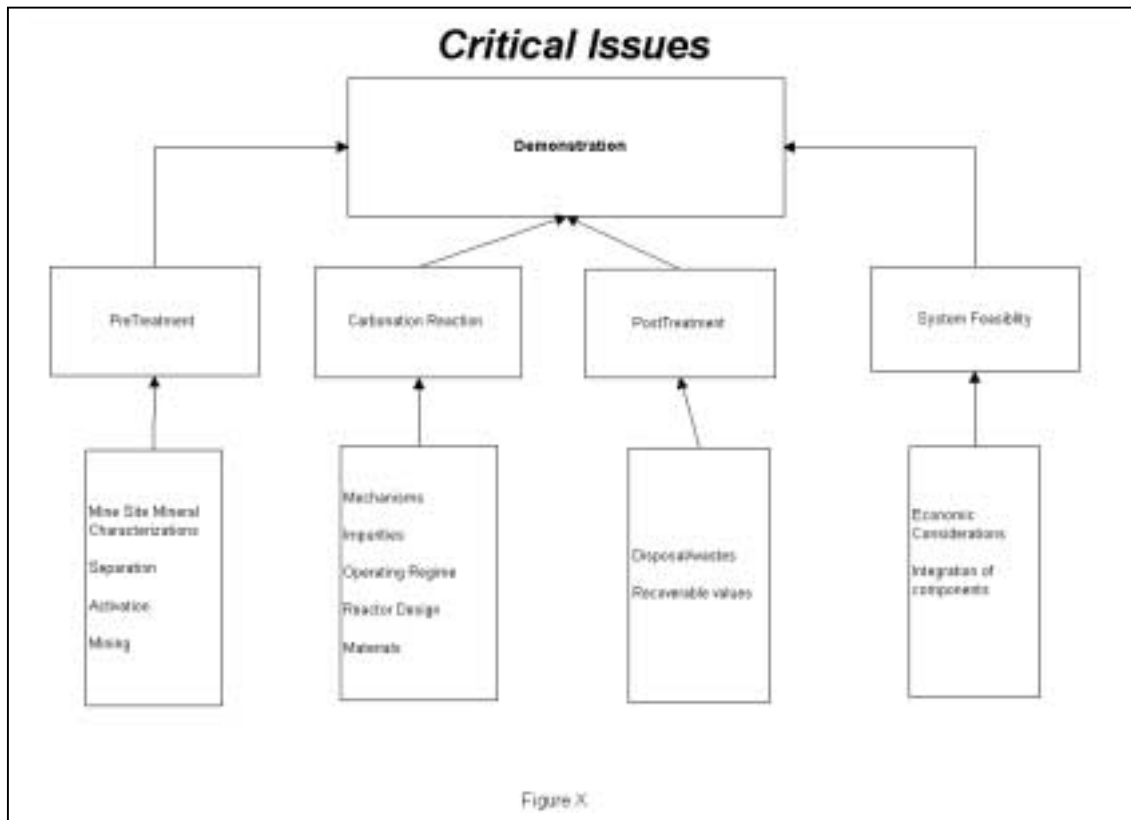
Figure 3. Critical Issues listed by Processing Step

Because of many fundamental advantages, such as long-term stability, large capacity, and favorable thermodynamics discussed in this paper, using minerals to sequester CO_2 appears attractive. Although currently a practical process is still yet to be developed, we have significantly reduced reaction times since the inception of the program. We also identified many critical areas to be studied. Additional support and industrial participation is welcomed so that progress can be accelerated and an early small-scale sequestration testing can be built.

REFERENCES

1) U. Siegenthaler and H. Oeschger, "Biospheric CO_2 Emissions During the Past 200 Years Reconstructed by Deconvolution of Ice Core Data," Tellus **39B,** (1987) 140-154.

2) C.D. Keeling, T.P. Whorf, M. Wahlen, and J. van der Plicht, "Interannual Extremes in the Rate of Rise of Atmospheric Carbon Dioxide since 1980," Nature **375,** (1995) 666-670.

3) EIA (Energy Information Administration) 1999, International Energy Outlook 1999, DOE/EIA-0383(99), U.S. Department of Energy, Washington, D.C.

4) S.I. Plasynski, C.B. Bose, P.D. Bergman, T.P. Dorchak, D.M. Hyman, H.P. Loh, and H.M. Ness, "Carbon Mitigation: A holistic Approach to the Issue," Paper presented at the 24th Intl. Tech. Conf. On Coal Utilization and Fuel Systems, March 8-11, 1999, Clearwater, FL.

5) Vision 21, Clean Energy for the 21st Century, U.S. Department of Energy, Office of Fossil Energy DOE/FE-0381, November, 1998. (Also available on www.fetc.doe.gov/publications/brochures/)

6) W. Seifritz, "CO_2 Disposal by Means of Silicates." *Nature,* **345,** (1990) 486.

7) T. Kojima, A. Nagamine, N. Ueno and S. Uemiya, "Absorption and Fixation of Carbon Dioxide by Rock Weathering." Proceedings of the Third International Conference on Carbon Dioxide Removal, Cambridge Massachusetts, September 9–11, 1996*, Energy and Conservation Management*, **38 Suppl,** (1997) S461–S466.

8) W. D. Gunter, E. H. Perkins and T. J. McCann, "Aquifer Disposal of CO_2 rich gases: Reaction Design for Added Capacity." Energy Conversion and Management, **34,** (1993) 941–948.

9) K. S. Lackner, C. H. Wendt, D. P. Butt, D. H. Sharp, and E. L. Joyce, "Carbon Dioxide Disposal in Carbonate Minerals," *Energy (Oxford)*, **20** [11] (1995) 1153-1170.

10) W. K. O'Connor, "Investigations into Carbon Dioxide Sequestration by Direct Mineral Carbonation." Presentation at Second Meeting of Mineral Sequestration Working Group, November 3, 1998, Albany Research Center, Albany, Oregon.

11) D. P. Butt, K. S. Lackner, C. H. Wendt, Y. S. Park, A. Benjamin, D. M. Harradine, T. Holesinger, M. Rising, and K. Nomura, "A Method for Permanent Disposal of CO_2 in Solid Form," *World Resource Review*, **9** [3] (1997) 324-336.

12) C. Drägulescu, P. Tribunescu & O. Gogu, "Lösungsgleichgewicht von MgO aus Serpentinen durch Einwirkung von CO_2 und Wasser." *Revue Roumaine de Chimie,* **17,** 9, (1972) 1518–1524.

13) W. K. O'Connor, D.C. Dahlin, D.N. Nilsen, R.P. Walters, and P.C. Turner., "Carbon Dioxide Sequestration by Direct Mineral Carbonation with Carbonic Acid." Presentation at 25th International Technical Conference on Coal Utilization & Fuel Systems, March 7, 2000, Clearwater, Florida.

14) F. Goff, G. Guthrie, D. Counce, E. Kluk, D. Bergfeld, and M. Snow, Preliminary Investigations on the Carbon Dioxide Sequestering Potential of Ultramafic Rocks. Los Alamos, NM: Los Alamos National Laboratory; LA-13328-MS; 1997.

15) P.M. Goldberg, Z.-Y. Chen, W. O'Connor, R. Walters, K. Lackner, and H. Ziock, "CO Mineral Sequestration Studies," Paper presented at GlobeEx 2000, August 2000, Las Vegas, NV.

Native Plants for Optimizing Carbon Sequestration in Reclaimed Lands

LAUR-01-1126

Pat J. Unkefer (punkefer@lanl.gov; 505-665-2554)
Biosciences Division (B-S1), Mail Stop E529
Los Alamos National Laboratory
Los Alamos, NM 87545

Michael H. Ebinger (mhe@lanl.gov; 505-667-3147)
Environmental Dynamics and Spatial Analysis Group (EES-10), Mail Stop J495
Los Alamos National Laboratory
Los Alamos, NM 87545

David D. Breshears (daveb@lanl.gov; 505-665-2803)
Environmental Dynamics and Spatial Analysis Group (EES-10), Mail Stop J495
Los Alamos National Laboratory
Los Alamos, NM 87545

Thomas J. Knight (tknight@usm.maine.edu; 207-780-4577)
Biological Sciences Department, 96 Falmouth Ave.
University of Southern Maine
Portland, ME 04103

Christopher L. Kitts (ckitts@calpoly.edu; 805-756-2949)
Associate Director, Environmental Biotechnology Institute
California Polytechnic State University
San Luis Obispo, CA 93407

Suellen A. VanOoteghem (svanoo@fetc.doe.gov; 304-285-5443)
Environmental Science and Technology, PO Box 880
National Energy Technology Laboratory
Morgantown, WV 26507-0880

Introduction

Carbon emissions and atmospheric concentrations are expected to continue to increase through the next century unless major changes are made in the way carbon is managed. Managing carbon has emerged as a pressing national energy and environmental need that will drive national policies and treaties through the coming

decades. Addressing carbon management is now a major priority for DOE and the nation. One way to manage carbon is to use energy more efficiently to reduce our need for major energy and carbon source-fossil fuel combustion. Another way is to increase our use of low-carbon and carbon free fuels and technologies. A third way, and the focus of this proposal, is carbon sequestration, in which carbon is captured and stored thereby mitigating carbon emissions.

Sequestration of carbon in the terrestrial biosphere has emerged as the principle means by which the US will meet its near-term international and economic requirements for reducing net carbon emissions (DOE Carbon Sequestration: State of the Science. 1999; IGBP 1998). Terrestrial carbon sequestration provides three major advantages. First, terrestrial carbon pools and fluxes are of sufficient magnitude to effectively mitigate national and even global carbon emissions. The terrestrial biosphere stores ~2060 GigaTons of carbon and transfers approximately 120 GigaTons of carbon per year between the atmosphere and the earth's surface, whereas the current global annual emissions are about 6 GigaTons. Second, we can rapidly and readily modify existing management practices to increase carbon sequestration in our extensive forest, range, and croplands. Third, increasing soil carbon is without negative environment consequences and indeed positively impacts land productivity.

The terrestrial carbon cycle is dependent on several interrelationships between plants and soils. Because the soil carbon pool (~1500 Giga Tons) is approximately three times that in terrestrial vegetation (~560 GigaTons), the principal focus of terrestrial sequestration efforts is to increase soil carbon. But soil carbon ultimately derives from vegetation and therefore must be managed indirectly through aboveground management of vegetation and nutrients. Hence, the response of whole ecosystems must be considered in terrestrial carbon sequestration strategies.

Objective

The complex interrelationships between plants and soils in the environment are not well understood. Our current understanding is based on an unsatisfactory combination of incomplete scientific knowledge and sound but often site-specific empirical observations. A better understanding of the basic principles governing the interrelations are needed to support the development of practical field approaches that are less site-specific and more generalizable from one site to another. Several knowledge gaps must be advanced to allow this better scientific understanding: (1) a better understanding of plant growth and associated fluxes of carbon from plants to soils is required and (2) a better understanding of the interrelationships between plant growth and soil quality improvement.

Approach

The effectiveness of terrestrial carbon sequestrated has been demonstrated on each of the continents, usually in the context of improving the land management and

particularly by reducing the cultivation of croplands. Less work has addressed the improvement of carbon in a broad class of lands that can be termed grazing lands. This term reflects the end use of a large fraction of the lands slated for re mediation and also reflects the current use of lands being grazed. Collectively these grazing lands are characterized by having the potential for improved carbon sequestration or storage where better management practices or inputs such as fertilizer or improved species can be used.

Many approaches to increasing terrestrial carbon storage are focusing upon the goals of increasing the carbon in the vegetation as well as the carbon in the soil. Accomplishing these goals depends upon fixing and storing greater amounts of atmospheric carbon. Fixing an increased amount of carbon can be most readily accomplished by increasing the biomass produced by increasing the vegetation growing at a site. Examination of the practical requirements for increasing biomass production reveals a positive, self-reinforcing cyclical process between the amount of biomass produced and the soils' capacity to support biomass production. Or re-stated the soils capacity for plant growth (its fertility) is profoundly impacted by the amount and type of plant life growing in the soil. The soil organic matter is derived from the vegetation grown at a site. The soil organic matter is a strong determinant of many of the properties that dictate the amount and type of plant life that can grow in a soil. These include the soil pH, the availability of plant nutrients, the soil's water holding capacity, and the extent to which water can infiltrate.

Re vegetation of reclaimed lands presents an excellent opportunity to optimize the carbon sequestration on these lands. An attractive re vegetation strategy for extreme environments is the use of native vegetation or vegetation that is well adapted for similar environments. The potential of native plant species for land reclamation is being recognized by those attempting to reclaim mine sites in regions with challenging climatic conditions and limiting soil quality. Workers at mine sites in Colorado (Long, 1999), Arizona (Pfannenstiel, 1999) and Utah (Daniels, 1999) all reported successful applications of native species. They reported the need to use an ecosystem approach. Pfannenstiel's (1999) work had spanned the longest period of time and thus had developed a more advanced understanding of successful practices. He noted the importance of including multiple types of plant species, growing sufficient ground cover to increase soil water, using natural associations between native species and matching soil with plant species. Thus he articulated key elements of an initial understanding of re vegetation with native species. The plant survival rates were acceptable but needed improvement to increase practicality and the number of types of plants used was limited.

Project Description (or Technology)

The factors that dictate the degree to which native or adapted species succeed at a site are not well understood; and this lack of understanding hampers our ability to efficiently re vegetate sites while optimizing carbon sequestration. Studies have been

initiated to address major key technical issues including (1) key plant growth conditions and (2) influences of soil organic matter on soil quality.

1. Key plant growth conditions: Effectiveness of amendments to native plant survival and establishment in native soils.

Recent work at LANL led to the discovery of a key molecular level nutrient monitoring and management system used by plants to regulate carbon fixation; this system is focused upon the nutrient, nitrogen (Knight and Langston-Unkefer, 1988, Unkefer et. al., 2000). Nitrogen is the growth-limiting nutrient for essentially all well watered plants in their natural environments. Plants have grown and reproduced for eons in an environment with uncertain supply of water and nutrients; survival has dictated a conservative assessment and husbanding of nutrients. Plants must also regulate their acquisition and metabolism of carbon and nitrogen to provide adequate amounts of these nutrients in the proper stoichiometry required to synthesize their various component proteins, carbohydrates, lipids, etc.   The discovery of this resource-based regulatory system governing plant metabolic rate, growth rate and overall accumulation of biomass, provides a much greater biochemical understanding of plant growth and is directly related to assessing plant carbon pools and fluxes.

This work has provided a means to increase the nitrogen use efficiency of plants which is a strongly linked with water use efficiency. This relationship will be explored in an attempt to find a practical means of enhancing the effectiveness of establishing greater vegetation on lands.

2. Influences of soil organic matter on soil quality

A major step in modernizing land management has been the recognition that the soil carbon content is an integral component of productive soils (a general reference, Lal et. al., 1998b). Soil carbon content is directly and positively correlated with such recognized characteristics of soil quality as bulk density, cation exchange capacity, pH, aggregate size, moisture holding capacity, the soil macrobes (earthworms, etc.) and the availability of plant nutrients because it increases the microbial activities mobilizing these nutrients. Previous investigations of these effects have been hampered by the limitations generated by the complexity of the processes and often by a lack of suitable experimental framework in which these processes can be addressed (Lal et. al., 1998b). We have found a way to overcome at least partially, these limitations.

A more suitable experimental framework is now available to us. Recent advancements in our understanding of ecosystems have provided a longer term conceptual model of the changes in these ecosystems as characterized by changes in their vegetation. Researchers such as Archer and Stokes (2000) have articulated four states of ecosystems and have begun to assess the potential for the effects of chronic and episodic stresses and disturbance to cause transitions from one state to another. These four states are as follows: Steady-state fluctuations; Suppressed re generation; Accentuated

degeneration; and Recovery. Work at Los Alamos by Breshears and coworkers has complimented and extended this work and as such provides additional sites for study (see ref's in Breshears et. al this volume). The recognition of these four states of ecosystem health or status and the existence of well characterized study sites provides the opportunity to examine the changes in the soil quality that accompany these changes in ecosystem vegetation. The changes in vegetation are linked to the changes in the soil.

Thus to study soil quality we will choose sites that represent these ecosystem states. Others have recognized the existence of and experimental utility of such states in soil status (Tongway and Hindley, 2000). Thus we will use sets of research sites that represent these four ecosystem states at various locations (mesic and semi arid) with different climates (colder and warmer) and will different soils. We can use gradients of climate (elevation) to provide transitions that can be studied. Such gradients exist within the Los Alamos Ecological Research Park and for which extensive data sets are available on climate, carbon inventory and vegetation (see refs in Breshears et. al., this volume). Basic site and soil characterization has either been done or will be done as a part of this work. This characterization includes such parameters as site plant biomass and plant community and soil carbon, pH, moisture, plant nutrients, and fundamental soil physical properties.

All of this work will be done within the larger scientific context of broader ecological investigations currently underway at these (Breshears et. al., 2001; Ebinger et. al., 2001) and other sites to be selected using these same criteria.

2A Microbial capability for decomposition of biomass: the fuel source for soil microbes and their soil building functions.

The decomposition of biomass is a vital component of healthy and fertile soil. This decomposition of biomass fuels the various microbial activities in the soil, including the essential microbial mobilization of nutrients. This microbial activity is a key determining factor in the availability of the plant nutrients nitrogen and phosphorous. Decomposition of biomass can also be expected to fuel other microbial activities as the deposition of carbonates. Thus understanding better the microbial decomposition of biomass is a key to a better understanding of soil quality and its management.

At sites where the decomposition rates for woody and herbaceous biomass have been determined, we will examine the microbial potential for this decomposition. Sites will be selected from the above mentioned gradients to allow us to examine the development of soil quality over timeframes extending far beyond the length of the study. The woody biomass has much greater proportion of lignin relative to cellulose while grassy biomass is more cellulosic in composition. Different microbial capabilities are needed to decompose these two general types of materials. Expect to be able to monitor he changes in the microbial capability as the vegetation changes at a site. For example as the soils microbial population changes to adapt to the decomposition of woody biomass in soils previously growing grass and then invaded by woody species. This information will tell us at what rate the soils are adapting.

2B Microbial capability for improving available N: a growth-limiting plant nutrient.

The microbial conversion of plant liter to energy and other nutrients feeds the microbial mobilization of plant nutrients from the soil. Thus the release of some carbon from the soil is necessary in order to improve a soil's capability to grow more biomass. These are cycles that must be enhanced together.

Several basic elements of microbial community structure and diversity are important in soil quality and ecosystem stability. Robust ecosystems with abundant nutrients are contrasted with stressed ecosystems with shortages of nutrients by the relative degrees of microbial diversity (Atlas and Bartha, 1997). More diverse microbial communities are often characterized by very efficient energy usage which to say that they are expected to use less energy per unit of microbial biomass. This difference in efficiency and diversity may also be expected to be manifested when comparing the improved vs. degraded soils. Relatively diverse microbial communities provide redundancy in functional capability and thus may well provide a degree of resiliency for community to be able to sustain itself when subjected to changes in environmental conditions or stresses. Because the availability of the key plant nutrient, nitrogen, is dependent upon microbial components of the soil we are examining the microbial function diversity with respect to its function of sustaining availability of nitrogen.

2C A new and simplified approach to soil microbial functions:

Existing methodologies for examining the soil microbes are inadequate to address such a complex system. The thousands of different types of microbes present in the soil present more complexity than can be addressed with existing tools. We will develop a simple method of assessing the microbial potential for carrying out specific functions. Specially we will develop tools for examining the key activities of biomass decomposition and mobilization of nitrogen using modern molecular biology techniques whose effectiveness was demonstrated in soil bioremediation studies (Clement et. al., 1998).

Several microbial activities carry out the decomposition of lignin and cellulose. These are distinguished as ligninase and cellulase activities. Several bacterial activities are involved in controlling the availability of nitrogen to plants. These activities are nitrogen fixation which increases available nitrogen and denitrification, which converts nitrogen from forms useful to the plant to nitrogen gas which is not useful to plants and which escapes to the atmosphere.

We will use the PCR-based DNA techniques with a different set of DNA probes to examine the functionalities of decomposition and nitrogen cycling in these soils. The laboratory at California Polytechnic State University is very experienced and expert in these studies, having pioneered the development of some of these techniques. The TRF patterns will be analyzed using three different pattern search/data display methods:

hierarchical cluster analysis, principal component analysis and canonical correlation analysis.

Application (or Benefits)

Improving our science-based methods for increasing the vegetation on lands can be expected to have net positive benefit on over terrestrial carbon sequestration. Lal and co authors (1998) estimated that a strong net gain in carbon sequestration is possible with improved soil management practices in the U. S. croplands. This group has more recently (Follett, et.al. 2001) estimated a similar strong net gain in carbon sequestration in the privately owned US grazing lands. They estimated that improved management practices for these lands would result in an increase of 70-205 MMT of carbon sequestered annually. They limited their estimates to the 212 Mha of privately owned grazing land and, as such, did not include the 124 Mha of publicly owned grazing lands. Furthermore they assumed only modest improvements in land management practices and assumed these improvements would actually be implemented on only a fraction of the lands. Thus their estimate was quite conservative.

Developing better science-based methods for establishing and increasing biomass production (or vegetation) on lands being reclaimed or improved will improve the carbon sequestration at these sites. Science-based methods can help practitioners to generalize and interpret results obtained at different sites, in different regions, climates, soils etc. This work will help to develop technologies is such a fashion that they can be more readily implemented. In order to a technology to be useful it must be implemented. If a technical approach is to be implemented it must meet certain criteria: it must be effective; it must be developed to such an extent that it can be practiced by those in the field; and it must be attractive to the practitioner by providing a valuable set of benefits. Other workers have demonstrated the effectiveness of re vegetating sites with native plants. This work will help to develop it for practical implementation and will help to document its expected benefits; the principle of which will be increased carbon sequestration and the consequential improvement of soil productivity.

The Department of Energy has established aggressive targets for low cost carbon sequestration (<$10 / T of C) technical approaches to avoid catastrophic increases in the nation's energy costs. Meeting this target cost range requires a technology that can be implemented inside an existing industry and thus gain cost leverage. The emerging carbon credits market in the US and Canada has established bio sequestered carbon values well within this range. Thus the DOE target cost range can be met using terrestrial bio sequestration of carbon.

References

Atlas, R. and R. Bartha. 1997 Chapter "Evolution and Structure of Microbial Communities", *In* Microbial Ecology, Addison Wesley Publishing.

Archer, S. and C. Stokes. 2000. Stress, disturbance and change in rangeland ecosystems. Pages 17-38. *In* Arnalds, O. and S. Archer, editors. Rangeland Desertification. Advances in Vegetation Science 19. Kluwer Academic Publishers, Boston, MA, USA.

Breshears, D.D., M.H. Ebinger and P.J. Unkefer. 2001 Assessing carbon dynamics in semiarid ecosystems: Balancing potential gains with potential large rapid losses. This volume.

Clement, B.G., L.E. Kehl, K.I. DeBord and C.L. Kitts. 1998. Terminal restriction fragment patterns (TRFPs), a rapid, PCR-based method for the comparison of complex bacterial communities. J Microbiol Methods 31: 135-142.

Daniels, R.W. 1999. Enhancement of reforestation at western surface coal mines. Pages 203-204.

Ebinger, M.H., D.A. Cremers, D.D. Breshears, P.J. Unkefer, S.A. Kammerdiener and M.J. Ferris. 2001. Total carbon measurement in soils using laser-induced breakdown spectroscopy: results from the field and implications for carbon sequestration. This volume.

Follett, R.F., J.M. Kimble and R. Lal. 2001. The Potential for U. S. Grazing Lands to Sequester Carbon and Mitigate the Greenhouse Effect. Lewis Publishers, Boca Raton, FL, USA.

IGBP Terrestrial Carbon Working Group. 1998.   The terrestrial carbon cycle: implications for the Kyoto protocol. Science **280**:1393-1394.

Knight, T.J and P.J. Unkefer. 1988. Enhancement of symbiotic dinitrogen fixation by a toxin-releasing plant pathogen. Science 241: 951-954.

Lal, R., J.M. Kimble, R.F. Follett and C.V. Cole. 1998a. The potential of U. S. Cropland to Sequester Carbon and Mitigate the Greenhouse Effect. Ann Arbor Press, Chelsea, MI, USA.

Lal, R. J.M. Kimble and R.F. Follett 1998b. Knowledge gaps and researchable priorities. Pages 595-604. *In* Lal R., J.M. Kimble, R.F. Follett and B.A. Stewart, editors. Soil Processes and the Carbon Cycle. Advances in Soils Science Series, CRC Press, Boca Raton, FL, USA.

Long, M. 1999. Reforestation in the western states. Pages 55-56. *In* Vories, K.C. and D. Throgmorton, editors. Enhancement of Reforestation at Surface Coal Mines: Technical Interactive Forum. U.S. Department of Interior, Office of Surface Mining, Alton, IL and Coal Research Center, Southern Illinois University, Carbondale, IL, USA.

Pfannenstiel, V. 1999. The arid and semiarid west. Pages 147-148. *In* Vories, K.C. and D. Throgmorton, editors. Enhancement of Reforestation at Surface Coal Mines: Technical Interactive Forum. U.S. Department of Interior, Office of Surface Mining, Alton, IL and Coal Research Center, Southern Illinois University, Carbondale, IL, USA.

Tongway, D. and N. Hindley. 2000. Assessing and monitoring desertification with soil indicators. Pages 889-98. *In* Arnalds, O. and S. Archer, editors. Rangeland

Desertification. Advances in Vegetation Science 19. Kluwer Academic Publishers, Boston, MA, USA.

Unkefer, P.J., T.K. Knight and R. Martinez. Use of prolines for improving growth and other properties of plants and algae. US Patent filed 1/27/00.

U.S. Department of Energy. 1999. Carbon Sequestration: State of the Science. Available at http://www.fe.doe.gov/coal_power/sequestration/index_rpt.html

A Proposal to Establish an International Network on Biofixation of CO_2 and Greenhouse Gas Abatement with Microalgae

Paola Pedroni (ppedroni@mail.enitecnologie.eni.it; 39 0252 046615)
EniTecnologie S.p.A., Environmental Technology Research Center
Via F. Maritano 26
20097   San Donato Milanese, Milan, Italy

John Davison (john@ieagreen.demon.co.uk; 44 1242 680753)
IEA Greenhouse Gas R&D Programme
StokeOrchard, Cheltenham, Gloucestershire
GL52 7RZ , United Kingdom

Heino Beckert (Heino.Beckert@netl.doe.gov; 304 286 4132)
National Energy Technology Laboratory, U.S. Department of Energy
3610 Collins Ferry Road
Morgantown, West Virginia 26507, USA

Perry Bergman (Perry.Bergman@netl.doe.gov; 412 386 4890)
National Energy Technology Laboratory, U.S. Department of Energy
P.O. Box 10940
Pittsburgh, Pennsylvania, 15236, USA

John Benemann, (jbenemann@aol.com; 925 939 5864)
Consultant
3434 Tice Creek Dr. No. 1
Walnut Creek, California, USA

SUMMARY

Microalgae mass cultures can use solar energy for the biofixation of power plant flue gas and other concentrated CO_2 sources into biomass that can be used to produce renewable fuels such as methane, ethanol, biodiesel, oils and hydrogen and for other fossil-fuel sparing products and processes. They thus can mitigate emissions of fossil CO_2 and other greenhouse gases. Microalgae are currently used commercially in the production of high-value nutritional products, in wastewater treatment and in aquaculture. One commercial microalgae production plant, in Hawaii, is already using flue gas from a small power plant as an exogenous source of the CO_2 required to grow algal biomass. Although still a relatively small industry (total production is only a few thousand tons of algal biomass per year world-wide), microalgae technologies have been extensively studied over the past decade in the context of greenhouse gas mitigation, specifically in Japan and the U.S.

In January of this year, a Workshop attended by 38 participants from major energy companies, the microalgae industry, governmental organizations, universities and others, was held in Monterotondo, near Rome Italy, to discuss the prospects of microalgae technologies in abating

greenhouse gases. The Workshop was organized by EniTecnologie (the R&D arm of ENI, the Italian oil company), the U.S. Department of Energy, and the IEA Greenhouse Gas R&D Programme. The consensus of the Workshop participants was that microalgae offer a variety of approaches to this goal, including the production of energy saving products (such as fertilizers and bioplastics) and applications in wastewater treatment and aquaculture. In addition, microalgae processes have potential for development of larger-scale systems, specifically for power plant CO_2 capture and renewable fuels production. Significant research, development and demonstration (R,D&D) efforts will be required to achieve the scientific and technical advances required, including high productivities, culture stabilities, control of biosynthetic pathways, and biomass harvesting and processing. Integrated processes in wastewater treatment and aquaculture were indicated as near-term applications of this technology. In addition to producing renewable fuels, such processes would, when compared to conventional processes, mitigate greenhouse gases by reducing CH_4 and N_2O emissions and by reduced fossil fuel consumption.

A formal proposal for establishment of an International Network for research coordination and collaboration, operating under the IEA Greenhouse Gas R&D Programme, was presented to the Executive Committee of the Programme at its meeting in Regina, Canada, in March 2001. The proposal focuses on practical R,D&D of microalgae systems that utilize concentrated sources of CO_2, in particular flue gas from stationary fossil fuel-burning power plants, and convert the algal biomass to renewable fossil fuel substitutes. The membership of this Network will comprise energy companies, government agencies, and other organizations interested in supporting the development of microalgae GHG mitigation technologies. The Network would start operations in 2002.

1. INTRODUCTION

The IEA (International Energy Agency) Greenhouse Gas R&D Programme was established ten years ago to evaluate technologies for the abatement/mitigation of greenhouse gas emissions, to disseminate information, to promote research activities and to develop targets for appropriate R,D&D. Some 16 countries and the EU participate in this Programme, which is also sponsored by several major energy companies. At the meeting of the IEA Greenhouse Gas R&D Programme Executive Committee in August 2000, in Cairns, Australia, the U.S. Department of Energy and EniTecnologie proposed the establishment of a new activity within the Programme to help coordinate and advance practical R,D&D in the area of microalgae technology for GHG mitigation. This activity was proposed to be organized as a "Network" of interested members and supporters of the IEA Greenhouse Gas R&D Programme, as well as other organizations and companies interested in promoting applied R&D in this area, and in coordinating and collaborating in such efforts.

Following up on this proposal, a Workshop was held in January of 2001, at the EniTechnologie research facility in Monterotondo, near Rome, Italy, to review the technological basis of this field and to discuss the proposal for this new activity. The U.S. Department of Energy and EniTecnologie supported this Workshop organized by the IEA Greenhouse Gas R&D Programme. About half of the 38 participants came from major energy companies, with the remainder representing microalgae companies, universities, government agencies, and private organizations. Aims of the Workshop were to:
1. review the technological basis and prospects of microalgae technologies in abating GHGs; and

2. elicit interest in the proposed "Microalgae Biofixation Network".

Technical presentations were followed by plenary and breakout sessions to develop consensus recommendations for R&D in microalgae technologies for CO_2 biofixation and GHG mitigation. These are discussed below, followed by a brief description of the Network proposal. A Workshop report is available on request from the authors.

2. TECHNICAL BACKGROUND

In recent years, major organized R,D&D efforts related to microalgae biofixation of CO_2 and production of renewable fuels were carried out in Japan and the U.S. (Usui and Ikenouchi, 1996; Sheehan et al., 1998). Although these prior efforts supported the potential of microalgae technologies, they also suggested the need for a more critical analysis of the proposed processes and R&D approaches, and the need to focus on both near- and long-term R&D goals. The Monterotondo Workshop brought together experts in microalgae mass culture to review the technical issues and provide a diversity of visions for microalgae applications in GHG mitigation. The main technical presentations (Table 1) provided the technical background to this Workshop (See the Workshop Report for summaries of the individual presentations).

TABLE 1.   Workshop Main Technical Presentations

- **Mario Tredici**, University of Florence, Italy ”Introduction to microalgae biotechnology”

- **John Benemann**, Consultant, USA ”The US experience in microalgae biofixation”

- **Yoshi Ikuta**, SeaAg Japan Inc., Japan ”The Japanese experience in microalgae biofixation"

- **Paul Roessler**, Dow Chemical, USA ”Microalgae genomics and molecular biology”

- **Norihide Kurano**, Marine Biotechnology Institute, Japan ”Biological CO_2 fixation and utilization project”

- **Avigad Vonshak**, Ben-Gurion University, Israel ”Stress physiology of dense outdoor algal cultures”

- **Miguel Olaizola**, Aquasearch Inc., USA ”The issue of cost of biological sequestration of CO_2: closed systems offer a solution”

- **Gerry Cysewski**, Cyanotech Corp., USA ”Carbon dioxide recovery in open pond culture of *Spirulina*”

- **Bailey Green**, Oswald Green, LLC, and University of California Berkeley, USA "Avoidance and mitigation of greenhouse gas emissions and microalgal biofixation of CO2 using the AIWPS”

- **David Brune**, Clemson University, USA ”Greenhouse gas mitigation with a sustainable aquaculture process”

- **Joseph Weissman**, SeaAg, Inc., USA “System and process design”

A practical example of a current microalgae production process is the case of *Spirulina*, a microalga already produced commercially in open ponds in many countries around the world. In these production systems, the algae are cultivated in large (typically 0.2 –0.4 hectares), raceway-type open ponds mixed by paddle wheels. Nutrients, most importantly CO_2, are added to the ponds and these filamentous algae are then harvested by fine mesh screens, spray dried and sold as specialty human foods and animal feeds. The CO_2 is typically purchased from commercial sources, although in some cases it is also derived from the flue gas emitted by the drying operation.

At the Cyanotech Corp. algal production facility in Kona, Hawaii, (Figure 1) a small power plant was build to produce both power and allow the capture of the CO_2 required for algal production ponds (Figure 2). Two 180 kW generators (with one spare) produce the electricity required to operate the paddle wheels on the 67 algal production ponds (avg. 0.3 ha in size) and other process power needs. The stack gas comes out at some $485^{\circ}C$ at 20 scm/min and contains 8% CO_2, or 188 kg/hr of CO_2. This is transferred to the bottom of a CO_2 absorption tower, 2.4 m diameter and with some 6.4 m high packing material. The spent culture medium (after harvesting the *Spirulina*) comes in at the top and is collected in the bottom. The countercurrent absorption system is 75% efficient and provides some 67 t CO_2/month, supporting 36 t/mo of *Spirulina* production, enough to provide CO_2 to 12 ha of ponds. The system generates an annual net income (credit) of almost $300,000 from power and CO_2 savings (Cysewski, Workshop Proceedings). This patented system provides a practical example of microalgae biofixation of CO_2. Biofixation of CO_2 into specialty foods, such as *Spirulina* does not, by itself, mitigate greenhouse gases. The most direct way for greenhouse gas mitigation is for the algal biomass to be converted to a renewable fuel, displacing fossil fuels.

It was pointed out by the Workshop participants that the current cost of commercial algal production in open ponds, such as for *Spirulina*, is some $5,000 per ton, but that the allowable cost for biofixation of CO_2 and renewable fuel production would be at most $250 per ton. This will require a large increase in the achievable productivities of microalgae systems as well as major cost reductions in the production process. These can be envisioned, in particular through an at least ten-fold increase in the scale of such ponds, as well as major cost reductions in essentially all aspects of the production systems. Asides from productivity, major technical and economic issues in large-scale algal mass culture include contamination and culture stability, algal biomass harvesting, and processing of the biomass to fuels. These will be the challenges faced in advancing this technology from its present status in specialty foods and feeds production to large-scale systems for fuels production and greenhouse gas mitigation.

A major theme of the technical presentations was the contrast between the production of microalgae in open (raceway, paddle wheel-mixed) ponds versus closed (typically tubular, optical fiber, flat plate) photobioreactors. Although closed photobioreactors have been used in some commercial microalgae production, they are too expensive for application to the low-cost production systems required for microalgae fuel production and greenhouse gas mitigation. A current commercial application of closed photobioreactors is in the cultivation of the unicellular alga *Haematococcus pluvialis*, a source of the very expensive pigment astaxanthin, used in salmon aquaculture and also as an antioxidant in food supplements (Olaizola, Workshop Report). Although this alga is difficult to maintain in mass cultures, it can be cultivated in open ponds (see Figure 1), with closed photobioreactors required in the start-up phase of the production process.

FIGURE 1. TYPICAL COMMERCIAL MICROALGAE PRODUCTION FACILITY
Cyanotech Corp., Kona, Hawaii. Note green ponds culturing *Spirulina*
and red ponds with *Haematococcus pluvialis*. Note paddle wheels.

FIGURE 2.
POWER PLANT AND CO₂ SCRUBBER FOR MICROALGAE PRODUCTION
Cyanotech Corp., Kona, Hawaii. See Text.

A similar process could be envisioned for larger-scale microalgae production processes for greenhouse gas mitigation: the initial starter cultures are cultivated in small closed photobioreactors and then transferred through increasingly larger systems to the final open production ponds. One potential application of such a scheme would be with the alga *Botryococcus braunii*, which contains up to 50% pure hydrocarbons by weight. Indeed, this alga blooms naturally in some Australian lakes and the algal biomass blown on shore has been used as fuel in Australia in the past (Wake and Hillen, 1980).

The application of closed photobioreactors was a focus of the very large (> $100 million) Japanese R&D program carried out during the 1990's to develop microalgae greenhouse gas mitigation technologies (Kurano, Workshop Report). This program involved a large number of private companies, as well as collaborative work with several research institutes and universities. Over 10,000 strains of microalgae were isolated and screened for tolerance to high CO_2, temperature, salinity, high growth rates, maximum cell densities, O_2 evolution rates, etc. Selected algal strains were investigated for optimized growth and production in photobioreactors of up to 200 liters in volume. In particular, designs using optical fibers were developed, although these are problematic due to the large light losses aside from their clearly excessive costs. Contrasting with this approach, at Tohuku Electric Power Co., in Sendai, Japan, a 16 month test of algal cultivation using the actual flue gas from a large oil-fired power plant was carried out using two small open raceway ponds (about 5 m^2 total) (Ikuta, Workshop Report). The strain cultured was a green alga, a *Tetraselmis* species that appeared spontaneously and replaced the initially inoculated strains. Seasonal productivities (Spring to Autumn) averaged some 17 g.m^{-2}.day^{-1} (all biomass units are ash-free dry weights). This project demonstrated that power plant flue gases can be used directly in a stable algal production in open raceway ponds. Presently, commercial diatom cultivation is being carried out in Japan in the context of commercial clam aquaculture, demonstrating that such systems can utilize flue gas CO_2 with 90% efficiency (Ikuta, Workshop Report).

A major focus of the technical presentations and discussions was how to achieve the very high productivities required for greenhouse gas mitigation. This issue has been studied since the initial development of this technology, starting with an international R&D effort some 50 years ago (Burlew, Algal Culture from Laboratory to Pilot Plant, 1953). The advantages of microalgae mass culture were already recognized at that time, including that algal densities can always be maintained near the optimum for light absorption and utilization, and that microalgae have the potential for very high productivities. However, solar conversion efficiency (productivity) is limited by the so-called "light saturation effect": microalgae cultures can utilize only a fraction of the sunlight to which algal cultures are exposed, typically one third or less. The reason for this is that the algal photosynthetic pigments (e.g. the chlorophylls, carotenoids, etc.) capture more photons under full sunlight conditions than can be processed by the biochemical machinery of photosynthesis. The four major approaches to overcoming this limitation were already recognized a half century ago (Burlew, 1953):
1. use short (microsecond) pulses of light ("flashing light");
2. expose the cells to high turbulence, achieving a similar effect;
3. dilution of sunlight (such as with the optical fiber photobioreactors or with vertical panels), and
4. improved strains of microalgae, "mutants … that can utilize light of very much higher intensity".

Although much work has been carried out with the first three approaches, in particular R&D on optical fiber bioreactors in Japan and the U.S., only the last approach, mutants that are not light saturated at high light intensities, is potentially practical, at least in the context of low-cost microalgae production. Recently, research in Japan and the U.S. has demonstrated that algal cultures and mutants with reduced antenna sizes can exhibit increased photosynthetic rates under high light intensities (Melis et al., 1999, Nakajima and Ueda, 2000). Application of such strains in large-scale, paddle-wheel mixed, raceway-type open ponds could achieve the very high productivities as well as the very low costs required for biofixation of CO_2 from power plant flue gases and their conversion to renewable fuels (Benemann, 1993). The molecular tools of modern genetic biotechnology are being developed for several microalgae species and are becoming available to allow the practical development of the improved strains required for high mass culture productivities (Roessler, Workshop Report).

Although the light saturation effect is perhaps the major limitation on productivity, it is not the only one. During cultivation, either in ponds or in closed photobioreactors, microalgae are subjected to diurnal variations in not only light intensity but also temperature and O_2 (which can accumulate to several-fold above air saturation levels, particularly in closed photobioreactors). High light intensities can often be detrimental to algal cultures: efficiencies for *Spirulina* drop dramatically during the middle of the day, due to the inhibitory effects of high sunlight. Temperature is another factor: the alga *Monodus subterraneus* growing in a diurnal temperature regime (13.5 to 28°C), exhibits a strong inhibition in photosynthetic parameters as well as biomass productivity compared to a constant temperature control (Vonshak, Workshop Report). Respiration, both during the night and also during day-time can, and often does, significantly reduce overall productivity.

Near-term applications of microalgae in greenhouse gas mitigation could come through the development of wastewater treatment and aquaculture processes that combine their waste treatment features with reduction in greenhouse gas emissions and biofuels production. Microalgae ponds have been used in wastewater treatment for over 50 years. A multipond "Advanced Integrated Wastewater Pond Systems Technology (AIWSP®)" was developed at the University of California Berkeley by Professor W. J. Oswald and colleagues over the past half century (Green, Workshop Report). This multi-stage process combines primary treatment (settleable solids removal and anaerobic digestion) in initial deep unmixed ("facultative") ponds, with secondary treatment (reduction of biochemical oxygen demand) taking place in shallow, paddle wheel-mixed, raceway ponds ("high rate ponds"). These are rather similar to those used for *Spirulina* production. In the facultative ponds, deep fermentation cells act as in-pond digesters where organic solids settle and undergo methane fermentation. In the high rate ponds, the O_2 produced by the microalgae supports the bacterial oxidation of waste organics. These are then followed by algal settling basins for removal and concentration of the algal cells. Alternatively, the algal biomass can be harvested by dissolved air flotation. A number of multipond systems are operating in California and around the world, treating municipal, agricultural and industrial wastes.

These systems could be applied to reduce greenhouse gas emissions by three main mechanisms:
1. The methane rich (typically >85%) biogas produced in the initial facultative ponds can be collected using submerged gas collectors, thereby reducing the atmospheric emission of this greenhouse gas.

2. The gas can then be used to generate power to mix the ponds and run the operating equipment, thus avoiding the fossil CO_2 emissions from the power consumed in conventional waste treatment.
3. Harvesting the algal biomass and its conversion to biofuels would replace additional fossil fuels.

The algal cultures in the high rate ponds are generally CO_2-limited, and supplemental CO_2 would greatly enhance algal production and biomass and thus, biofuels production.

Similarly, it is possible to consider microalgae greenhouse gas mitigation being carried out in connection with aquaculture systems. For example, a "Partitioned Aquaculture System (PAS)", developed at Clemson University (Brune, Workshop Report, Figure 3) uses paddle wheel-mixed raceway ponds to separate the pond fish culture into a series of separate physical/chemical/biological processes linked together hydraulically. The paddle wheel mixing provides good hydraulic control and maximizes algal growth, outgasing and waste treatment functions, thus greatly reducing the environmental impacts of such systems. Algal photosynthesis increases from about 1-3g C $m^{-2}.d^{-1}$ in conventional catfish ponds to 10 – 12 g C $m^{-2}.d^{-1}$ in the PAS system. This leads to greatly increased levels of O_2 in the ponds, reducing the mechanical aeration required in catfish aquaculture by 75 to 90%, saving power in excess of that required for paddle wheel mixing. Most importantly, from an economic perspective, these systems greatly increase fish production. Calculations of their GHG emissions reductions potential show an overall reduction of over 50%, from 2.0 kg C-CO_2eq/kg of product (fish flesh) for conventional systems to some 0.8 kg C-CO_2eq/kg of product for current PAS systems. The major part of this difference is due to the much lower CH_4 emissions from the PAS compared to conventional aquaculture ponds. Over 60,000 hectares (150,000 acres) of catfish ponds are currently operating in the Southeastern U.S., providing an opportunity for significant impacts in greenhouse gas mitigation through application of this technology, particularly if the much lower greenhouse gas emissions of such fish production compared to meat production are considered (Brune, Workshop Report).

The development and application of advanced microalgal waste treatment and aquaculture technologies required supplying CO_2 to the algal cultures in order to maximize productivities and utilization of waste nutrients. This greatly increases algal biomass and thus, the amount of biofuels that, as a byproduct of this process, can function in greenhouse gas mitigation. The application of such processes to animal wastes, food processing and other industrial wastes would greatly increase the potential of such integrated microalgae systems in GHG abatement.

The ultimate objective of microalgae biofixation of CO_2 is to operate large-scale systems that are able to convert a significant fraction of the CO_2 outputs from a power plant into biofuels. This will require considerable scale-up of such systems, high CO_2 utilization efficiencies, very high algal productivities and very low costs. These requirements cannot be easily achieved with closed photobioreactors that have inherently small-scale units, and where temperature and O_2 control are major problems. Ponds, due to their large open surface area, are self-limiting in oxygen accumulation and temperature increases, and contamination problems are not greater than with closed photobioreactors (Weissman, Workshop Report). CO_2 can be transferred with high efficiency into ponds, using in-pond sumps operated either with, or in the case of flue gas, against the current. Outgasing of CO_2 from ponds can be limited to a small fraction by operating within a defined range of alkalinity, pH, and mixing velocities.

FIGURE 3.
AQUACULTURE–MICROALGAE PONDS FOR FISH AQUACULTURE
(Clemson University, South Carolina)

Results from operation of a pilot plant (two ponds, 1,000 m^2 each) operated in Roswell, New Mexico (1988-1990), demonstrated high (90%) CO_2 transfer and overall utilization efficiencies, and little difference was noted between plastic lined and unlined ponds. This resolved a major uncertainty, as plastic liners would be too expensive for large-scale, low-cost applications. In small-scale ponds, productivities with several diatom species averaged over 30 g.m^{-2}.d^{-1} of ash-free dry weight in experiments of up to several months, with light conversion efficiencies averaging over 7% of PAR (photosynthetically active radiation, about 3.5% of total solar energy). The larger ponds had lower productivity, maximally about 20 g.m^{-2}.d^{-1} in summer, probably due to the less optimal hydraulic and other conditions achieved in these large-scale experiments (Weissman, Workshop Report). Overall, this pilot plant work demonstrated that it is possible to stably mass culture green algae and diatoms in low-cost unlined, relatively large-scale open ponds.

Finally, several participants highlighted the potential of microalgae, specifically the nitrogen fixing cyanobacteria, in biofertilizer production. One concept is to grow such algae in rice field, where

they could be relatively cheaply integrated into rice cultivation. Considerable R&D is still required for such applications, in particular the development of strains that can successfully colonize rice fields. However, because in such rice-field applications there would be no requirement for CO2 fertilization, these potential applications are not further considered in the context of the microalgae biofixation of CO_2 R&D needs.

3. R&D NEEDS FOR MICROALGAE BIOFIXATION

The major technical challenges for microalgae biofixation of CO_2 for greenhouse gas abatement are the very large cost reductions required in the overall process, compared to current commercial production technologies. Absent other economic considerations, such as in wastewater treatment, very high solar conversion efficiencies, approaching 10% of total solar energy into biomass, will be required for stand-alone algal processes, where biofuels are the main output. This corresponds to a productivity of some 60 g ash-free organic dry weight.m^{-2}.day^{-1}, depending on location and biomass C-content. The cost of producing the algal biomass could be at most about $250/ton. This suggest total system capital costs, depending on productivity, of not more than $100,000 to 150,000/ha, including harvesting, infrastructure, and the processing of the biomass to fuels. This would exclude all but the lowest cost designs, e.g. large-scale open pond systems without plastic liners. Operating costs would also have to be quite low, not higher than $100 to 150/ton of algal biomass.

Engineering and costs analyses of large-scale (several hundred hectare) pond systems have projected such low costs, sufficient to allow for their use in fuel production and greenhouse gas mitigation (Weissman and Goebel, 1987; Benemann and Oswald, 1996). These studies assumed favorable sites, optimized production systems and, most importantly, the ability to achieve very high productivities, approaching 10% of solar energy conversion. Processes integrated with waste treatment would be competitive at much smaller scales and lower productivities, as their environmental functions would cover many, if not all, of the process costs.

Productivities of algal mass cultures are dependent on many factors, from algal strains to weather and culture techniques. However, under optimal conditions of sunlight and temperature, average algal biomass productivities are projected to be as high as 30 g.m^{-2} .d^{-1} using current or near-term future technology. It should be noted that commercial production rates for *Spirulina* are given only as 10 g.m^{-2}.d^{-1}, even in the rather ideal climate of Hawaii. One reason for these low productivities is that, to lower cost of harvesting, these cultures are operated to maximize cell density rather than productivity. Also, *Spirulina*, as other cyanobacteria, are not as highly productive as green algae and diatoms, because they exhibit high respiration rates and are easily photoinhibited. Work with green algae and diatoms has demonstrated productivities that could be extrapolated to an annual average approaching 30 g.m^{-2}.day^{-1}, if operated in a similar climate as Hawaii. Pilot plant work at Roswell, New Mexico, mentioned above, also suggested that relatively high productivities of these organisms are achievable with low-cost unlined (e.g. dirt bottom) ponds and that CO_2 utilization can be very high (>90%) in open ponds.

The main obstacles to further increasing algal productivities are light saturation and respiration (both night-time dark respiration and day-time photorespiration). Light saturation is the largest

single factor limiting the productivity of algal mass cultures, and genetic selection of algal strains with smaller antenna sizes (fewer chlorophylls per photosynthetic unit) is the most plausible approach to overcoming this limitation. Respiration is another area requiring applied R&D, if the goal of high productivities is to be achieved. Other issues, such as how to stably cultivate and maintain highly productive algal strains in mass cultures, must also be addressed in any applied microalgae biofixation R&D program.

One central issue is whether closed photobioreactors exhibit higher productivities than open ponds, and whether they can avoid, not just delay, contamination with competing microalgae or other invaders. The high costs of such systems would, in any event, make them unsuitable for applications in biofixation of CO_2. However, closed photobioreactors would be useful in the building up of inoculum cultures from the laboratory for applications in large-scale outdoor systems, and as R&D tools.

In addition to productivity, the major objective of future R&D must be to reduce the very high capital and operating cost of microalgae production in current commercial systems. As stated above, the current costs of microalgae biomass production (e.g. for *Spirulina*) is some \$5,000/t of biomass, some twenty-fold higher than is currently allowable for greenhouse gas abatement and renewable fuels production. Indeed, compared to lignocellullosic biomass, which can be produced for some \$50/t (all biomass weights are given on a dry ash-free basis), even \$250/t is high, though allowable if the algal biomass can be more easily converted at higher yields to liquid and gaseous fuels (biodiesel, ethanol, hydrocarbons, methane or even hydrogen). In any event, such a large cost reduction from current technology would need to be accomplished through major increases in productivity, process improvements and economies of scale. Process improvements would include development of a lower cost algal harvesting process. Economies of scale suggest that algal systems of several hundred hectares, at a minimum, will be required in power plant fossil CO_2 biofixation. To accomplish this objective will require long-term R&D efforts and funding.

In the near-term, the most likely applications of microalgae technologies are wastewater treatment and aquaculture where the algae provide both dissolved O_2 (for bacterial breakdown of wastes and for fish production) and excess nutrient removal. Such wastewater treatment and aquaculture processes can also reduce anaerobically generated CH_4 and N_2O, which are more potent greenhouse gases than CO_2.

The relative potential of the various microalgae biomass production processes in reducing GHGs still needs to be determined. It must be emphasized that microalgae biomass used as human foods or animal feeds do not mitigate GHGs. Also, high value byproducts would have very small markets, leading to negligible GHG reductions. In wastewater treatment, as in some aquaculture processes, the use of CO_2 for increasing microalgae biomass production would greatly increase the amounts of algal biomass produced and biofuel generated from such processes. Through CO_2 fertilization, GHG reductions can be maximized in wastewater treatment processes along with other environmental benefits, such as nutrient reductions. Thus, such processes do not require the large scales, very high productivities, or low costs required for stand-alone power plant flue-gas CO_2 utilization and biofuel-producing processes. Wastewater treatment and aquaculture systems provide an opportunity for near-term practical demonstration projects for biofixation of CO2, which could serve to highlight both the potential of these processes and provide practical

experience for future development of microalgae processes designed for power plant flue gas CO_2 utilization.

The overall consensus of the Workshop participants was that microalgae systems could indeed be developed to achieve the very high productivities and very low capital and operating costs required for production of renewable microalgae fuels and to abate fossil fuel CO_2 emissions from power plants. On the issue of productivity, the saturating light effect should be a central focus of future R&D. However, this is not the only factor limiting productivity, respiration and photoinhibition also being important. It must be recognized that actually achieving these goals will require relatively long-term R&D efforts. The greatest potential for microalgae biofixation processes is in developing countries, which should be included in any future development of this technology.

4. THE INTERNATIONAL NETWORK FOR BIOFIXATION OF CO_2

The advantage of microalgae systems lies in their potential for high productivity, giving them a small footprint compared to other biological systems, their ability to use otherwise unsuitable water and land resources, their integration with waste treatment and their production of liquid and gaseous fuels not readily obtained from other biomass sources. These potential advantages still must be realized and will require extensive R,D&D to be achieved in practice. A specific R&D plan will need to be developed by the proposed International Network. Early pilot plant work, preferably at already established microalgae facilities, such as at wastewater treatment plants or commercial aquaculture systems, would help to more rapidly achieve these long-term goals. From such practical work, larger-scale systems could be extrapolated and more fundamental research issues identified and addressed.

At present, the major limitations are technological and economic; however resources (e.g. climate, suitable land, available CO_2, water or waste flows, etc.) will limit the ultimate potential of this technology. Estimates of the potential for GHG reductions by microalgae processes must still be developed, both geographically and for various applications, such as power plant flue gas utilization and waste treatment. A resource and potential impacts assessment should be one of the early activities by the proposed Network. More detailed economic and systems analyses are also required. Some higher value, energy-saving products, such as bioplastics and fertilizers, can be considered in microalgae biofixation, but require further analysis. Engineering and economic studies would be another early goal for the proposed Network. The major recommendation arrived at during this Workshop was to proceed with the preparation of a formal proposal for establishing an International Network on Microalgae Biofixation of CO_2 for GHG Abatement.

The Network would serve as a vehicle to encourage the practical development of this technology through coordination and collaboration in approaches identified as most promising in both the short- and long-term. It will be organized under the auspices of the IEA GHG R&D Programme as a Project under the existing Annex 1. The Network will focus on practical R&D of microalgae processes that use concentrated CO_2 sources and produce renewable fuels. The Network will be led by stakeholders, namely private companies, government agencies and other organizations interested in funding and promoting, internally and/or through cooperative R&D activities, the development of microalgae biofixation technologies and the practical applications of the results.

The specific objectives of the proposed International Network would be to:
- Encourage practical development of this technology.
- Identify the most promising R&D objectives for both the short- and long-term.
- Develop an overall multi-year R&D plan with specific technical goals.
- Carry out supporting engineering, systems, technology, and resource analyses.
- Coordinate R&D activities and facilitate joint R&D projects, including pilot plant work.
- Pool and provide technical expertise and resources to Network participants.
- Promote worldwide collaboration in this field, including with Less Developed Countries.

The general R&D topics required for practical development and applications include:
- Selection and improvement of algal strains able to be mass cultured in open ponds.
- Maximization of algal productivity under sunlight conditions.
- Maximization of algal biomass C-storage products.
- Development of large-scale, low cost systems for algal cultivation.
- Development of low cost algal-harvesting technologies.
- Improvements in the processes for converting algal biomass into fuels.
- Practical demonstrations in wastewater treatment, aquaculture and other near-term applications.
- Ongoing engineering and economic feasibility analyses to help focus R&D priorities.

At the Meeting of the IEA Greenhouse Gas R&D Programme Executive Committee in Regina, Canada, at the end of March, 2001, EniTecnologie and the U.S. DOE National Energy Technology Laboratory formally presented a proposal to move forward with the establishment of this Network. The Network would be comprised some of the of member countries and supporting energy companies participating in the IEA Greenhouse Gas R&D Programme, as well as other companies and organizations wishing to carry out and support microalgae biofixation R&D. The formal establishment of the Network is anticipated at the next Executive Committee meeting in August 2001, with Network activities starting by 2002.

REFERENCES

Benemann, J.R., "Utilization of Carbon Dioxide from Fossil Fuel-Burning Power Plants with Biological Systems", *Energy Conserv. Mgmt.,* 34: 999 - 1004 (1993).

Benemann, J. R., and W.J. Oswald, "Systems and Economic Analysis of Microalgae Ponds for Conversion of CO_2 to Biomass". Final Report to the U.S. Dept. of Energy, Pittsburgh Energy Technology Center. Dept. of Civil Engineering, University of California Berkeley. March, 1996.

Burlew, J., "Algae Culture: From Laboratory to Pilot Plant", Carnegie Institute, Washington D.C. (1953).

Melis, A., J. Neidhardt and John R. Benemann, "*Dunaliella salina* (Chlorophyta) with small chlorophyll antenna sizes exhibit higher photosynthetic productivities and photon use efficiencies than normally pigmented cells". *J. App. Phycol.* 10: 515 - 525 (1999).

Nakajima, Y. and R. Ueda, "The effect of reducing light-harvesting pigment on marine microalgal productivity". *J. App. Phycol*., 12: 285 –290 (2000).

Sheehan, J., T. Dunahay, J. Benemann and P. Roessler, "A Look Back at the U.S. Department of Energy's Aquatic Species Program - Biodiesel from Algae". NERL/TP-580-24190. National Renewable Energy Laboratory, Golden, CO, 80401, July 1998.

Usui, N., and M. Ikenouchi, The Biological CO2 Fixation and Utilization Project, RITE (1) – Highly-effective Photobioreactor System. Energy Conserv. Mgmt. 38: S487 – S492 (1996).

Wake, L.V., and L.W. Hillen. "Study of a Bloom of the Oil-rich Alga *Botryococcus braunii* in the Darwin River Reservoir". *Biotech. Bioeng*., 22: 1637 - 1656 (1980).

Weissman, J. C. and R. P. Goebel, "Design and Analysis of Pond Systems for the Purpose of Producing Fuels", Solar Energy Research Institute, Golden Colorado SERI/STR-231-2840 (1987).